ADENOVIRUS STRATEGIES TO REGULATE THE ASSOCIATION OF

CELLULAR PROTEINS WITH VIRAL GENOMES

Neha J. Pancholi

A DISSERTATION

in

Cell and Molecular Biology

Presented to the Faculties of the University of Pennsylvania

in

Partial Fulfillment of the Requirements for the

Degree of Doctor of Philosophy

2018

Supervisor of Dissertation

_____

Matthew D. Weitzman, Ph.D.

Professor of Microbiology and Pathology and Laboratory Medicine

Graduate Group Chairperson

_____

Daniel S. Kessler, Ph.D.

Associate Professor of Cell and Developmental Biology

Dissertation Committee

Eric J. Brown, Ph.D., Associate Professor of Cancer Biology

Paul M. Lieberman, Ph.D., Professor of Gene Expression and Regulation

Susan R. Weiss, Ph.D., Professor of Microbiology

Jianxin You, Ph.D., Associate Professor of Microbiology

ADENOVIRUS STRATEGIES TO REGULATE THE ASSOCIATION OF CELLULAR PROTEINS

WITH VIRAL GENOMES

ACKNOWLEDGMENTS

I would like to thank my advisor, Matt Weitzman, for his mentorship throughout the past five and half years. His high expectations and critiques motivated me to keep improving, and his guidance has allowed me to grow as a scientist, public speaker, and writer. The challenge to think independently, ask meaningful questions, and drive a research project has been at many points daunting and frustrating, but Matt's trust, encouragement, and willingness to step in when needed gave me the confidence and skills to tackle this challenge.

I would also like to thank the past and present members of the Weitzman lab. Life in the lab would not have been nearly as wonderful without their support and friendship. I thank them for all of the scientific discussions and for helping me put out fires, both metaphorically and literally. In particular, I am incredibly grateful to have shared my time in the lab with Daphne Avgousti and Emigdio Reyes. So much of my scientific growth is due to my conversations and collaborations with them. I thank them for sharing their expertise and for their perpetual willingness to offer advice on anything and everything.

I would also like to thank my committee members, Eric Brown, Paul Lieberman, Susan Weiss, and Jianxin You, for their input on my projects throughout the years.

I am also grateful for the friends I have made through CAMB. From the early years spent exploring the city, studying for prelims, and playing dodgeball to the more recent weddings, thesis defenses, and wine nights, it has been wonderful sharing both my scientific and personal lives with them.

I would like to thank my parents, grandparents, and brother for their love and support throughout my life and for instilling in me the importance of education. I am extremely grateful to spend my life with my husband Andrew, who supports my goals and shares my love of learning, and with our cats Jack and Sophie, who support my head while I sleep and share my love of eating.

ABSTRACT

ADENOVIRUS STRATEGIES TO REGULATE THE ASSOCIATION OF CELLULAR PROTEINS WITH VIRAL GENOMES

Neha J. Pancholi

Matthew D. Weitzman

Successful viral propagation relies on the careful regulation of cellular proteins. Controlling the cellular proteins that interact with viral genomes is an important regulatory strategy, since these interactions control a myriad of processes relevant to viral infection. Nuclear replicating DNA viruses face an especially difficult challenge, as their genomes are accessible to DNA-binding proteins that can promote or impair viral processes. Understanding the manipulation of host proteins associated with viral genomes provides insight into the role of cellular proteins in viral infection and provides targets for anti-viral therapeutics. Furthermore, these interactions can provide insight into the regulation of fundamental cellular processes, and have broader implications in understanding viral or cellular evolution. Here, we employed different strategies to understand how interactions with viral genomes are regulated. We studied adenovirus, a DNA virus that replicates in the nucleus, where its linear double-stranded DNA genome is accessible to nuclear DNA-binding proteins. First, we utilized evolutionary diverse adenovirus serotypes with distinct tissue tropisms to study interactions with known anti-viral proteins within the cellular DNA damage response (DDR). This project demonstrated that serotypes across the adenovirus family target DDR proteins, but do so with varying success. Some serotypes completely overcome inhibitory effects of the DDR, while other serotypes fail to do so. Further analysis demonstrated differences in the mechanisms used to target the DDR. Findings from this project showed that

comparison of diverse adenovirus serotypes can provide mechanistic insight, and these findings may have broader implications in understanding tissue tropism and viral evolution. In the second project, we used proteomics to identify host proteins associated with viral genomes and uncovered a novel role for the histone-like viral protein VII in regulating these interactions. We found that protein VII promotes association of cellular proteins involved in transcription, splicing, and mRNA export. Furthermore, we found that protein VII suppresses the anti-viral interferon response. Together, our results demonstrate that defining interactions of cellular proteins with viral genomes is a useful strategy to identify cellular proteins that promote or impair viral processes and to understand viral mechanisms used to regulate their association with viral genomes.

TABLE OF CONTENTS

LIST OF TABLES

LIST OF ILLUSTRATIONS

CHAPTER 1:

Introduction

A portion of this chapter has been previously published in:

> **Pancholi, N.J.**, A.M. Price, and M.D. Weitzman, *Take your PIKK: tumour viruses and DNA damage response pathways.* Philos Trans R Soc Lond B Biol Sci, 2017. **372**(1732).

Virus-host interactions

As obligate intracellular pathogens, viruses must manipulate the host cell environment in favor of viral replication. Such manipulation can have dire consequences for cellular processes, thus cells have evolved mechanisms to defend against viruses by impairing viral replication. Studying virus-host interactions is crucial to identifying the cellular obstacles that defend against viruses and the mechanisms by which viruses evade cellular defenses. This information provides potential targets for anti-viral therapies, and provides insight into basic cellular processes and viral and host evolution. Studying the interactions between viruses and cells has also been instrumental in dissecting fundamental cellular pathways (Berk, 2005; Daugherty & Malik, 2012), as the cellular proteins that viruses target are often regulatory nodes in cellular signaling pathways. Virus-host interactions have therefore also been important resources to uncover key regulatory mechanisms of cellular processes.

Viruses must regulate protein-DNA interactions

One of the multiple ways that viruses manipulate cellular environments to promote viral replication is through regulation of protein-DNA interactions, as these interactions control several critical processes, including DNA replication, gene expression, and the interferon

response. In the case of nuclear-replicating DNA viruses, cellular DNA-binding proteins that usually interact with cellular DNA can often recognize and associate with viral DNA. This can be beneficial or detrimental to viral replication, depending on the function of the cellular DNA-binding protein. For example, recognition by DNA replication or transcription enzymes can benefit the virus, but recognition by DNA sensors that activate immune signaling can impair viral replication and spread. Therefore, viruses must tightly regulate the cellular proteins that interact with viral genomes. Viruses must recruit cellular proteins to their genomes that aid DNA replication and transcription of viral genes, but must evade interaction with cellular proteins that can trigger anti-viral processes. My thesis work examined how viruses regulate these interactions with cellular DNA-binding proteins. To address this topic, we studied adenovirus, which is a nuclear-replicating DNA virus that has been a historically useful model to study viral manipulation of cellular processes. In **Chapter 2**, we demonstrate how diverse adenoviruses evade recognition by a previously defined anti-viral DNA-binding protein complex. In **Chapter 3**, we utilize proteomics to identify host proteins that interact with viral DNA and describe how a viral DNA-binding protein may regulate these interactions.

Adenovirus

Adenovirus (Ad) was originally isolated from pediatric adenoid tissue in 1953 (Rowe, Huebner, Gilmore, Parrott, & Ward, 1953) and has proven to be an especially powerful model to study basic cellular processes (Berk, 2005). Interest in understanding the interaction of Ad with the cell expanded following the 1962 observation that rodents infected with Ad developed tumors (Trentin, Yabe, & Taylor, 1962). Later research showed that Ad proteins transform human cells in culture and seize control of the cell cycle (Endter & Dobner, 2004). There are many benefits to using Ad to study cellular pathways: Ad propagates well in cell culture, and the life cycle of the virus has been well

characterized. Here, I will first describe the Ad family and the viral life cycle before discussing strategies used by adenovirus to manipulate cellular processes that are activated by interactions between host proteins and viral DNA.

Adenovirus family and classification

Ad is a non-enveloped DNA virus that replicates in the nucleus of host cells (Berk, 2013). At least fifty-six human types comprise the Ad family, and there are additional Ads that infect other vertebrate species (Berk, 2013). Human Ad types were originally classified by serology and hemagglutination assays (Berk, 2013), and have therefore been referred to as “serotypes” historically. Ads have more recently been categorized by genome similarity (Davison, Benko, & Harrach, 2003); however, I will continue to use the term “serotype” here due to convention in the literature. Human serotypes are classified into seven subgroups, A-G, and cause a variety of illnesses (Berk, 2013). There is a moderate level of conservation between subgroups, and all serotypes examined to date have similar genome structure and express homologous proteins (Berk, 2013; Davison et al., 2003).

Viral capsid structure and core proteins

The adenovirus capsid is an icosehdral structure composed of the major capsid proteins, hexon, penton, and fiber (H. Liu et al., 2010; Maizel, White, & Scharff, 1968; Reddy, Natchiar, Stewart, & Nemerow, 2010; van Oostrum & Burnett, 1985). Hexon proteins form the icosahedral structure, and penton is found at each vertex. Fiber proteins form shafts that protrude from the vertices and play an important role in binding to the viral receptor (Philipson, Lonberg-Holm, & Pettersson, 1968). The minor capsid proteins are IIIa, VIII, and IX, and these stabilize interactions between hexon proteins (H. Liu et al., 2010; Reddy et al., 2010). Many viral proteins are also found inside the capsid, and

these proteins are referred to as “core proteins” (**Figure 1.1**). Proteins VII, V, and μ are small, basic core proteins that interact with the viral genome and likely contribute to condensation (C. W. Anderson, Young, & Flint, 1989; Chatterjee, Vayda, & Flint, 1986; Russell, Laver, & Sanderson, 1968). Protein VII is the major core protein, as it is the most abundant, with over 800 copies found in each virion (Chelius et al., 2002; van Oostrum & Burnett, 1985). In addition, a single terminal protein (TP) is found at the 5’ end of each DNA strand (Smart & Stillman, 1982; Van der Vliet, 1995), where it serves as the primer for DNA replication during infection (Van der Vliet, 1995). Protein VI associates with both hexon and protein V to tether the capsid to the interior DNA-protein core (Reddy et al., 2010). Additionally, the virion contains the viral protease, which cleaves viral proteins during entry (Cotten & Weber, 1995; Greber, Webster, Weber, & Helenius, 1996) and during the final stages of packaging (Weber, 2007). The virion also contains protein IVa2, which aids packaging by binding the packaging sequence in the viral genome (Ostapchuk, Yang, Auffarth, & Hearing, 2005). Adenovirus virions do not contain any cellular proteins.

Viral entry

Adenoviruses enter the cell through receptor-mediated endocytosis. Adenoviruses within subgroups A, C, D, E, and F utilize the coxsackie and adenovirus receptor (CAR) (Bergelson et al., 1997), while subgroup B adenoviruses use CD46 as a receptor (Gaggar, Shayakhmetov, & Lieber, 2003). Entry is initiated by the binding of the capsid fiber protein with the cellular receptor (Philipson et al., 1968), and virions enter the cell in endosomes (Chardonnet & Dales, 1970; Greber, Willetts, Webster, & Helenius, 1993). Acidification of the endosome results in activation of the viral protease, which cleaves protein VI (Greber et al., 1996). Cleavage of protein VI is required for the complete disassembly of viral particles that occurs at the nuclear membrane and for DNA import

into the nucleus (Cotten & Weber, 1995; Greber et al., 1996). Upon acidification and endosome lysis, viral particles are released into the cytosol and transported on microtubules to the nucleus through interactions between hexon and dynein proteins (Dales & Chardonnet, 1973; Greber et al., 1993).

Interaction of the viral particles with the nuclear pore complex is required to trigger final disassembly (Greber et al., 1997), likely as an attempt to prevent detection by cytoplasmic DNA sensors. DNA import into the nucleus is aided by the interaction of protein VII with the cellular transportin protein (Hindley, Lawrence, & Matthews, 2007). Most capsid and core proteins remain associated with the nuclear pore complexes (Greber et al., 1997), but protein VII and terminal proteins remain bound to viral genomes as they enter the nucleus (Greber et al., 1997). Nuclear Ad genomes are then transcribed and replicated to generate viral progeny.

Adenovirus genome and gene expression

Ad genomes are linear double-stranded DNA and range in size from 25-45 kb (Davison et al., 2003). The ends of the viral genome are inverted terminal repeat sequences that contain the origins of replication. There are five early transcription units (E1A, E1B, E2, E3, and E4), four intermediate transcription units (IX, IVa2, L4 intermediate, and E2 late), and one late transcription unit (major late unit) (**Figure 1.2**). The intermediate and late transcription units are expressed after the onset of viral DNA replication.

Ad expresses early proteins to establish a cellular environment conducive to viral replication and late proteins to form viral particles. Early proteins are expressed from genomic regions E1-E4, each of which expresses multiple proteins through alternative splicing of transcripts (Berget, Moore, & Sharp, 1977) (**Figure 1.2**). E1 and E4 proteins manipulate the cellular environment to promote viral processes, E2 expresses proteins

involved in viral DNA replication, and E3 expresses proteins to suppress the host innate immune response. Early proteins are expressed before the onset of viral DNA replication. Initiation of DNA replication marks the transition into the late stage of infection, when the intermediate and late transcription units are transcribed.

Early proteins

E1A from the E1 genomic region is the first viral protein to be transcribed, due its strong enhancer (Hearing & Shenk, 1983; Nevins, Ginsberg, Blanchard, Wilson, & Darnell, 1979). The E1A transcript produces two proteins, called large and small E1A. Large E1A is a transactivator and stimulates transcription of E1A and the other early transcription units by recruiting host transcription enzymes to viral genomes (Pelka et al., 2009; Winberg & Shenk, 1984). In addition to promoting viral transcription, both small and large E1A manipulate the cell cycle in order to promote entry into S phase so that viral DNA replication can occur. This is achieved through interaction between E1A and the cellular retinoblastoma (Rb) family of proteins. E1A binding to Rb releases E2F transcription factors, allowing them to activate transcription of genes required for progression into S phase (Bagchi, Raychaudhuri, & Nevins, 1990). The E1 region also encodes two proteins expressed from the E1B transcription unit: E1b55K and E1b19K. These proteins regulate apoptosis and the cell cycle in order to promote viral replication. Together with E1A, E1B proteins can transform human cells in culture, and E1 proteins are the transformative agents of the widely used 293 cells (Endter & Dobner, 2004). E1b19K is a viral mimic of the anti-apoptotic MCL-1 protein (Cuconati & White, 2002), whose degradation induces apoptosis. As an MCL-1 mimic, E1b19K is able to prevent apoptosis even when MCL-1 has been degraded (Cuconati & White, 2002). E1b19K inhibits apoptosis by binding the cellular BAK and BAX proteins, preventing their interaction and pro-apoptotic activity (Cuconati & White, 2002). E1b55K regulates

cellular function partially through its ability to target cellular proteins for proteasome-mediated degradation (Baker, Rohleder, Hanakahi, & Ketner, 2007; Cheng et al., 2011; Dallaire, Blanchette, Groitl, Dobner, & Branton, 2009; Forrester et al., 2011; Harada, Shevchenko, Shevchenko, Pallas, & Berk, 2002; Orazio, Naeger, Karlseder, & Weitzman, 2011; Querido, Blanchette, et al., 2001; Querido et al., 1997; Schwartz et al., 2008; Steegenga, Riteco, Jochemsen, Fallaux, & Bos, 1998; Stracker, Carson, & Weitzman, 2002). E1b55K interacts with the viral E4orf6 protein (expressed from the E4 region), which recruits cellular proteins to form a VHL-like E3 ubiquitin ligase (Harada et al., 2002; Querido, Blanchette, et al., 2001; Querido, Morrison, et al., 2001). E1b55K is thought to provide substrate specificity to the ubiquitin ligase (Berk, 2005; Blackford & Grand, 2009; Schwartz et al., 2008), which targets proteins involved in a myriad of cellular processes, including the DNA damage response and cell cycle control (Baker et al., 2007; Berk, 2005; Blackford & Grand, 2009; Forrester et al., 2011; Orazio et al., 2011; Querido et al., 1997; Stracker et al., 2002). Activity of the E1b55K-E4orf6 ubiquitin ligase is required for optimal viral replication, protein expression, and export of viral mRNA (Blackford & Grand, 2009; Blanchette et al., 2008; Halbert, Cutt, & Shenk, 1985; Lakdawala et al., 2008). In addition to targeting proteins for degradation, E1b55K suppresses the activity of the tumor suppressor p53 by directly binding its transcriptional activation domains (Sarnow, Ho, Williams, & Levine, 1982). This inhibits p53-mediated transcriptional activation of cellular genes that promote cell cycle arrest.

The E2 region expresses proteins involved in replication of the viral genome. Activation of the E2 transcription unit is mediated by the cellular E2F proteins (SivaRaman & Thimmappaya, 1987), which function during S phase. This ensures that expression of viral DNA replication proteins occurs only after cells have entered S phase (Berk, 2013). E2 expresses the viral DNA polymerase (Ad Pol), pre-terminal protein (pTP), and the

single-stranded DNA binding protein (DBP). pTP associates with the 5' ends of newly replicated viral genomes and functions as a protein primer for DNA replication by providing the 5' hydroxyl group necessary for elongation (Smart & Stillman, 1982; Van der Vliet, 1995). DBP binds and stabilizes single-stranded DNA intermediates produced during replication (Van der Vliet, 1995; van der Vliet & Levine, 1973), and also promotes strand separation (Dekker et al., 1997; Van der Vliet, 1995).

The E4 region expresses seven proteins: orf1, orf2, orf3, orf3/4, orf4, orf6, and orf6/7. These proteins are involved in regulation of several different cellular processes, including transcription, translation, apoptosis, mRNA splicing, protein stability, and DNA damage responses, among others (reviewed in (Tauber & Dobner, 2001; Weitzman, 2005). While deletion or mutation of individual E4 orfs only moderately affects viral replication (Halbert et al., 1985), deletion of both E4orf6 and E4orf3 or the entire E4 region results in a dramatic reduction of viral growth (Bridge & Ketner, 1989; Huang & Hearing, 1989; Lakdawala et al., 2008; Weiden & Ginsberg, 1994). Therefore, E4orf3 and E4orf6 are considered redundant in promoting optimal lytic viral replication (Bridge & Ketner, 1989; Huang & Hearing, 1989). E4orf3 and E4orf6 each manipulate cellular proteins in multiple ways in order to evade anti-viral cellular pathways. E4orf3 forms characteristic nuclear track structures (Carvalho et al., 1995; Doucas et al., 1996; Ou et al., 2012) and disrupts PML nuclear bodies into nuclear tracks (Carvalho et al., 1995; Doucas et al., 1996). E4orf3 can promote viral replication by mislocalizing cellular proteins to these nuclear tracks in order to sequester them away from viral genomes (Bridges, Sohn, Wright, Leppard, & Hearing, 2016; Reyes et al., 2017; Stracker et al., 2002). In addition to mislocalization to E4orf3-PML tracks, E4orf3 recruits cellular proteins involved in translation inhibition and mRNA degradation to perinuclear aggresomes to prevent inhibition of viral protein synthesis (Greer, Hearing, & Ketner,

2011). E4orf3 also suppresses expression of p53-responsive genes through H3K9 methylation of p53 target gene promoters (Soria, Estermann, Espantman, & O'Shea, 2010) and has been demonstrated to suppress interferon signaling (Ullman & Hearing, 2008; Ullman, Reich, & Hearing, 2007). E4orf6 also manipulates cellular proteins to evade anti-viral pathways. E4orf6, together with E1b55K, promotes degradation of several cellular proteins (described in E1b55K section above) to promote viral replication, mRNA export, and protein synthesis (Blackford & Grand, 2009; Blanchette et al., 2008; Halbert et al., 1985; Lakdawala et al., 2008). In addition, E4orf6 has been shown to interact with and inhibit tumor suppressors p53 and p73 independently of E1b55K (Dobner, Horikoshi, Rubenwolf, & Shenk, 1996; Higashino, Pipas, & Shenk, 1998; Steegenga, Shvarts, Riteco, Bos, & Jochemsen, 1999).

Early viral proteins manipulate the cell to promote viral replication and to express the viral proteins necessary to replicate the viral genome. Thus, once early proteins are expressed, the viral genome is replicated and expression of late viral genes begins.

Late proteins

Late viral genes are expressed from a single transcription unit under the control of the major late promoter (MLP) (Shaw & Ziff, 1980). The major late transcript is processed by alternative splicing and alternative poly(A) usage to produce five families of late transcripts (L1-L5). Further processing of each family generates at least 14 late mRNAs. Viral DNA replication is a prerequisite to activation of the MLP (Thomas & Mathews, 1980), ensuring that late proteins are not expressed until they are needed to package replicated viral genomes. Late proteins largely form the viral capsid and are involved in DNA compaction and packaging. Functions of these proteins are described in the *Viral*

capsid structure and core proteins and *Viral assembly and release* sections of this chapter.

Protein VII

Protein VII is a late protein expressed from the L2 region that has important roles at several stages of infection, including viral entry (Greber et al., 1997), evasion of the DNA damage response (Karen & Hearing, 2011), viral transcription (Komatsu, Haruki, & Nagata, 2011; Matsumoto, Nagata, Ui, & Hanaoka, 1993; Okuwaki & Nagata, 1998), and DNA condensation (Johnson et al., 2004). As an incoming viral protein, it is present even before *de novo* viral protein synthesis (J. Chen, Morral, & Engel, 2007; Karen & Hearing, 2011), and new copies are produced during the late stage of infection (Xue, Johnson, Ornelles, Lieberman, & Engel, 2005). As a result, protein VII is present throughout infection. Protein VII is produced as a pre-cursor protein, and the pro-peptide sequence is cleaved by the viral protease in the final stage of packaging (C. W. Anderson, Baum, & Gesteland, 1973). The mature cleaved protein is found in viral particles and on incoming genomes. Protein VII is the major core protein, with over 800 copies found in each viral particle (van Oostrum & Burnett, 1985). This small, basic protein associates with and condenses viral genomes (Chatterjee et al., 1986; Russell et al., 1968), and contributes to nuclear entry of the genome (Hindley et al., 2007). While other core proteins remain cytoplasmic (Greber et al., 1997), protein VII enters the nucleus in association with viral genomes (Greber et al., 1997) and has been suggested to protect incoming viral genomes from detection by DNA damage machinery before early viral gene expression (Karen & Hearing, 2011). Surprisingly, deletion of protein VII does not preclude packaging of the viral genome into capsids (Ostapchuk et al., 2017). This suggests that other core proteins are redundant with protein VII for condensing DNA to be packaged. While production of viral particles is not affected by protein VII deletion,

the viruses that are produced in the absence of protein VII are non-infectious (Ostapchuk et al., 2017). Protein VII-deleted viruses are unable to escape from endosomes during the initial steps of infection (Ostapchuk et al., 2017). This defect raises the possibility that protein VII contributes to endosomal escape. However, the defect could also be an indirect consequence of the ineffective protein VI cleavage that was observed in the absence of protein VII (Ostapchuk et al., 2017) since protein VI plays an important role in endosomal escape (Cotten & Weber, 1995; Greber et al., 1996). Furthermore, it is possible that the protein-VII-deleted virus particles are structurally distinct from wild-type viruses, and viral entry could be affected by any structural abnormalities.

Protein VII has been described to impact viral transcription, but there are conflicting reports as to its role. While protein VII-mediated DNA condensation is beneficial for packaging genomes into capsids, it does not allow for efficient transcription of viral genes (Matsumoto et al., 1993; Okuwaki & Nagata, 1998). Therefore, it would be expected that protein VII is displaced to promote active transcription. There is some evidence of gradual protein VII dissociation before the onset of transcription (Haruki, Okuwaki, Miyagishi, Taira, & Nagata, 2006; Komatsu et al., 2011). However, protein VII is also detected on viral genomes during later stages as well (Chatterjee et al., 1986; Reyes et al., 2017; Xue et al., 2005). Since cellular histones interact with adenoviral DNA during infection (Giberson, Davidson, & Parks, 2012; Komatsu & Nagata, 2012), it is likely that some protein VII dissociates from genomes to make room for histones to bind. The protein VII that remains associated with viral genomes is likely remodeled to regulate the timing of viral genes (Giberson et al., 2012). Consistent with this theory, protein VII was found associated with the major late promoter but not with the E1A promoter at 6 hours post-infection (Haruki, Gyurcsik, Okuwaki, & Nagata, 2003), when

late transcription has not yet begun. Furthermore, protein VII interacts with the cellular chromatin remodeling protein SET (also known as template activating factor 1β) (Haruki et al., 2003; Haruki et al., 2006; Komatsu et al., 2011; Matsumoto et al., 1993; Xue et al., 2005). SET promotes viral replication and early viral gene expression by increasing DNA accessibility (Matsumoto et al., 1993). Deletion of SET results in a moderate decrease in viral gene expression and replication (Haruki et al., 2006). Despite the negative impact that protein VII-mediated DNA condensation has on transcription, it appears that protein VII is also capable of activating transcription in *in vitro* assays (Komatsu et al., 2011). Furthermore, protein VII has been suggested to recruit the viral transactivator protein E1A to viral DNA (Johnson et al., 2004). While some data suggest that protein VII must be removed before transcription can begin, other data suggest that transcription is actually required for protein VII dissociation (J. Chen et al., 2007). The impact of protein VII on viral transcription remains unclear, as does the timing and extent of dissociation from viral genomes.

Viral DNA replication and viral replication centers

Adenovirus DNA replication relies on three viral proteins from the E2 region: pre-terminal protein (pTP), DNA-binding protein (DBP), and the adenovirus DNA polymerase (Ad Pol) (Van der Vliet, 1995). The functions of these proteins are described in the *Adenovirus genome and gene expression* section of this chapter. Several cellular proteins, such as topoisomerase I, contribute to adenovirus DNA replication (Reyes et al., 2017; Van der Vliet, 1995). Cellular helicases are not required for adenovirus DNA replication because of the strand separating function of DBP (Dekker et al., 1997; Dekker et al., 1998). Replication occurs in two rounds to duplicate the viral genome. In the first round of replication, only one of the two DNA strands serves as the template, and the second strand is displaced as the nascent DNA strand is elongated (Van der

Vliet, 1995). Therefore, the first round of replication produces one double-stranded viral genome and a displaced DNA strand. The displaced strand circularizes by self-annealing through the complementary inverted terminal ends found at each end of the DNA strand, generating a panhandle structure (Van der Vliet, 1995). The annealed portion of the panhandle has the same sequence and structure as the replication origin of the viral genome. This allows replication initiation to occur through the same mechanism as the first round of replication. By the end of the second round of replication, two complete viral genomes have been produced.

Adenovirus DNA replication occurs in structures called viral replication centers (VRCs). VRCs have been visualized in multiple ways: by immunofluorescence of single-stranded DNA-binding proteins viral DBP or cellular RPA32 (Evans & Hearing, 2005; Pombo, Ferreira, Bridge, & Carmo-Fonseca, 1994; Stracker et al., 2002; Stracker et al., 2005), by incorporation of nucleotide analogs and subsequent visualization (Pombo et al., 1994; Reyes et al., 2017), and by *in situ* hybridization using probes specific to the viral genome (Pombo et al., 1994; Puvion-Dutilleul & Puvion, 1990a, 1990b; Weitzman, Fisher, & Wilson, 1996). Representative images of VRCs from multiple adenovirus serotypes are shown in **Figure 1.3**. The structure of VRCs changes throughout the course of infection. VRCs begin as small foci that enlarge as replication produces more genomes, and the sites of single-stranded DNA eventually become donut-shaped (Pombo et al., 1994; Puvion-Dutilleul & Puvion, 1990a, 1990b). At very late stages of infection, VRCs disassemble and can be seen as clusters of irregularly shaped aggregates. As viral genomes replicate, newly synthesized double-stranded viral genomes are displaced to the periphery of single-stranded DNA accumulation sites (Pombo et al., 1994; Puvion-Dutilleul & Puvion, 1990a). Viral transcription of late genes occurs at the periphery of VRCs, using the displaced genomes as templates (Pombo et al., 1994).

Virion assembly and release

Viral DNA replication and late gene expression result in accumulation of capsid proteins and viral genomes that are assembled into viral particles. Once translated, the major core proteins – hexon, penton, and fiber – form distinct fragments of the capsid in the cytoplasm (Horwitz, Scharff, & Maizel, 1969; Velicer & Ginsberg, 1970). These fragments are hexon trimers, which form the faces of the icosahedral capsid, and penton capsomers, which are complexes of penton and fiber shafts (Horwitz et al., 1969; Velicer & Ginsberg, 1970). Hexon trimers and penton capsomers are then imported into the nucleus, where they associate to form the pro-capsid and where viral genomes are packaged. Packaging of the viral genome requires seven AT-rich packaging sequences located at the left end of the genome (Hearing, Samulski, Wishart, & Shenk, 1987; Ostapchuk & Hearing, 2005), which are bound by the viral proteins IVa2, L4-22K, and L1-52/55K (Ostapchuk & Hearing, 2005; Ostapchuk et al., 2005). IVa2 associates with viral genomes and pro-capsids (Christensen et al., 2008), and using its ATPase activity (Koonin, Senkevich, & Chernos, 1993), IVa2 works as an ATP-dependent motor to encapsidate viral genomes (Ostapchuk & Hearing, 2005). Core viral proteins associated with viral genomes are packaged as pre-cursors, and their pro-peptide sequences are cleaved by the viral protease to generate mature core proteins in the final steps of virion assembly (C. W. Anderson et al., 1973; Freimuth & Anderson, 1993). Cleavage by the viral protease is required for stability and infectivity of the virions (Ostapchuk & Hearing, 2005).

Viral particles are released upon cellular lysis. Adenovirus increases cellular susceptibility to lysis by disrupting cellular integrity through viral protease-dependent cleavage of a cellular cytokeratin (P. H. Chen, Ornelles, & Shenk, 1993). Cell death and lysis at the end of the viral replication cycle result from accumulation of the viral E3 11.6

kDa protein (Tollefson, Ryerse, Scaria, Hermiston, & Wold, 1996; Tollefson, Scaria, et al., 1996), which has been referred to as the viral death protein due to its induction of cell death. Released viral particles spread to uninfected cells to begin another round of viral infection. Viral dissemination is facilitated by degradation of integrin α3 (Dallaire et al., 2009) and disruption of tight junctions (Latorre et al., 2005; Walters et al., 2002).

Adenovirus manipulation of cellular processes that respond to viral DNA

DNA damage response

Maintenance of cellular genome integrity is paramount to preventing cellular transformation. Thus, cells have a plethora of mechanisms in place to preserve genome integrity. The pathways activated by DNA damage to protect genome integrity are collectively called the DNA damage response (DDR), and they function to sense and repair damage in cellular DNA (reviewed in (Ciccia & Elledge, 2010; Harper & Elledge, 2007; Jackson & Bartek, 2009; Polo & Jackson, 2011)). The DDR also responds to viruses, which trigger DDR activation through several means (Luftig, 2014). For example, viral genomes and replication intermediates may activate the DDR due to their resemblance to damaged DNA structures. In addition, rapid viral DNA replication may cause replication stress or errors that trigger the DDR. Viral inactivation of cell cycle checkpoints may also allow mutations to accumulate in cellular DNA. Activation of the DDR during infection can have a myriad of consequences for virus replication, and several viruses therefore manipulate the DDR to promote infection (Hollingworth & Grand, 2015; Lilley, Schwartz, & Weitzman, 2007; Luftig, 2014; Ryan, Hollingworth, & Grand, 2016; Turnell & Grand, 2012).

Cellular genomes are damaged on average 100,000 times per day (Ciccia & Elledge, 2010). Sources of damage include exogenous assaults such as radiation, and

endogenous events such as replication fork collapse and DNA replication errors. DNA damage occurs in multiple forms, including mismatched base pairs, pyrimidine dimers, replication stress, and single-strand or double-strand DNA breaks (Ciccia & Elledge, 2010). Unchecked DNA damage has dramatic effects on cells since the accumulation of mutations and DNA breaks can lead to cell death, chromosomal translocations, and oncogenesis.

The DDR is a network of signal transduction pathways that respond to DNA damage. Signaling is mediated by serine/threonine kinases within the PIKK family and the downstream proteins that are activated (Ciccia & Elledge, 2010; Harper & Elledge, 2007; Jackson & Bartek, 2009; Polo & Jackson, 2011). DDR signaling leads to arrest of the cell cycle to allow recruitment of proteins to repair the damaged DNA (Ciccia & Elledge, 2010; Harper & Elledge, 2007; Jackson & Bartek, 2009; Polo & Jackson, 2011). Alternatively, signaling can induce apoptosis to eradicate the damaged cell. The DDR is activated by recognition of DNA damage via proteins called “sensors.” Sensors bind DNA at the site of damage and recruit PIKK “transducers.” Transducers in turn activate multiple downstream “effectors” to amplify signaling that mediates DNA repair and cell cycle arrest at the G1/S, intra-S, and G2/M checkpoints (Ciccia & Elledge, 2010; Harper & Elledge, 2007; Jackson & Bartek, 2009; Polo & Jackson, 2011). Effectors include tumor suppressors, which halt cell division by activating cell cycle checkpoints or apoptosis. Loss or inhibition of tumor suppressors can lead to unregulated cellular proliferation and transformation. Viruses regulate the DDR through manipulation of proteins at all three stages of the DDR.

The primary transducers of the DDR are ataxia telangiectasia mutated (ATM), ataxia telangiectasia and Rad3 related (ATR), and DNA-dependent protein kinase (DNA-PK).

ATM, ATR, and DNA-PK are all members of the PIKK family and have similar domain structures, including kinase and protein-binding domains (Bakkenist & Kastan, 2004; Lovejoy & Cortez, 2009). The specific PIKK activated depends on the type of DNA damage encountered. ATM and DNA-PK respond to double-strand DNA breaks (DSBs), while ATR responds to replication stress and single-stranded DNA (ssDNA) (Bakkenist & Kastan, 2004; Lovejoy & Cortez, 2009). The specific proteins activated in each pathway are illustrated in **Figure 1.4**. Briefly, the MRE11-RAD50-NBS1 complex (MRN) senses DSBs and promotes activation of ATM (Carson et al., 2003; Lee & Paull, 2005). ATM is activated by auto-phosphorylation and through interactions with TIP60 (Bakkenist & Kastan, 2003; Y. Sun, Jiang, Chen, Fernandes, & Price, 2005), and activated ATM then phosphorylates downstream effectors to amplify signaling. Effectors include histone H2A variant H2AX (γH2AX when phosphorylated), NBS1, BRCA1, CHK2, and p53 (Banin et al., 1998; Burma, Chen, Murphy, Kurimasa, & Chen, 2001; Cortez, Wang, Qin, & Elledge, 1999; Lim et al., 2000; Matsuoka, Huang, & Elledge, 1998; Rogakou, Boon, Redon, & Bonner, 1999). BRCA1 and RAD51 are required for repair of DSBs by homologous recombination during S-phase, and CHK2 and p53 activate the G1/S, intra-S, and G2/M checkpoints (Banin et al., 1998; Hirao et al., 2000; Kastan & Bartek, 2004; Matsuoka et al., 1998). Another repair pathway for DSBs is non-homologous end joining (NHEJ), which requires DNA-PK activity. The Ku complex senses DSBs and recruits the catalytic subunit of DNA-PK (DNA-PKcs) (Ciccia & Elledge, 2010). The Ku-DNA-PKcs complex recruits XRCC4 and DNA ligase IV to join broken ends (Nick McElhinny, Snowden, McCarville, & Ramsden, 2000). Accumulation of ssDNA at resected DSBs and replication forks promotes activation of the ATR pathway. Exposed ssDNA is coated and protected by RPA, which recruits ATR through the ATR binding partner ATRIP (Zou & Elledge, 2003). The ATR activator TOPBP1 is recruited by interacting with the 9-1-1

complex (RAD9, RAD1, HUS1) (Delacroix, Wagner, Kobayashi, Yamamoto, & Karnitz, 2007). ATR activation signals through downstream effectors CHK1 and p53 to cause cell cycle arrest at the G2/M and intra-S checkpoints or apoptosis (Kastan & Bartek, 2004). Since cell cycle arrest or cell death could limit viral replication, viruses employ multiple strategies to misregulate the cell cycle, most notably through inactivation of tumor suppressors p53 and RB (Endter & Dobner, 2004; Howley & Livingston, 2009; Jha, Banerjee, & Robertson, 2016; Moody & Laimins, 2010; Pipas, 2009). Misregulation of the cell cycle via disruption of tumor suppressors is a significant contributor to transformation by tumor viral oncoproteins (Endter & Dobner, 2004; Howley & Livingston, 2009; Jha et al., 2016; Moody & Laimins, 2010; Pipas, 2009).

The intricate relationship between viruses and the DDR has been extensively demonstrated with adenovirus serotype 5 (Ad5). All three of the PIKKs are targeted by adenoviral proteins, and these interactions revealed principles that have since been extended to other viruses. Adenovirus has a linear, double-stranded DNA genome, and one of the first indications that the DDR responded to adenovirus was the observation that infection with genetic mutants of Ad5 resulted in fusion of viral genomes into concatemers (Weiden & Ginsberg, 1994). This observation led to the hypothesis that the blunt, double-stranded DNA ends of the Ad5 viral genome are recognized as DNA breaks. Several DDR proteins are necessary for concatemer formation, supporting a role for the DNA repair machinery (Boyer, Rohleder, & Ketner, 1999; Stracker et al., 2002). This was the first demonstration that the cellular DDR recognizes and acts on viral DNA. While the DDR responds to mutant Ad5 infection, wild-type Ad5 infection does not produce concatemers (Carson et al., 2003; Stracker et al., 2002; Weiden & Ginsberg, 1994), indicating that Ad5 evades the DDR. Inactivation of DDR components is critical for efficient Ad5 replication (Boyer et al., 1999; Evans & Hearing, 2005; Gautam &

Bridge, 2013; Lakdawala et al., 2008; Shah & O'Shea, 2015), suggesting a role for the DDR in restricting adenoviral replication.

MRN

The cellular MRE11, RAD50, and NBS1 proteins comprise the MRN complex (MRN), which can act as a sensor of double-strand DNA breaks (Figure 1). Ad5 regulates MRN localization and protein levels to minimize the impacts of host detection of viral DNA. During Ad5 infection, early viral proteins both degrade MRN and mislocalize MRN into nuclear tracks and perinuclear aggresomes (Araujo, Stracker, Carson, Lee, & Weitzman, 2005; Cheng et al., 2011; Evans & Hearing, 2003, 2005; Forrester et al., 2011; Karen, Hoey, Young, & Hearing, 2009; Ou et al., 2012; Shah & O'Shea, 2015; Stracker et al., 2002). The MRN proteins become immobilized, preventing localization to Ad5 replication centers (Carson et al., 2009; Stracker et al., 2002). Mislocalization is also necessary for SUMOylation of MRE11 and NBS1 by an early viral protein, although the consequences of SUMOylation are unclear (Sohn & Hearing, 2012).

Evading MRN appears to be important for the Ad5 life cycle. In the absence of MRN mislocalization or degradation, MRN is present at viral replication centers where it associates with viral DNA in an NBS1-dependent manner (Mathew & Bridge, 2007, 2008; Stracker et al., 2002). Ad5 mutants unable to target MRN are severely impaired in viral DNA replication, late protein expression, and virion production (Evans & Hearing, 2005; Lakdawala et al., 2008; Mathew & Bridge, 2007). Although MRN is required for concatemers (Stracker et al., 2002), MRN can also impair viral replication independently of concatemer formation (Evans & Hearing, 2003; Lakdawala et al., 2008; Mathew & Bridge, 2007). Loss of MRN rescues replication of Ad5 mutants that neither mislocalize nor degrade MRN (Lakdawala et al., 2008; Mathew & Bridge, 2007). Ad5 mutants that

target MRN by only one of these mechanisms are not impaired for viral replication, demonstrating that each mechanism is sufficient to evade MRN (Lakdawala et al., 2008).

There are several potential models for MRN restriction of adenovirus replication. One model is that MRE11 removes the viral terminal protein (TP) from the 5' ends of the adenovirus genome through its nuclease activity. TP provides the 3' hydroxyl group to initiate DNA replication and may protect viral DNA from digestion, so its removal would have a profound effect on adenovirus replication. This model is supported by the loss of DNA sequences at concatemer junctions and the requirement for MRE11 exonuclease activity for concatemer formation (Karen et al., 2009; Stracker et al., 2002; Weiden & Ginsberg, 1994). Alternatively, recruitment of DDR proteins to viral DNA could physically obstruct the interaction of viral and cellular replication proteins with viral genomes (Karen & Hearing, 2011). A third model is that MRN indirectly impairs replication through activation of downstream ATM signaling, which is supported by enhanced viral replication during ATM inhibition (Gautam & Bridge, 2013; Shah & O'Shea, 2015). While it is clear that MRN is a major obstacle for Ad5 replication, the mechanism by which it restricts replication requires further study.

ATM

Observations from Ad5 were the first to demonstrate that MRN promotes ATM activation in response to viruses and cellular double-strand breaks in mammalian cells (Carson et al., 2003). Since MRN is the sensor that activates ATM signaling, it would be expected that MRN targeting by Ad5 abrogates ATM activation. Multiple groups have observed that degradation of MRN by wild-type Ad5 can prevent activation of ATM or downstream substrates at viral replication centers (Carson et al., 2003; Gautam & Bridge, 2013; Shah & O'Shea, 2015). Ad5 also employs means to prevent ATM activation before viral

proteins are expressed. Protein VII, a viral core protein bound to incoming viral DNA, is negatively correlated with phosphorylated ATM on mutant Ad5 genomes early during infection (Karen & Hearing, 2011). This suggests a role for protein VII in preventing DDR recognition of incoming viral genomes. Furthermore, protein VII is sufficient to suppress DDR signaling in response to breaks in the cellular genome (Cheng et al., 2013). The effect of protein VII on the DDR in response to cellular and viral genomes may depend on its interaction with the cellular SET/TAF1β protein (Cheng et al., 2013). Another mechanism by which Ad5 may regulate ATM activation is through degradation of the ATM activator TIP60 (Gupta, Jha, Engel, Ornelles, & Dutta, 2013). Together, these studies demonstrate multiple ways that Ad5 infection can affect ATM activation and signaling.

While there is consensus that ATM is not activated during early infection or at wild-type Ad5 replication centers, some findings demonstrate pan-nuclear distribution of activated ATM late in infection (Shah & O'Shea, 2015), suggesting MRN-independent ATM activation during virus infection. This is consistent with the reported phosphorylation of the ATM substrate KAP1 and replication-dependent widespread γH2AX during wild-type Ad5 infection (Forrester et al., 2011; Nichols, Schaack, & Ornelles, 2009; Shah & O'Shea, 2015). KAP1 phosphorylation is also seen during infection with other Ad serotypes (Forrester et al., 2011).

The effect of ATM activation on Ad5 infection may vary between cell types and stages of the viral life cycle. When viral replication was measured by quantitative PCR in ATM hypomorphic fibroblasts, ATM loss did not enhance replication of an Ad5 mutant unable to target MRN (Lakdawala et al., 2008). However, when viral replication was measured by dot blot hybridization in transformed cell lines, increased viral DNA from the mutant

Ad5 was observed when ATM was inhibited or depleted (Gautam & Bridge, 2013). In primary lung epithelial cells, ATM has distinct effects on Ad5 at different stages of replication (Shah & O'Shea, 2015). An Ad5 mutant incapable of targeting MRN was impaired by ATM activation at replication centers early during infection in small airway epithelial cells (Shah & O'Shea, 2015). In these cells, wild-type Ad5 avoided ATM activation at replication centers by targeting MRN and progressed to late infection when diffuse ATM activation occurred. Inhibition of ATM kinase activity during wild-type Ad5 infection does not affect replication in transformed or primary cells (Gautam & Bridge, 2013; Shah & O'Shea, 2015). Together, these findings suggest that ATM does not impair wild-type Ad5 but may inhibit replication of specific Ad5 mutants in various cellular settings.

ATR

ATR signaling is also abrogated during adenovirus infection. While ATR is generally associated with prolonged exposure of ssDNA due to replication stress, double-strand breaks can induce ssDNA exposure and subsequent ATR activation due to MRE11-mediated resection at broken ends (Jazayeri et al., 2006). Ad5 mutants that do not target MRN induce robust activation of ATR signaling (Carson et al., 2009; Carson et al., 2003), which could occur due to replication intermediates or resection at genome ends. ATR activation is prevented during infection with wild-type Ad5 due to MRN degradation and mislocalization (Carson et al., 2003; Forrester et al., 2011). ATR and several downstream proteins are found at viral replication centers (Blackford et al., 2008; Carson et al., 2009) but ATR does not appear to affect Ad5 replication (Gautam & Bridge, 2013; Lakdawala et al., 2008; Shah & O'Shea, 2015). Adenovirus serotype 12 (Ad12) inhibits ATR through degradation of the ATR regulator TOPBP1 (Blackford et al., 2010). Interestingly, Ad12 does not mislocalize MRN and therefore does not inhibit ATR

through this mechanism (Stracker et al., 2005). It appears that Ad12 and Ad5 employ distinct mechanisms to inhibit ATR, while some other adenovirus serotypes induce robust ATR signaling (Forrester et al., 2011). Inactivation of ATR by adenoviruses may simply be a downstream consequence of MRN manipulation, or it may be specifically targeted to promote some undetermined aspect of the life cycle.

DNA-PK

The formation of adenoviral genome concatemers requires DNA-PK and NHEJ proteins to ligate DNA ends, and correlates with decreased late protein expression and DNA packaging (Boyer et al., 1999; Jayaram & Bridge, 2005). Adenovirus proteins overcome these limitations by disabling the DNA-PK pathway. All adenovirus serotypes examined to date degrade DNA Ligase IV (Baker et al., 2007; Cheng et al., 2011; Forrester et al., 2011), and Ad5 early proteins also interact with DNA-PK to inhibit its functions (Boyer et al., 1999).

Adenovirus has been a powerful model to uncover fundamental principles of virus-host interactions, including interactions with the DDR. Studies with Ad5 were the first to demonstrate that the host DDR responds to viral DNA. In the case of Ad5, DDR proteins seem to be inhibitory, and Ad5 thus disables DDR pathways to overcome anti-viral defense and promote viral replication.

Interferon response

The innate immune response serves as a frontline of defense against invading pathogens and is critical to preventing viral spread. The detection of pathogen associated molecular patterns (PAMPs) triggers signaling that leads to production of interferon proteins and extracellular release of cytokines. These events lead to the synthesis of several anti-viral proteins and the recruitment of innate immune cells.

Therefore, suppression of interferon signaling is crucial to ensure success of viral replication. Interferon signaling in response to viruses is most often activated upon detection of viral genomes or viral nucleic acids by cellular DNA or RNA sensors (Barbalat, Ewald, Mouchess, & Barton, 2011; Barber, 2011; Keating, Baran, & Bowie, 2011). Detection of viral DNA by DNA sensors leads to activation of the 'stimulator of interferon genes' protein (STING) (Ishikawa & Barber, 2008; Ishikawa, Ma, & Barber, 2009; Jin et al., 2008; W. Sun et al., 2009; Zhong et al., 2008). The TANK-binding kinase-1 (TBK-1) is subsequently recruited to STING, where it phosphorylates STING (S. Liu et al., 2015) and the interferon regulatory factor-3 (IRF3) (Fitzgerald et al., 2003; Sharma et al., 2003). Phosphorylated IRF3 dimerizes and complexes with the CBP/p300 acetyltransferase (R. Lin, Heylbroeck, Pitha, & Hiscott, 1998; Sato, Tanaka, Hata, Oda, & Taniguchi, 1998; Wathelet et al., 1998; Yoneyama et al., 1998). The IRF3-CBP/p300 complex translocates to the nucleus to activate transcription of IFNβ, which is then secreted from the cell (R. Lin et al., 1998; Sato et al., 1998; Wathelet et al., 1998; Yoneyama et al., 1998). Binding of IFNβ to a cell surface receptor activates autocrine and paracrine signaling that triggers transcriptional activation of hundreds of interferon-stimulated genes (ISGs) to combat viral infection in infected cells and to prevent infection of neighboring cells (De Andrea, Ravera, Gioia, Gariglio, & Landolfo, 2002; Haller, Kochs, & Weber, 2006). Binding of IFNβ to the cellular receptor activates JAK-STAT signaling, resulting in phosphorylation of STAT-1 and STAT-2 (De Andrea et al., 2002; Haller et al., 2006). Phosphorylated STAT proteins recruit IRF9, and the resulting complex is called the IFN-stimulated gene factor 3 (ISGF3) (De Andrea et al., 2002; Haller et al., 2006). ISGF3 complexes translocate to the nucleus, where they activate expression of ISGs by binding IFN stimulated response elements (ISRE) found in the promoters of these genes (De Andrea et al., 2002; Haller et al., 2006). Interferon

signaling is depicted in **Figure 1.5**. The proteins encoded by ISGs challenge viral replication in several ways, including inhibition of viral transcription, degradation of viral nucleic acids, manipulation of the cell cycle, and recruitment of immune cells (De Andrea et al., 2002). The IFN response is therefore an important cellular defense against viral infection.

In order to establish successful viral replication, adenovirus employs multiple mechanisms to dismantle IFN signaling at various steps of the IFN pathway. The first of these methods to be defined was inhibition of the RNA-activated protein kinase (PKR) by a viral non-coding RNA called viral associated RNA, or VA-RNA I (Kitajewski, Schneider, Safer, Munemitsu, et al., 1986; Kitajewski, Schneider, Safer, & Shenk, 1986; Mathews & Shenk, 1991; Thimmappaya, Weinberger, Schneider, & Shenk, 1982). PKR exists as an inactive monomer in the absence of infection. During viral infection, PKR can recognize double-stranded RNA species generated by viral transcription. Recognition of dsRNA leads to dimerization, autophosphorylation, and activation of PKR (Cole, 2007; Dey et al., 2005; F. Zhang et al., 2001). In addition, PKR is an ISG and is therefore upregulated in response to IFN signaling (Mathews & Shenk, 1991). Activated PKR phosphorylates eIF-2α, which results in inhibition of translation as a method to block viral protein synthesis. During adenovirus infection, VA-RNA I binds PKR and prevents its activation to avoid phosphorylation of eIF-2a and subsequent translational inhibition (Kitajewski, Schneider, Safer, Munemitsu, et al., 1986; Thimmappaya et al., 1982). Another strategy used by adenovirus to lessen the impact of the IFN response is through E1A-mediated suppression of ISG expression (K. P. Anderson & Fennie, 1987; Fonseca et al., 2012). Infection of an E1A-deleted mutant into cells pre-treated with IFN resulted in dramatically reduced viral yield compared to wild-type virus, which is refractory to IFN treatment. Furthermore, this effect was found to be independent of the effects of VA-RNA I on PKR

(K. P. Anderson & Fennie, 1987), demonstrating distinct mechanisms used by adenovirus to evade IFN signaling. The ability of E1A to subvert effects of IFN signaling is dependent on N-terminal binding to hBre1, a cellular E3 ubiquitin ligase that is responsible for the transcription activating monoubiquitination of histone H2B at ISGs (Fonseca et al., 2012). Another viral protein expressed from the E1 region of the genome, E1b55K, has also been shown to suppress transcription of ISGs (Chahal, Qi, & Flint, 2012; Miller, Rickards, Mashiba, Huang, & Flint, 2009). By comparing microarray analyses from cells infected with either wild-type or E1b55K-deleted virus, it was found that the absence of E1b55K during infection resulted in higher levels of ISG transcripts (Miller et al., 2009). This suggested that E1b55K suppresses ISG expression. Consistent with this finding, E1b55K-deleted viruses were significantly impaired when cells were pre-treated with IFN. In the presence of IFN treatment, E1b55K-deleted viruses had lower viral yields and failed to form viral replication centers (Chahal et al., 2012). These effects were found to be independent of other known E1b55K functions, such as association with E4orf6, prevention of apoptosis, and localization to PML tracks (Chahal et al., 2012). Together, these findings demonstrated that both E1A and E1b55K can suppress ISG expression. The mechanism by which E1b55K regulates ISG expression remains to be uncovered, but E1A has been shown to regulate transcription of ISGs through histone PTMs. While E1A and E1b55K each regulate ISG expression, their effects do not appear to be redundant, as deletion of either E1A or E1b55K results in increased sensitivity to IFN treatment (K. P. Anderson & Fennie, 1987; Chahal et al., 2012; Fonseca et al., 2012; Miller et al., 2009). It is possible that the effects of E1A and E1b55K are cell-type dependent, or that they regulate distinct ISGs. An additional mechanism suggested to counter IFN is through E4orf3-mediated disruption of PML bodies (Ullman & Hearing, 2008; Ullman et al., 2007). E4orf3-deleted viruses were

shown to be defective for replication in the presence of IFN (Ullman et al., 2007). However, E1A levels were also decreased under these conditions (Ullman et al., 2007). Since E1A contributes to suppression of the IFN response (K. P. Anderson & Fennie, 1987; Fonseca et al., 2012), the inability of an E4orf3-deleted virus to overcome the IFN response could be an indirect effect of decreased E1A levels. As a result, the role for E4orf3 in suppressing the IFN response during infection remains unclear. The authors also demonstrated that expression of an E4orf3 mutant unable to disrupt PML bodies did not rescue the defect of the E4orf3-deleted virus in the presence of IFN (Ullman et al., 2007), supporting their conclusion that disruption of PML is necessary for adenovirus to overcome IFN. Furthermore, PML depletion restored replication of the E4orf3-deleted virus in IFN-treated cells (Ullman & Hearing, 2008). Depletion of cellular DAXX, which is found in PML bodies, similarly rescued the replication defect of E4orf3-deleted virus in the presence of IFN (Ullman & Hearing, 2008). These data suggest that E4orf3 reorganization of PML bodies allows adenovirus to overcome effects of IFN by inhibiting the interferon-induced proteins, PML and DAXX. However, the decreased E1A levels observed during infection with the E4orf3-deleted virus in IFN-treated cells confound interpretation of these findings. Together, these works demonstrate that adenovirus has evolved to suppress multiple steps of the IFN pathway, including ISG expression (through E1A and E1b55K-mediated effects on transcription) and ISG activity (through VA-RNA inhibition of PKR and E4orf3-mediated disruption of PML and DAXX).

Thesis goals

The adenovirus life cycle relies on the careful regulation of cellular proteins with viral genomes. As described in this chapter, viral proteins recruit transcription factors, chromatin remodeling complexes, and topoisomerase to promote viral DNA replication and transcription. At the same time, adenoviruses prevent association of anti-viral

proteins with viral genomes by manipulating cellular pathways through several strategies, including protein degradation, viral mimicry, and suppression of cellular transcription. We aimed to identify novel DNA-protein interactions and mechanisms used by adenoviruses to control the cellular proteins that associate with their genomes. In the following chapters, I describe two distinct strategies we used to study these interactions. In **Chapter 2**, we compared interactions of several evolutionary distinct adenovirus serotypes with the cellular DNA damage response, which has been shown to respond to viral DNA and restrict Ad5 replication. Comparing multiple serotypes allowed us to uncover different interactions with the known anti-viral MRN complex and suggested that some serotypes utilize unidentified mechanisms to target this cellular complex. In **Chapter 3**, we employed proteomics to identify novel interactions between cellular proteins and adenovirus DNA. Furthermore, we identified new functions for the viral DNA-binding protein VII in regulating host proteins associated with both viral and cellular DNA. We also present evidence supporting a role for protein VII in suppressing the IFN response, potentially by blocking binding of a DNA sensor with viral DNA. Together, results from **Chapters 2** and **3** demonstrate the significance of DNA-protein interactions in controlling viral infection and highlight how different strategies can be used to study these interactions.

Figures

Figure 1.1

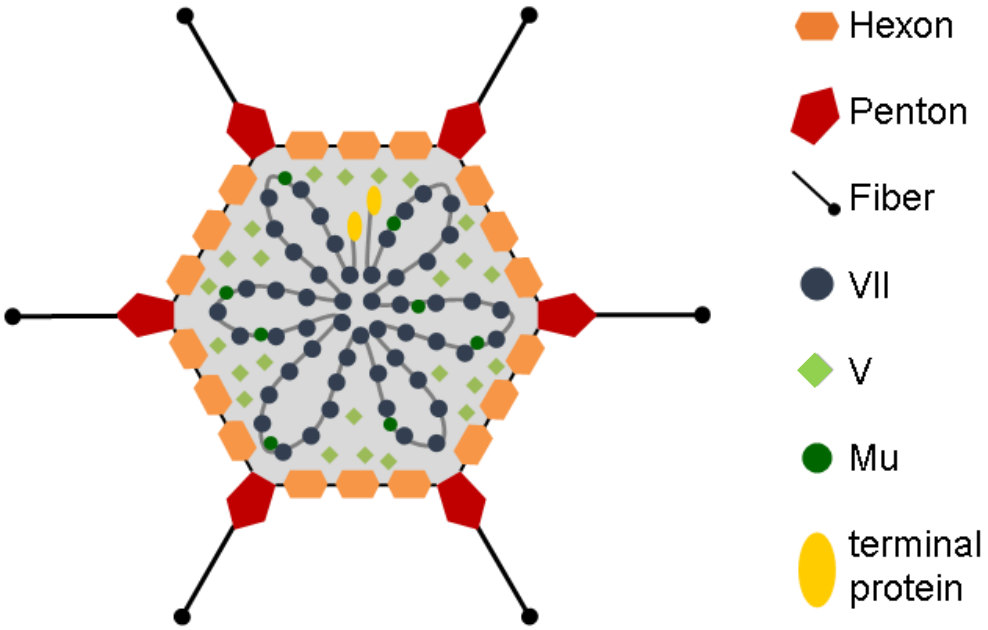

Figure 1.1: Adenovirus capsid and core proteins. Hexon, penton, and fiber comprise the viral capsid. Protein VII is associated with viral genomes and is the most abundant core protein. Terminal protein is bound to the 5' end of each DNA strand. Protein V and mu are additional core proteins. *Figure courtesy of Christin Herrmann.*

Figure 1.2

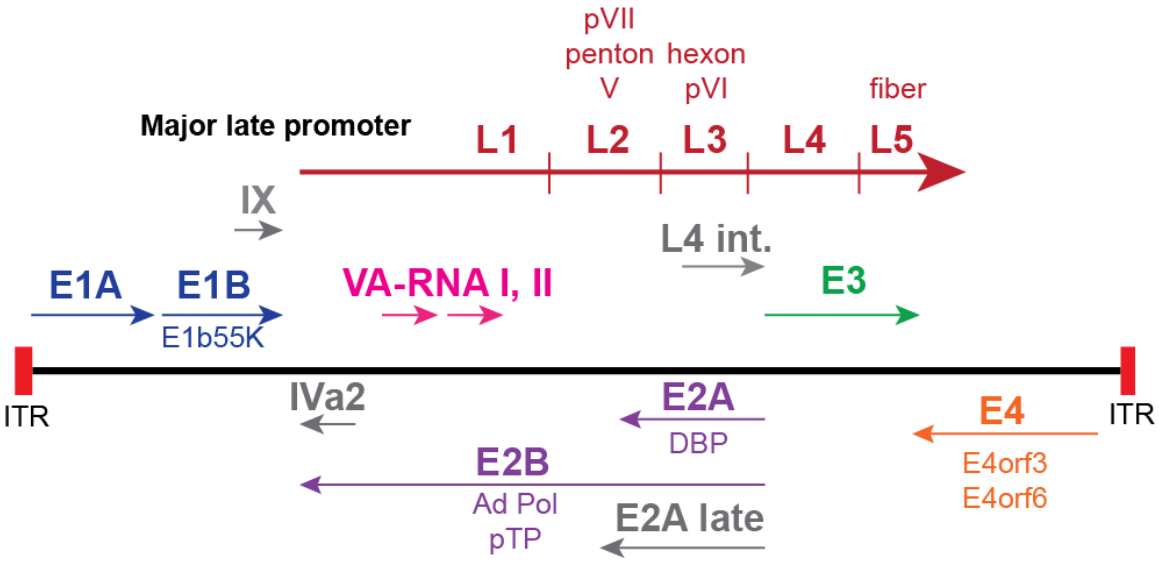

Figure 1.2: Adenovirus genome and transcription units. Inverted terminal repeats (ITR) are found at each end of the genome. Early proteins are expressed from E1 (blue), E2 (purple), E3 (green), and E4 (orange) transcription units. Late proteins are expressed from one transcription unit (red) under the control of the major late promoter. Intermediate transcription units are in grey. In addition, non-coding RNAs, VA RNA I and VA RNA II (pink) are expressed. Viral proteins discussed in the thesis are listed in the schematic next to the transcription unit from which they are expressed.

Figure 1.3

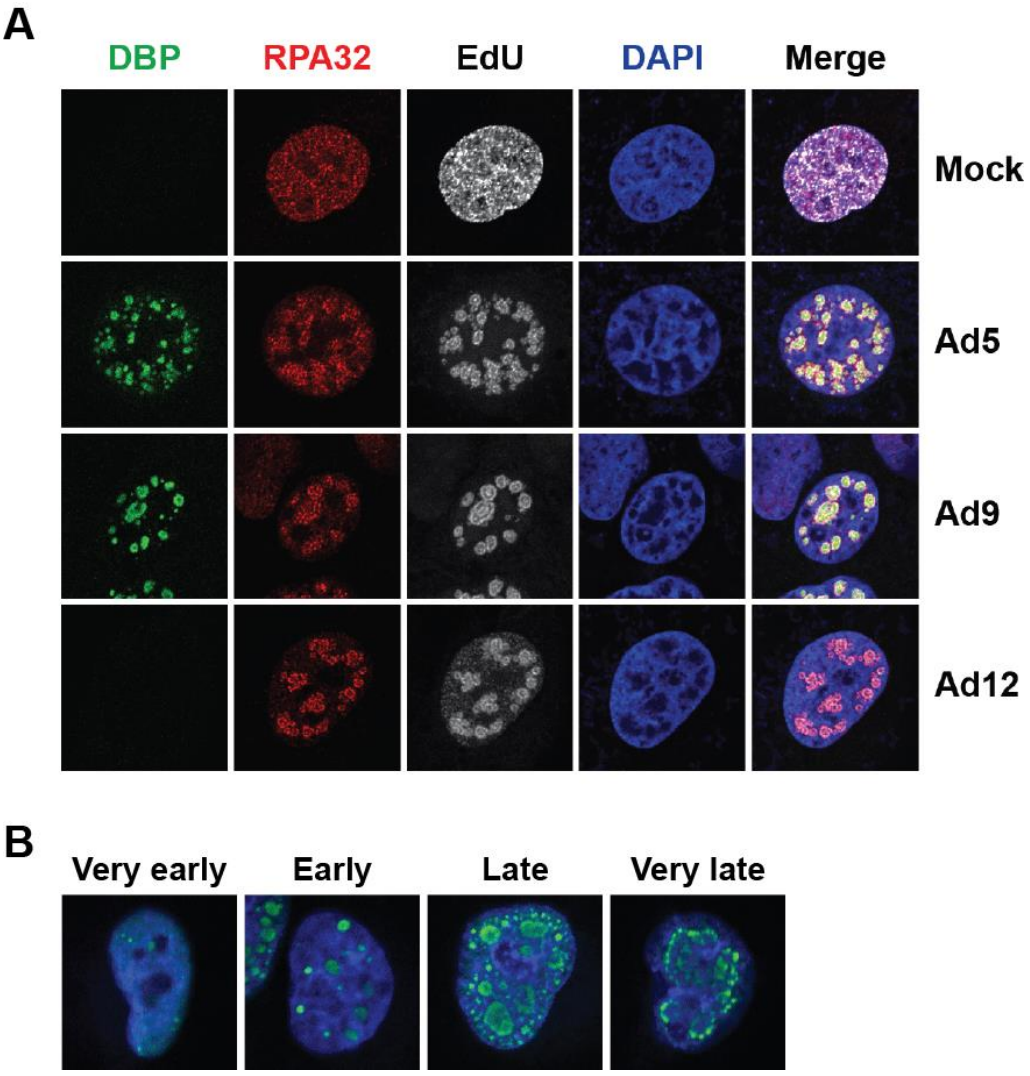

Figure 1.3: Viral replication centers. (A) Images of viral replication centers from adenovirus-infected cells. DBP is a viral DNA replication protein that accumulates at sites of single-stranded viral DNA and marks viral replication centers. RPA32 is a cellular single-stranded DNA-binding protein and also marks viral replication centers. EdU is a thymidine analog that is incorporated into replicating DNA. Colocalization of DBP, RPA32, and EdU demonstrate that any of these methods can be used to visualize viral replication centers. **(B)** Representative images from different stages of Ad5 infection. Viral replication centers change as infection progresses.

Figure 1.4

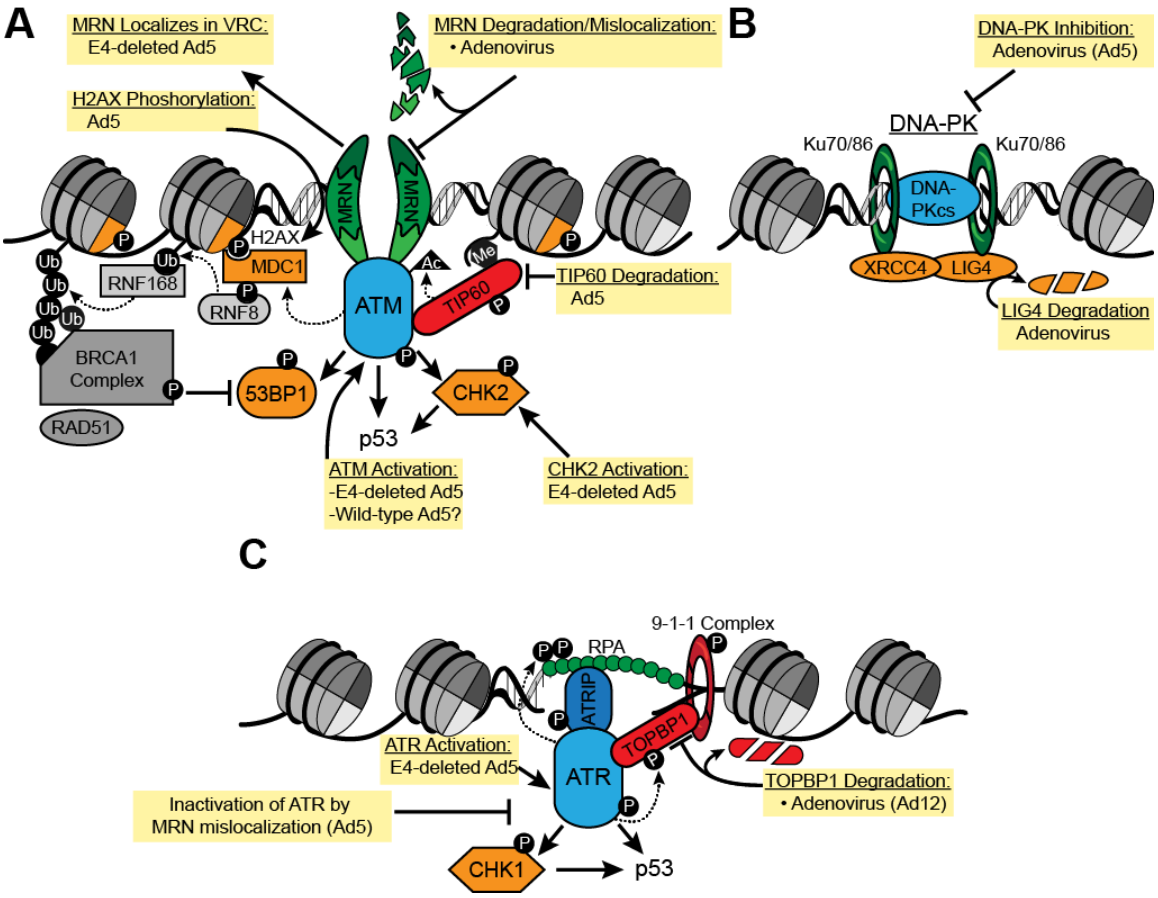

Figure 1.4: Adenovirus manipulates several steps of the DNA damage response. (A) ATM signaling is activated in response to double-strand DNA breaks (DSBs). The MRN sensor responds to DSBs and activates ATM auto-phosphorylation and phosphorylation of downstream substrates. Wild-type Ad5 mislocalizes and degrades MRN and degrades Tip60. Some reports demonstrate that wild-type Ad5 inhibits ATM activation, while other reports demonstrate widespread ATM activation during late stages of infection. **(B)** Signaling through DNA-PK is activated by recognition of DSBs by the Ku70/Ku80 complex and results in DNA repair by non-homologous end joining. Adenovirus suppresses the DNA-PK pathway in multiple ways. All serotypes examined

to date can degrade DNA ligase IV. **(C)** The ATR pathway responds to prolonged exposed single-stranded DNA. Wild-type Ad5 mislocalizes MRN, which prevents ATR activation. Ad12 degrades TOPBP1.

Figure 1.5

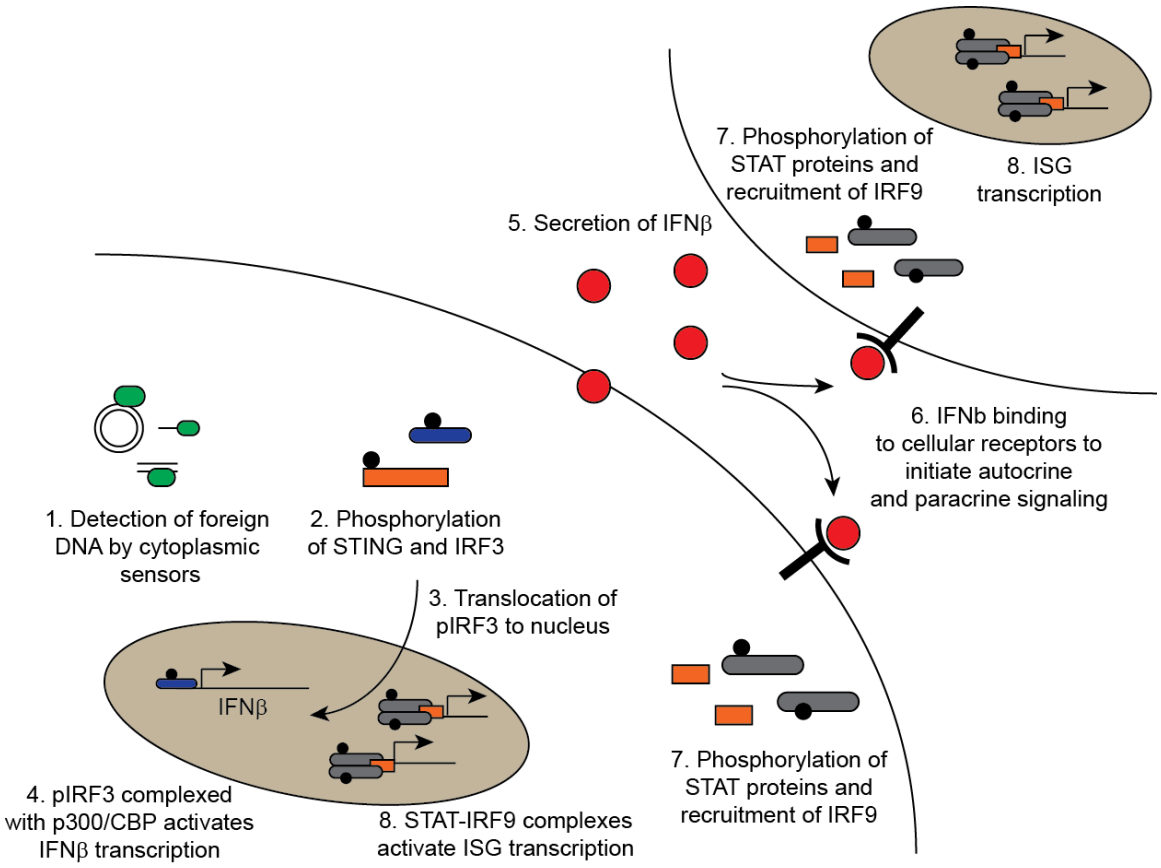

Figure 1.5: Overview of interferon signaling. Cytoplasmic DNA sensors recognize viral DNA, which leads to activation of STING and interferon regulatory factor 3 (IRF3). IRF3 translocates to the nucleus where it activates transcription of IFNβ. Newly synthesized IFNβ protein is released from the infected cell and binds cellular receptors on the infected and adjacent cells. This activates JAK-STAT signaling and expression of interferon-stimulated genes in infected and adjacent cells. The protein products of ISGs impair viral processes through multiple mechanisms.

CHAPTER 2:

Serotype-specific restriction of wild-type adenoviruses by the cellular Mre11-Rad50-Nbs1 complex

Portions of this chapter are currently in press:

> **Pancholi, N.J.** and Weitzman, M.D. Serotype-specific restriction of wild-type adenoviruses by the cellular Mre11-Rad50-Nbs1 complex. *Virology.* (in press)

A figure from this chapter has been previously published in:

> Lou, D. I.*, Kim, E. T.*, Meyerson, N. R., **Pancholi, N. J.**, Mohni, K. N., Enard, D., . . . Sawyer, S. L. (2016). An Intrinsically Disordered Region of the DNA Repair Protein Nbs1 Is a Species-Specific Barrier to Herpes Simplex Virus 1 in Primates. *Cell Host Microbe*, 20(2), 178-188.

Introduction

It has been well established that the DDR is an obstacle for wild-type Ad5 replication and that Ad5 employs redundant mechanisms to evade its negative effects (see Chapter 1). However, there has been relatively little research into the interactions between other adenovirus serotypes and the DDR. Analysis of known Ad5 degradation substrates during infection with other Ad serotypes revealed that all serotypes examined to date lead to degradation of DNA ligase IV (Forrester et al., 2011). In contrast, some serotypes appear not to degrade MRN, p53, or integrin α3, and only Ad12 has been found to degrade the DDR regulatory protein TOPBP1 (Blackford et al., 2010; Bridges et al., 2016; Cheng et al., 2011; Forrester et al., 2011). Interestingly, substrate degradation by non-Ad5 serotypes does not always correlate with interaction with E1b55K (Cheng et al.,

2013), suggesting that degradation of host proteins by adenoviruses may be regulated in additional unknown ways. Furthermore, infection with some serotypes does not result in MRN mislocalization to tracks or to aggressomes (Blanchette, Wimmer, Dallaire, Cheng, & Branton, 2013; Forrester et al., 2011; Stracker et al., 2005). These findings demonstrate that although the ability to evade recognition by MRN is critical for optimal wild-type Ad5 replication, this may not necessarily be representative across the whole adenovirus family.

Since cellular restriction factors can influence tissue tropism and virulence, we reasoned that there may be differences among serotypes in their ability to overcome MRN inhibition. While previous studies have demonstrated that some serotypes do not degrade or mislocalize MRN, it remains unknown how the different interactions with MRN impact virus replication. Given the importance of inactivating MRN and downstream responses during wild-type Ad5 replication, it is possible that virulence and/or tissue tropism of adenoviruses are partially influenced by their potential to evade inhibition by MRN. Furthermore, it is unclear whether MRN targeting by other serotypes is accomplished by the analogous viral proteins as Ad5. Here, we examined more closely the fate of MRN during infection with multiple adenovirus serotypes representing several subgroups, and we determined the impact on wild-type viral DNA replication. Consistent with previous reports (Cheng et al., 2011; Forrester et al., 2011), we identified serotypes that target MRN through both degradation and mislocalization, and other serotypes incapable of one or both of these mechanisms. We found that serotypes Ad9 and Ad12 can target MRN by mislocalization or degradation but are still impaired for DNA replication, demonstrating differences between these serotypes and Ad5. By examining the viral proteins that target MRN, we found that Ad9-E4orf3 alone is not sufficient to induce MRN mislocalization even though it is observed during Ad9 infection,

suggesting that MRN mislocalization by Ad9 may be regulated through additional viral mechanisms. This work adds to our growing understanding of adenoviruses and the DDR, and suggests that diverse strategies have evolved across the adenovirus family to overcome MRN during wild-type virus infections.

Materials and Methods

Cell lines

U2OS were purchased from the American Tissue Culture Collection. Immortalized NBS cells (ILB1) transduced to express Nbs1 or empty vector were previously described (Cerosaletti et al., 2000; Kraakman-van der Zwet et al., 1999). Immortalized A-T cells (AT22IJE-T) and matched cells complemented with ATM as previously described were gifts from Y. Shiloh (Ziv et al., 1997; Ziv et al., 1989). All cells were maintained in Dulbecco modified Eagle medium (Corning MT10-013-CV) supplemented with 10% fetal bovine serum and 1% penicillin-streptomycin (Invitrogen 15140122) at 37°C in a humidified incubator with 5% CO_2. Acceptor cells for the generation of doxycycline-inducible cell lines were provided by E. Makeyev and were used as previously described (Khandelia, Yap, & Makeyev, 2011). Briefly, FLAG-Ad9-E4orf3 was PCR amplified from the pL2-FLAG-Ad9-E4orf3 plasmid described below and inserted into the inducible plasmid backbone. The inducible plasmid containing FLAG-Ad9-E4orf3 was transfected into U2OS acceptor cells together with a plasmid expressing the Cre recombinase. Recombined clones were selected with 1 μg/mL Puromycin. Cells were induced with 0.2 μg/mL doxycycline for 24 hours to express FLAG-Ad9-E4orf3. Expression was confirmed by immunoblot and immunofluorescence. Inducible cells were maintained in medium supplemented with tetracycline-free fetal bovine serum.

Plasmids and transfections

The Ad9-E4orf3 cDNA was obtained from cells infected with Ad9, PCR amplified, and cloned into the pL2-FLAG plasmid backbone (described in (Stracker et al., 2005)). Transfections were performed using the standard protocol for Lipofectamine 2000 (Invitrogen).

Viruses and infections

Wild-type Ad5, Ad2, Ad4, Ad9, Ad12, and Ad35 were purchased from American Tissue Culture Collection. Mutant Ad5 viruses *dl*1004, *dl*110, and *dl*1006 were previously described (Babiss & Ginsberg, 1984; Bridge & Ketner, 1989) and were gifts from G. Ketner and D. Ornelles. Wild-type Ad5, Ad2, Ad4, Ad9, Ad12, Ad35, *dl*110, and *dl*1006 were propagated on 293 cells. The E4-deleted virus *dl*1004 was propagated on W162 cells. All viruses were purified by two sequential rounds of ultracentrifugation of cesium chloride gradients and stored in 40% glycerol at -20°C. Viral titers were determined by plaque assay on 293 cells. Infections were carried out by standard protocols using a multiplicity of infection of 20 (Ad5 wild-type and mutants, Ad2, Ad4, Ad12, Ad35) or 50 (Ad9). Viruses were diluted in Dulbecco modified Eagle medium supplemented with 2% fetal bovine serum and 1% penicillin-streptomycin and added to cell monolayers. Cells were incubated with the virus for 2 hours at 37°C before supplementing infection medium with medium containing 10% fetal bovine serum.

Antibodies and inhibitors

Primary antibodies to cellular proteins were purchased from commercial sources: Mre11 (Novus NB100-142), Rad50 (GeneTex [13B3] GTX70228), Nbs1 (Novus NB100-143), ATM pS1981 (Epitomics 2152-1 and Abcam [EP1890Y] ab81292), ATM (Abcam [Y170] ab32420 and Epitomics 1549-1), Actin (Sigma a5441), RPA32 (Abcam ab2175 and

Bethyl A300-244A), PML (Santa Cruz [PG-M3] sc-966), and FLAG (Sigma F3165 and F7425). Primary antibodies to adenoviral proteins DBP and E4orf3 were gifts from A. Levine and T. Dobner, respectively. Horseradish peroxidase-conjugated secondary antibodies for immunoblotting were purchased from Jackson Laboratories. Fluorophore-conjugated secondary antibodies for immunofluorescence were purchased from Life Technologies. The ATM kinase inhibitor KU55933 was purchased from Abcam. The proteasome inhibitor MG132 was purchased from Sigma-Aldrich.

Immunoblotting

Immunoblot analysis was carried out using standard methods. Briefly, protein samples were prepared in lithium dodecyl sulfate loading buffer (NuPage) with 10% dithiothreitol and boiled. Equal amounts of protein were separated by electrophoresis. Proteins were transferred to nitrocellulose membranes (GE Healthcare Amersham) and blocked in 5% milk in tris buffered saline with Tween (TBST). Proteins were detected by enhanced chemiluminescence (Thermo Scientific) on film (HyBlot CL) or on a Syngene G-Box.

Immunofluorescence

Cells were plated on glass coverslips. Cells were washed with phosphate buffered saline (PBS) and fixed with cold 4% paraformaldehyde for 15 minutes. Cells were permeabilized for ten minutes with 0.5% Triton X-100 and coverslips were blocked for 1 hour with 3% bovine serum albumin (BSA) in PBS, incubated with each primary antibody diluted in 3% BSA for one hour, and incubated with a mixture of secondary antibodies and 4,6-diamidino-2-phenylindole (DAPI) in 3% BSA for one hour. Coverslips were mounted onto glass slides using ProLong Gold AntiFade Reagent (Life Technologies) and fluorescence was visualized using a Zeiss LSM 710 confocal microscope. Images were processed using ImageJ and Adobe Creative Suite 6.

Virus genome accumulation by quantitative PCR

Cells were infected and harvested by Trypsin at 4 hours post-infection (hpi) and at the times indicated. Total DNA was isolated using the PureLink Genomic DNA kit (Invitrogen). Quantitative PCR was performed using primers specific for a conserved sequence in the viral genome (5' atcaccaccgtcagtgaa and 5' gtgttattgctgggcga) or cellular tubulin (5' ccagatgccaagtgacaagac and 5' gagtgagtgacaagagaagcc). Values for viral DNA were normalized internally to tubulin and externally to the 4 hour time point to control for any variation in virus input. Quantitative PCR was performed using Sybr Green (Thermo) and data were collected using the ViiA 7 Real-Time PCR System (Thermo). At least three biological replicates were included, and statistical analyses were performed with the Prism v7 software (GraphPad).

Results

Effect of adenovirus infection on MRN protein levels and localization

We selected five serotypes to investigate MRN during adenovirus infection, each serotype representing a different adenovirus subgroup. We included Ad2, a subgroup C virus that is closely related to Ad5 (92.6% genome identity), as well as viruses that are less closely related to Ad5: Ad12 (subgroup A, 56.8% genome identity), Ad35 (subgroup B, 63.9% genome identity), Ad9 (subgroup D, 61.0% genome identity), and Ad4 (subgroup E, 61.4% genome identity). We first defined their impact on MRN by examining MRN protein levels by western blot over a time course of infection. We observed that infections for several serotypes progressed at a slower rate than observed for Ad5 (**Figure 2.1**). We therefore examined MRN protein levels up to 72 hours post-infection, when CPE could be observed for all serotypes (**Figure 2.1**). Infections for Ad2, Ad4, Ad5, Ad9, and Ad35 were confirmed by western blot for the viral DNA-binding protein (DBP) (**Figure 2.2A**). The antibody generated against Ad5 DBP does not

recognize DBP expressed from Ad12, and therefore Ad12 infection was instead confirmed by the presence of cytopathic effect (see **Figure 2.1**). We observed that Ad2, Ad4, Ad5, and Ad12 degrade MRN, as indicated by decreased protein levels of Mre11, Rad50, and Nbs1 during infection (**Figure 2.2A**). Ad9 does not degrade MRN, and the protein levels for Mre11, Rad50, and Nbs1 remained steady throughout infection (**Figure 2.2A**). Interestingly, Mre11 and Nbs1 protein levels remained steady throughout infection with Ad35, but Rad50 protein levels were dramatically reduced (**Figure 2.2A**). To confirm that the decrease in Rad50 levels during Ad35 infection was due to degradation, we treated infected cells with the proteasome inhibitor MG132 and compared to results obtained during Ad5 infection (**Figure 2.2B**). MG132 treatment rescued Rad50 levels, suggesting that Ad35 somehow leads to degradation of Rad50 but not Mre11 or Nbs1 (**Figure 2.2B**).

We also examined subcellular localization of Mre11 in relation to viral replication centers (VRCs) by immunofluorescence (**Figure 2.3**). VRCs were visualized using antibodies for viral DBP or cellular RPA32, which are both known to localize to sites of single-stranded adenovirus DNA (Pombo et al., 1994; Stracker et al., 2005). VRCs begin as small foci, which transition to large, pleomorphic structures as viral DNA replication progresses (Pombo et al., 1994). In an asynchronous infection, there will be a mixture of cells with small and large VRCs, depending on the stage of viral replication. We examined Mre11 localization in cells with small and large VRCs to determine how Mre11 localization is affected at different stages of infection. Representative images from early and late stages of infection are shown in **Figure 2.3**. During Ad2, Ad4, Ad9, and Ad5 infections, Mre11 was redistributed to sites distinct from VRCs early during infection (**Figure 2.3**). We previously demonstrated that Nbs1 can colocalize with VRCs during late stages of Ad4 infection, although much of the Nbs1 was reorganized in structures separate from

VRCs earlier during Ad4 infection (Stracker et al., 2005). The results presented here suggest that the effect of infection on Nbs1 localization can differ from that of Mre11. This is consistent with other reports, where Nbs1 was found colocalized with VRCs during late stages of Ad5 infection even though Mre11 was mislocalized to nuclear tracks or degraded (Evans & Hearing, 2005). During late stages, Mre11 was undetectable in Ad2, Ad4, and Ad5 infections, consistent with MRN degradation by these serotypes (**Figure 2.3**). Mre11 was detected during late stages of Ad9 infection but remained sequestered from VRCs. In contrast, during infection with Ad12 and Ad35, Mre11 colocalized with VRCs at early stages of infection, demonstrating that these serotypes do not mislocalize Mre11 (**Figure 2.3**). Mre11 was undetectable at late stages of Ad12 infection, consistent with degradation (**Figure 2.3**), but remained colocalized with Ad35 VRCs late during infection since Mre11 is not degraded by this serotype (**Figure 2.3**). In line with previous reports (Cheng et al., 2011; Forrester et al., 2011; Stracker et al., 2005), we conclude that these representative adenovirus serotypes interact differently with MRN: some serotypes degrade and mislocalize MRN (Ad2, Ad4, and Ad5), and some only degrade (Ad12) or only mislocalize (Ad9) MRN complex members (**Table 2.1**). In the case of Ad35, it appears that this serotype can selectively degrade a single component of the MRN complex without degrading the entire complex (**Table 2.1**). This could be through direct interaction and targeting of Rad50 or indirectly by removal of an additional protein required for its stability within the complex.

ATM is activated during infection with multiple serotypes

Since the MRN complex is required for full activation of ATM in response to DNA breaks (Carson et al., 2003; Paull & Lee, 2005), we examined how differences in MRN manipulation by diverse adenovirus serotypes affect ATM activity. Previous research has shown that ATM substrate KAP1 is phosphorylated during infection with several

serotypes (Forrester et al., 2011), but no studies have examined ATM activation directly or ATM localization during infection with serotypes other than Ad5. We assessed ATM activation by western blot and immunofluorescence using an antibody specific to phosphorylation at serine 1981, the ATM autophosphorylation site (Bakkenist & Kastan, 2003). The E4-deleted Ad5 (dl1004 (Bridge & Ketner, 1989)) served as a positive control for ATM activation (Carson et al., 2003). We found that ATM autophosphorylation increased during infection with all serotypes except Ad5 (**Figure 2.4A and 2.4B**) and that phosphorylated ATM colocalized with DBP or RPA32-stained VRCs (**Figure 2.4A**). These data suggest that ATM is activated in response to viral DNA during infection with these serotypes. Most cells infected with Ad5 did not show ATM activation (representative image, **Figure 2.4A**), although in some cells a small amount of phosphorylated ATM colocalized with VRCs (data not shown). The phosphorylated ATM signal with Ad5 was much less intense than in cells infected with the E4-deleted Ad5 (**Figure 2.4B**). Together, these data suggest that wild-type Ad5 suppresses ATM activation at VRCs, but that ATM signaling is activated during infection with wild-type forms of other serotypes.

MRN impairs DNA replication for Ad9 and Ad12 serotypes

Based on observed differences for MRN components during infection with different wild-type Ad serotypes, we asked to what extent MRN inhibits replication of the different serotypes. To determine whether the observed differences between serotypes affect viral DNA replication, we measured viral DNA accumulation by quantitative PCR in the presence and absence of a functional MRN complex (**Figure 2.5**). NBS-ILB1 cells harbor a hypomorphic Nbs1 mutation that prevents formation of the MRN complex (Kraakman-van der Zwet et al., 1999), and complementation of these cells with wild-type Nbs1 restores MRN complex formation (Cerosaletti et al., 2000). We infected NBS-ILB1

cells (NBS+Vector) and matched cells expressing wild-type Nbs1 (NBS+Nbs1) with each serotype, as well as with Ad5 mutants. As expected, replication of wild-type Ad5 was similar in the presence or absence of the MRN complex (**Figure 2.5A**). We also observed that the presence of Nbs1 did not impact replication of Ad5 mutants that were E1b55K-deleted (dl110 (Babiss & Ginsberg, 1984), retains mislocalization of MRN), or E4orf1-3-deleted (dl1006 (Bridge & Ketner, 1989), retains degradation of MRN). In contrast, DNA replication of complete E4-deleted virus (dl1004 (Bridge & Ketner, 1989)) was inhibited in cells complemented with Nbs1 to generate the functional MRN complex, but was rescued in cells that lack functional Nbs1. This demonstrates that in wild-type Ad5 infection, either mislocalization or degradation of MRN is sufficient to overcome the inhibitory effects of the MRN complex, as previously reported (Lakdawala et al., 2008). Similar to Ad5, both Ad2 and Ad4 were not affected by MRN, since replication was similar in mutant and complemented cells (**Figure 2.5A**). This is consistent with our observation of MRN degradation and mislocalization by both viruses (**Figures 2.2 and 2.3**). Interestingly, Ad35, which does not mislocalize or degrade Mre11, was not impaired in the presence of functional Nbs1. In fact, Ad35 replication significantly decreased in the absence of Nbs1. It was also interesting to observe that replication of Ad9, which mislocalizes but does not degrade MRN, was significantly increased in the absence of functional Nbs1 at multiple stages of infection (**Figure 2.5A-B**). Similarly, replication of Ad12, which degrades but does not mislocalize MRN, was significantly increased in the absence of the functional MRN complex (**Figure 2.5A-B**). We verified that Ad9 and Ad12 retained the ability to manipulate MRN in these cells by examining Mre11 by immunofluorescence (**Figure 2.5C**). Together, these data suggest that serotypes differ in their susceptibility to inhibition by the MRN complex. Ad5, Ad2, Ad4, and Ad35 are not inhibited by MRN. In contrast, MRN impairs replication of Ad9 and

Ad12, despite being targeted by each of these viruses. These data suggest that in contrast to Ad5, neither MRN mislocalization by Ad9 nor MRN degradation by Ad12 is sufficient to overcome inhibition of viral DNA replication by the MRN complex during wild-type virus infection.

ATM does not impair Ad9 or Ad12

Since neither MRN targeting by Ad9 nor Ad12 was sufficient to overcome inhibition by MRN, we investigated these serotypes further to identify potential reasons for their inability to overcome MRN. ATM signaling has been suggested to impair infection of certain Ad5 mutants (Gautam & Bridge, 2013; Shah & O'Shea, 2015). Since ATM signaling is activated during infection by wild-type Ad9 and Ad12 (**Figure 2.4**), we examined whether inhibition of Ad9 and Ad12 by MRN could be due to the downstream effects of ATM activation. To determine the effect of ATM activity on viral replication, we measured viral genome accumulation by quantitative PCR in cells treated with the ATM inhibitor KU55933 (Hickson et al., 2004). ATM inhibition was demonstrated by decreased signals for the autophosphorylation mark at S1981 (**Figure 2.6A-B**). We found that ATM inhibition did not affect accumulation of viral DNA genomes for Ad9 or Ad12 (**Figure 2.6A-B**). We also assessed the impact of ATM by infecting A-T cells, which are ATM deficient, and matched cells complemented with ATM (Ziv et al., 1997; Ziv et al., 1989). Neither Ad9 nor Ad12 DNA replication was impaired by ATM in these cells (**Figure 2.6C-D**). We conclude that ATM does not impair replication of these serotypes, and therefore inhibition of viral DNA replication by MRN is unlikely to be through ATM.

Degradation of MRN by Ad12 occurs similarly to Ad5

We reasoned that mechanistic differences between Ad5, Ad9, and Ad12 targeting of MRN may explain the inability of Ad9 and Ad12 to overcome the inhibitory effects of MRN. We therefore more closely examined MRN mislocalization and degradation by each of these serotypes. We compared MRN degradation between Ad5 and Ad12 to identify any mechanistic differences. We found that Ad12 degradation of MRN is proteasome-dependent (**Figure 2.7A**) and that Ad12-E1b55K and Ad12-E4orf6 are together sufficient to degrade MRN (**Figure 2.7B**). Therefore, MRN degradation by Ad12 appears to occur through a mechanism similar to that of Ad5.

MRN colocalizes with E4orf3 and PML during Ad9 infection

We also compared MRN mislocalization between Ad5 and Ad9 to uncover potential differences. We first compared MRN localization between Ad5 and Ad9. During wild-type Ad5 infection, MRN is colocalized with E4orf3 and PML into nuclear tracks (Stracker et al., 2002). We used an antibody raised against the Ad5-E4orf3 to detect E4orf3 expressed during Ad9 infection by immunofluorescence (**Figure 2.8A**). We found that Ad9-E4orf3 formed nuclear structures similar to those characterized for Ad5-E4orf3 (Carvalho et al., 1995; Doucas et al., 1996). We also found that Mre11 colocalized with E4orf3 during Ad9 infection (**Figure 2.8A**). Immunofluorescence of Ad9 infected cells showed that PML was also disrupted from PML bodies into track-like structures that partially colocalized with Mre11 (**Figure 2.8B**). Staining for Mre11 and Nbs1 showed colocalization into these structures, suggesting that MRN components are redistributed as a complex during Ad9 infection (**Figure 2.8C**). These results suggest that Ad9 disrupts PML and mislocalizes MRN to nuclear structures containing E4orf3 and PML, similar to Ad5.

Ad9-E4orf3 is not sufficient to alter MRN localization

Since Ad5-E4orf3 is sufficient for MRN mislocalization and disruption of PML bodies by transfection (Doucas et al., 1996; Stracker et al., 2002), we investigated the role of Ad9-E4orf3 in MRN mislocalization to PML tracks. We transfected an expression vector for FLAG-tagged Ad9-E4orf3 and found that it formed characteristic track-like structures, although the E4orf3 tracks formed in the absence of infection are notably longer than those formed during infection (**Figure 2.9A,** compare to **Figures 2.8A** and **7B**). Ectopically expressed Ad9-E4orf3 was sufficient to reorganize PML into tracks (**Figure 2.9A**) similar to Ad5-E4orf3. However, we found that Ad9-E4orf3 was not able to alter the localization of MRN, since Mre11 retained a diffuse nuclear pattern when Ad9-E4orf3 was expressed (**Figure 2.9B**). Additional immunofluorescence showed that Mre11 results are representative of all three MRN components (data not shown). FLAG-Ad9-E4orf3 expressed from a doxycycline-inducible cell line was also insufficient to alter Mre11 localization (**Figure 2.9C**). However, the MRN complex colocalized with Ad9-E4orf3 when transfected cells were subsequently infected with Ad9 (**Figure 2.9B**). Together with data from **Figure 2.8**, these observations show that although Ad9 mislocalizes MRN to E4orf3-PML tracks during infection, Ad9-E4orf3 is not sufficient to mislocalize MRN. This suggests that expression of additional viral proteins or viral-induced changes are required for MRN mislocalization by Ad9 during infection.

Single residue site-directed mutagenesis does not affect mislocalization by Ad9-E4orf3

To address potential explanations for the inability of Ad9-E4orf3 to mislocalize MRN when expressed in the absence of infection, we considered a known requirement for mislocalization by Ad5-E4orf3. Our lab previously determined that the isoleucine at residue 104 of the Ad5-E4orf3 is necessary for mislocalization of MRN (Stracker et al.,

2005). When I104 was mutated to arginine, Ad5-E4orf3 was unable to alter the localization of MRN (Stracker et al., 2005). An alignment of the primary sequences of Ad5-E4orf3 and Ad9-E4orf3 demonstrates that the corresponding residue in Ad9-E4orf3 is arginine (R105) (**Figure 2.10A**). We used site-directed mutagenesis to mutate the arginine in Ad9-E4orf3 to isoleucine (R105I) to determine if this residue difference is the reason that Ad9-E4orf3 is not sufficient to mislocalize MRN. We transfected the R105I mutant plasmid and visualized Mre11 localization in transfected cells. We found that both wild-type and mutant Ad9-E4orf3 proteins formed nuclear tracks but did not affect MRN localization (**Figure 2.10B**). We conclude that mutation of residue R105 to isoleucine in Ad9-E4orf3 is not sufficient to enable MRN mislocalization.

Divergent Nbs1 proteins from non-human primates impair E4-deleted Ad5

The work presented thus far has examined the effect of MRN, a host anti-viral protein complex, on adenovirus. However, viral manipulation also affects host proteins since virus-host interactions can influence host evolution as cellular proteins evolve to escape viral antagonism. Therefore, we also investigated the potential for viruses to influence MRN evolution in a collaborative project with Dr. Sara Sawyer. Since MRN influences several viruses (Anacker, Gautam, Gillespie, Chappell, & Moody, 2014; Lilley, Carson, Muotri, Gage, & Weitzman, 2005; Turnell & Grand, 2012; Wu et al., 2004), the Sawyer group analyzed sequences of Mre11, Rad50, and Nbs1 across multiple non-human primate species to identify any evidence of potential positive selection. Multiple sequence alignments demonstrated that Mre11 and Rad50 are highly conserved, but Nbs1 is variable across primate species (Lou et al., 2016). We investigated whether differences in Nbs1 would affect the ability of MRN to impair the E4-deleted Ad5 mutant. We reasoned that if adenovirus had provided positive selection for MRN evolution, then MRN that contains human Nbs1 would be most effective at impairing replication of the

human E4-deleted Ad5. We used human NBS-ILB1 cells (described above) complemented with Nbs1 from human, gibbon, or siamang. We infected NBS-ILB1 and complemented cells with the E4-deleted Ad5 mutant and measured viral DNA accumulation by quantitative PCR (**Figure 2.11**). As expected, cells complemented with human Nbs1 dramatically impaired the E4-deleted Ad5 (**Figure 2.11**). We found that replication of the E4-deleted Ad5 was suppressed to a similar level in cells complemented with gibbon or siamang Nbs1 (**Figure 2.11**). These data demonstrate that the differences between human, gibbon, and siamang Nbs1 proteins do not affect the ability of MRN to impair replication of Ad5. Since the observed differences between human and non-human primate Nbs1 proteins do not confer an advantage in suppressing human adenovirus, the observed sequence variability of Nbs1 between these primate species is unlikely to have been selected for by adenovirus.

Table 2.1

Serotype	Subgroup	MRN degradation	Mre11 mislocalization
Ad12	A	✓	-
Ad35	B	Rad50 only	-
Ad2	C	✓	✓
Ad5	C	✓	✓
Ad9	D	-	✓
Ad4	E	✓	✓

Table 2.1: Summary of MRN degradation and mislocalization during adenovirus infection. Findings from **Figures 2.2** and **2.3** are summarized.

Figures

Figure 2.1

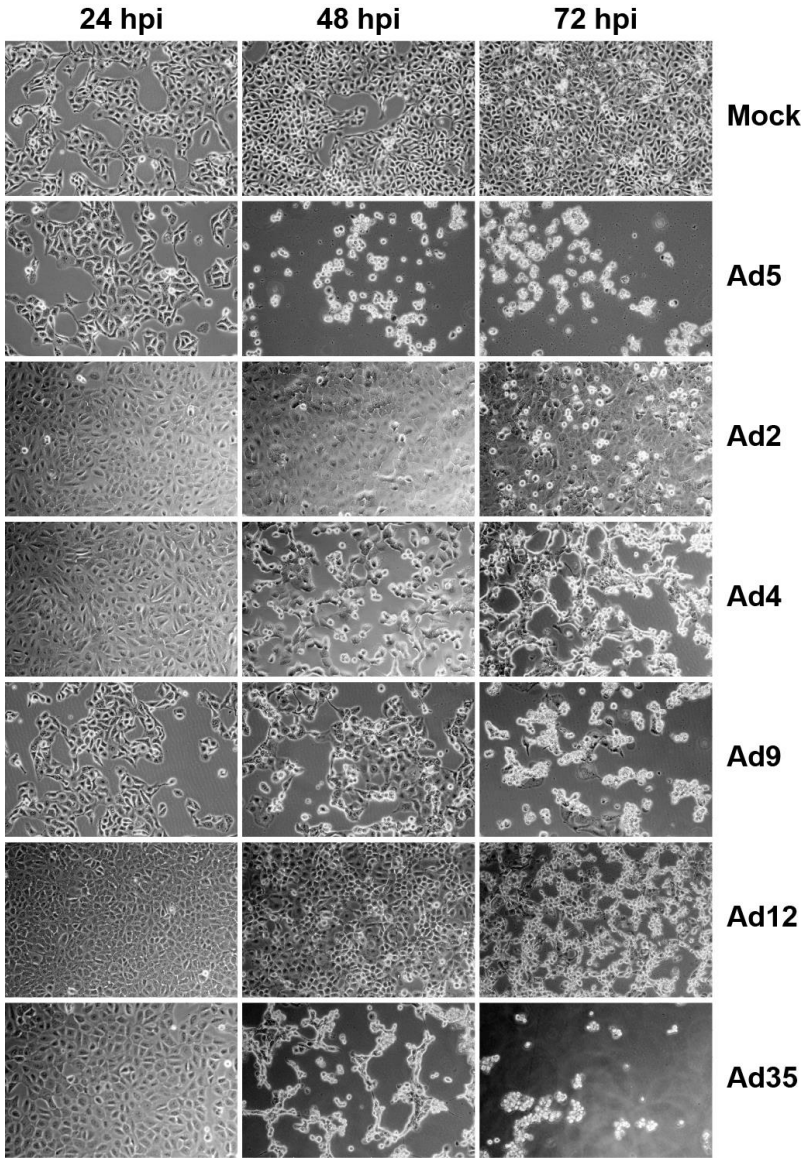

Figure 2.1: Cytopathic effect (CPE) during infection with multiple adenovirus serotypes. Images show cell morphology of mock and infected U2OS cells at the time points indicated. Rounding, clustering, and detachment of cells indicate adenovirus-induced CPE. Ad2, Ad4, Ad9, and Ad12 infection cause CPE at later time points than Ad5.

Figure 2.2

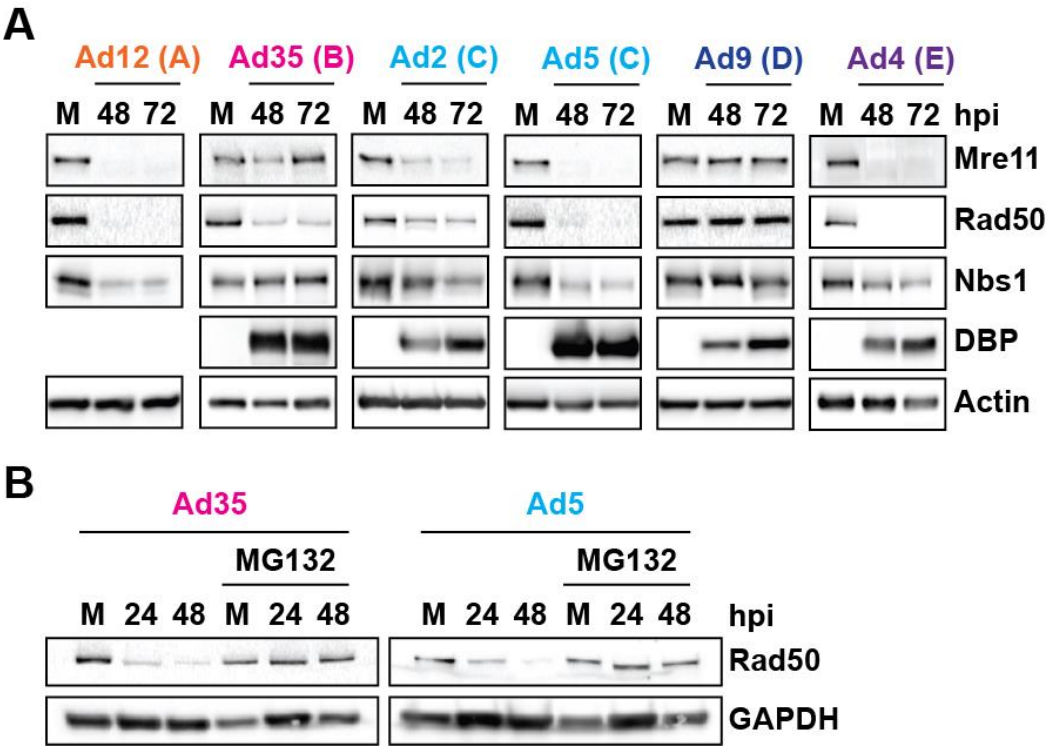

Figure 2.2: Effect of adenovirus infection on MRN protein levels. (A) Western blot analysis of Mre11, Rad50, and Nbs1 using infected cell lysates. U2OS cells were infected with serotypes from subgroups A-E and harvested at 48 and 72 hours post-infection (hpi). Subgroups are indicated in parentheses. Viral DBP confirms infection for all serotypes except Ad12. **(B)** Western blot analysis of Rad50 during Ad35 and Ad5 infection in the presence of the proteasome inhibitor MG132. Cells were treated with 20 uM MG132 or equal volume DMSO 8 hpi and harvested at the indicated time points. MG132 and DMSO were refreshed every 24 hours.

Figure 2.3

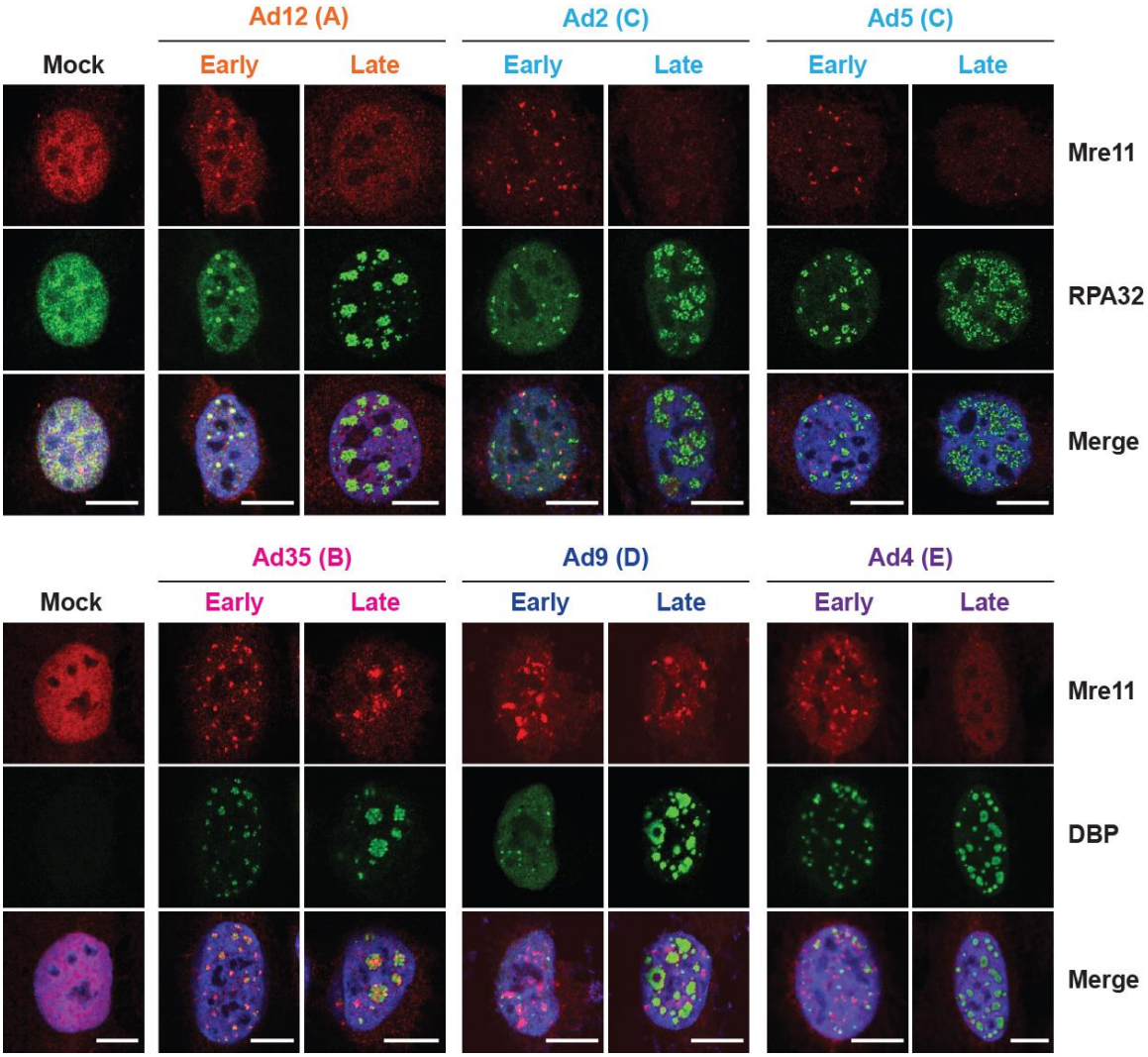

Figure 2.3: Effect of adenovirus infection on MRN localization. Immunofluorescence results of Mre11 (red) during infection of U2OS cells with each serotype at 18-24 hpi. Cellular RPA32 or viral DBP (green) mark viral DNA replication centers (VRC), which enlarge over the course of infection. Representative early and late infection images based on VRC size are shown. Merged images include DAPI stain in blue. Scale bar = 10 μm.

Figure 2.4

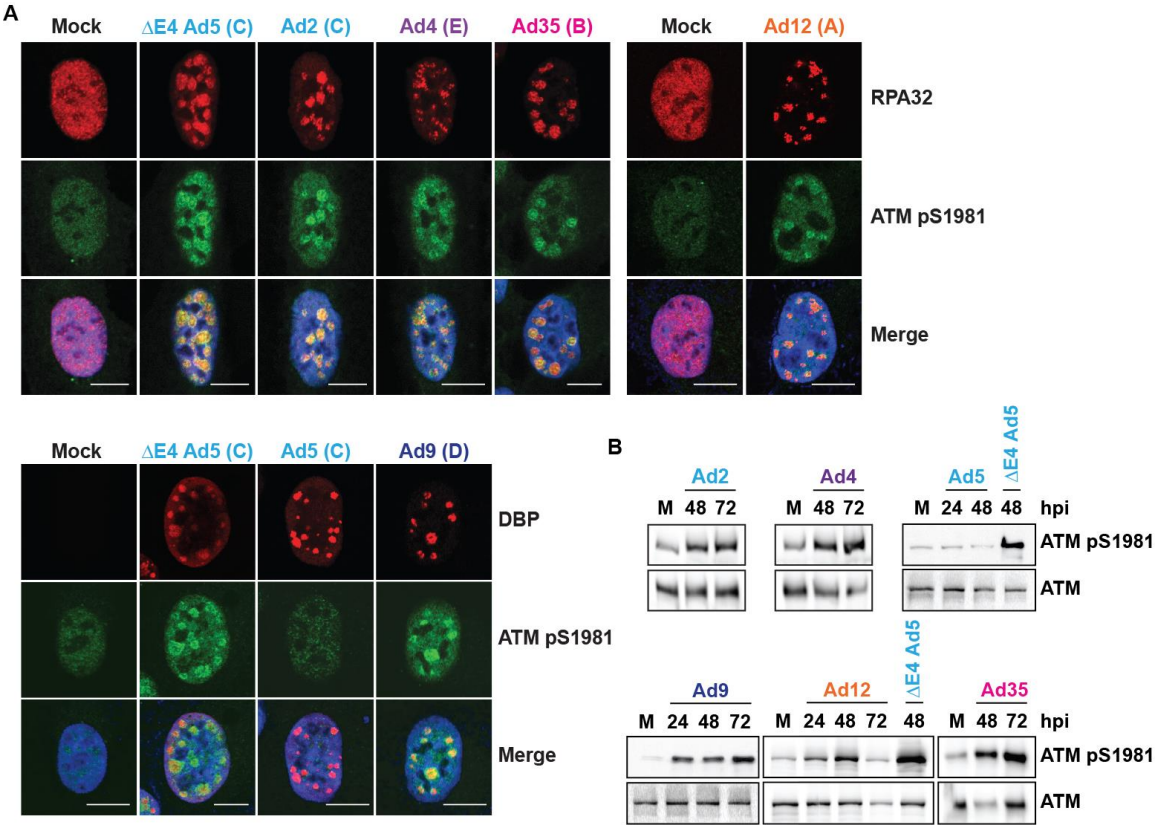

Figure 2.4: ATM is activated during infection with multiple serotypes. (A) Immunofluorescence of phosphorylated ATM (pS1981) (green) during infection of U2OS cells with each serotype at 24 hpi. The E4-deleted Ad5 mutant dl1004 serves as a positive control for ATM phosphorylation. Cellular RPA32 or viral DBP (red) mark sites of viral replication. Merged images include DAPI stain in blue. Scale bar = 10 μm. Representative images are shown. **(B)** Western blots of phosphorylated ATM (pS1981) and total ATM with infected cell lysates. U2OS cells were infected with each serotype and harvested at the indicated time points.

Figure 2.5

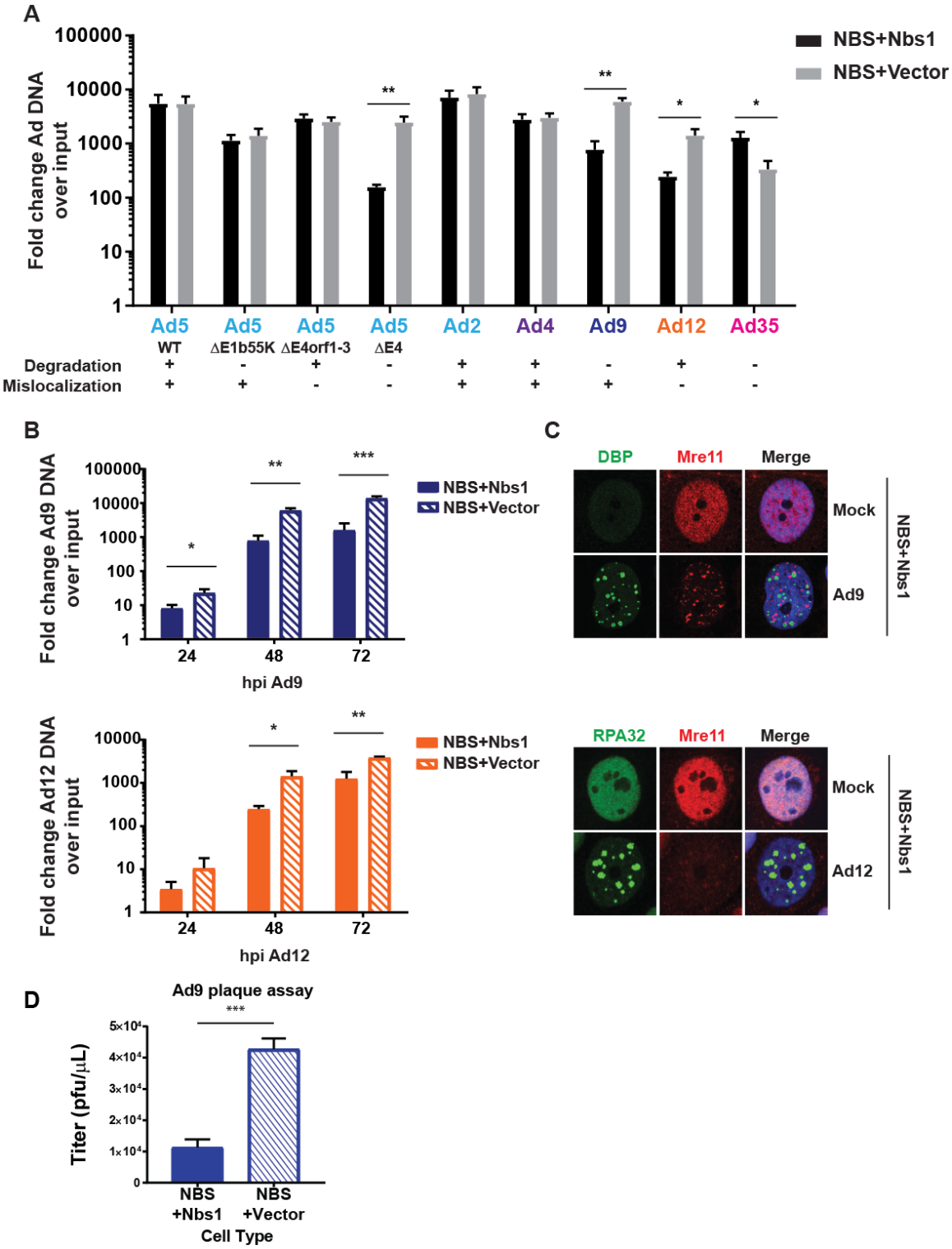
A
Fold change Ad DNA over input
100000
10000
1000
100
10
1
NBS+Nbs1
NBS+Vector
**
**
*
*
Ad5 WT
Ad5 ΔE1b55K
Ad5 ΔE4orf1-3
Ad5 ΔE4
Ad2
Ad4
Ad9
Ad12
Ad35
Degradation + - + - + + - + -
Mislocalization + + - - + + + - -
B
Fold change Ad9 DNA over input
*
**
***
NBS+Nbs1
NBS+Vector
24
48
72
hpi Ad9
Fold change Ad12 DNA over input
*
**
NBS+Nbs1
NBS+Vector
24
48
72
hpi Ad12
C
DBP
Mre11
Merge
Mock
Ad9
NBS+Nbs1
RPA32
Mre11
Merge
Mock
Ad12
NBS+Nbs1
D
Ad9 plaque assay
***
Titer (pfu/μL)
5×10⁴
4×10⁴
3×10⁴
2×10⁴
1×10⁴
0
NBS +Nbs1
NBS +Vector
Cell Type

Figure 2.5: MRN impairs Ad9 and Ad12 replication. (A) Hypomorphic Nbs1 cells complemented with wild-type Nbs1 (NBS+Nbs1) or empty vector (NBS+Vector) were infected to determine the effect of MRN on viral replication. Cells were harvested 48 hpi, and viral DNA accumulation was measured by quantitative PCR using primers specific for a conserved region of the viral genome. Values were normalized internally to tubulin and also to a 4-hour time point to control for input virus. Fold increase over input is shown, and error bars represent standard deviation from at least three biological replicates. Statistical significance was determined by a student's T test (* = $p < 0.05$, ** = $p < 0.01$). **(B)** Viral DNA accumulation was measured in NBS+Vector and NBS+Nbs1 cells as in panel A over a time course of infection with Ad9 and Ad12. MRN impairs DNA accumulation at multiple time points of infection. Error bars represent standard deviation from at least three biological replicates. Statistical significance was determined by a student's T test (* = $p < 0.05$, ** = $p < 0.01$, *** = $p < 0.001$). **(C)** Immunofluorescence of complemented NBS cells (NBS+Nbs1) 48 hpi confirms that Ad9 mislocalizes MRN and that Ad12 decreases MRN levels in these cells. Mre11 is shown in red. Viral DBP and cellular RPA32 (green) mark sites of viral DNA replication, and merged images include DAPI in blue. Scale bar = 10μm. **(D)** Plaque assay results from Ad9 infection in NBS cells. Ad9-infected NBS+Nbs1 or NBS+Vector cells were harvested at 72 hpi, and virus was released by freeze-thaw cycles. Virus titer was measured by plaque assay on 293 cells. Error bars represent standard deviation across three biological replicates. *** = $p<0.001$

Figure 2.6

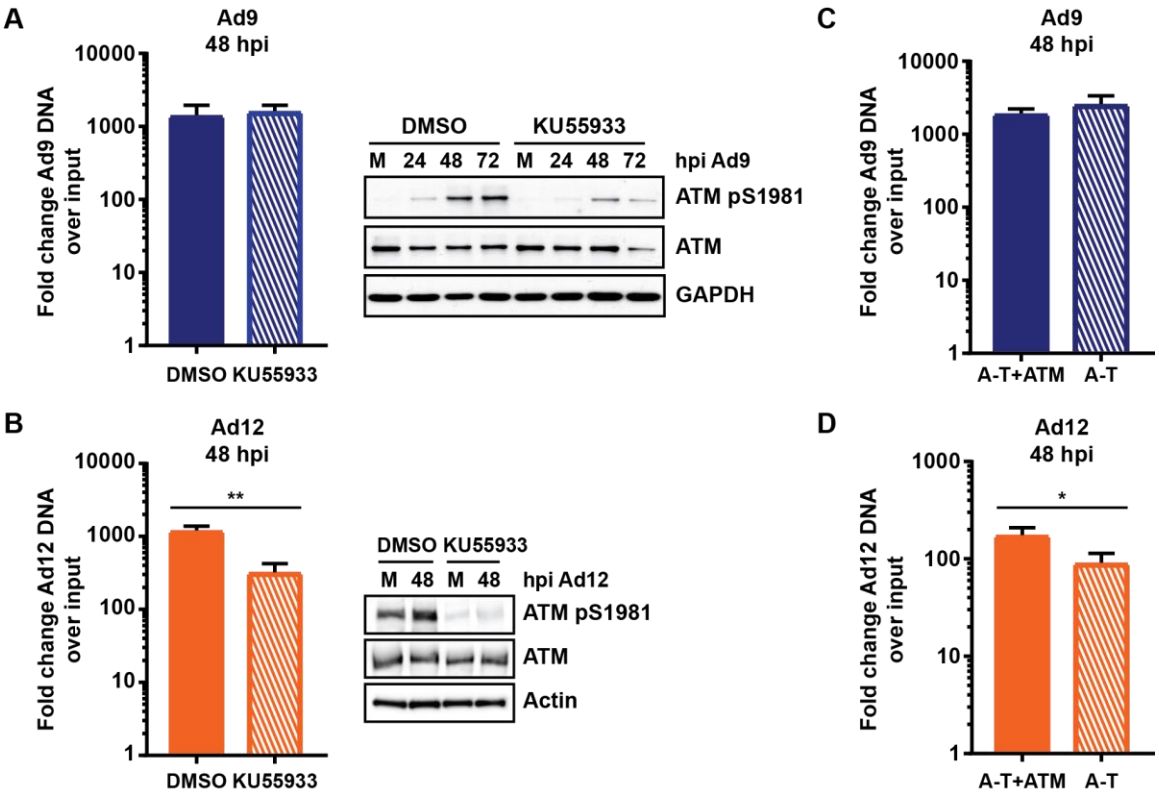

Figure 2.6: ATM does not impair Ad9 or Ad12. (A-B) U2OS cells were treated with the ATM inhibitor KU55933 or DMSO at 1 hour prior to infection with Ad9 **(A)** or Ad12 **(B)**. Cells were harvested 48 hpi and viral genome accumulation measured by quantitative PCR as in **Figure 2.4**. Averages from at least three biological replicates are shown. Statistical analyses were performed using a student's T test. Western blots demonstrate reduced ATM phosphorylation in cells treated with KU55933. **(C-D)** ATM-deficient A-T cells or matched cells complemented with ATM were infected with Ad9 **(C)** or Ad12 **(D)**. Cells were harvested 48 hpi and viral genome accumulation was measured by quantitative PCR as described in **Figure 2.4**. Averages from at least three biological replicates are shown. Statistical significance was determined using a student's T test (* = $p < 0.05$).

Figure 2.7

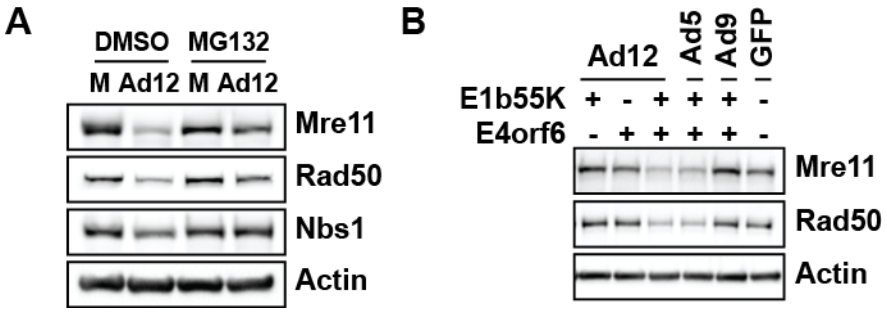

Figure 2.7: Ad12 E1b55K and E4orf6 are sufficient to degrade MRN. (A) Western blot analysis of MRN protein levels during Ad12 infection under proteasome inhibition. U2OS cells were infected with Ad12 and treated with 20uM MG132 or equal volume DMSO at 8 hpi. Cells were harvested 48 hpi. **(B)** Cells were transfected with plasmids expressing E1b55K and/or E4orf6 from Ad12, Ad5, or Ad9 and harvested 24 hours post-transfection.

Figure 2.8

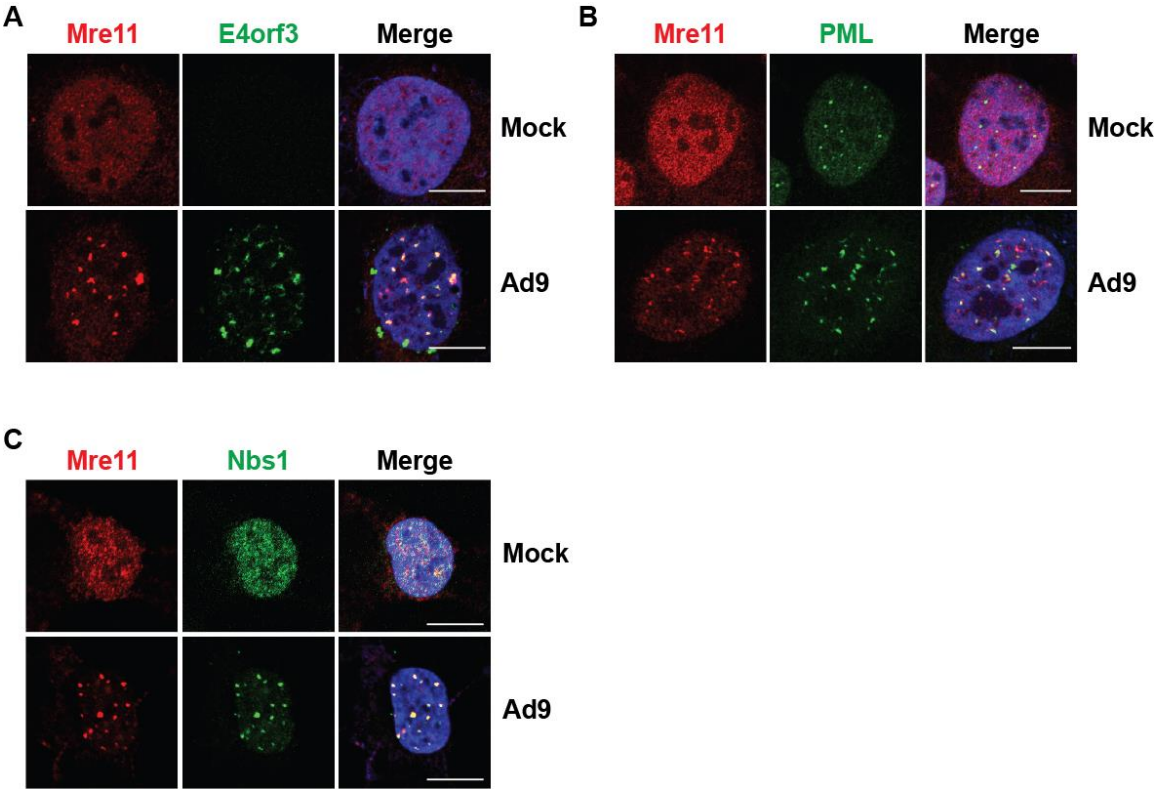

Figure 2.8: MRN colocalizes with E4orf3 and PML during Ad9 infection. (A) Representative immunofluorescence results from Ad9-infected U2OS cells (24 hpi) showing Mre11 (red) and Ad9-E4orf3 **(A)**, PML **(B)**, or Nbs1 **(C)** in green. Merged images include DAPI in blue. Scale bar = 10 μm.

Figure 2.9

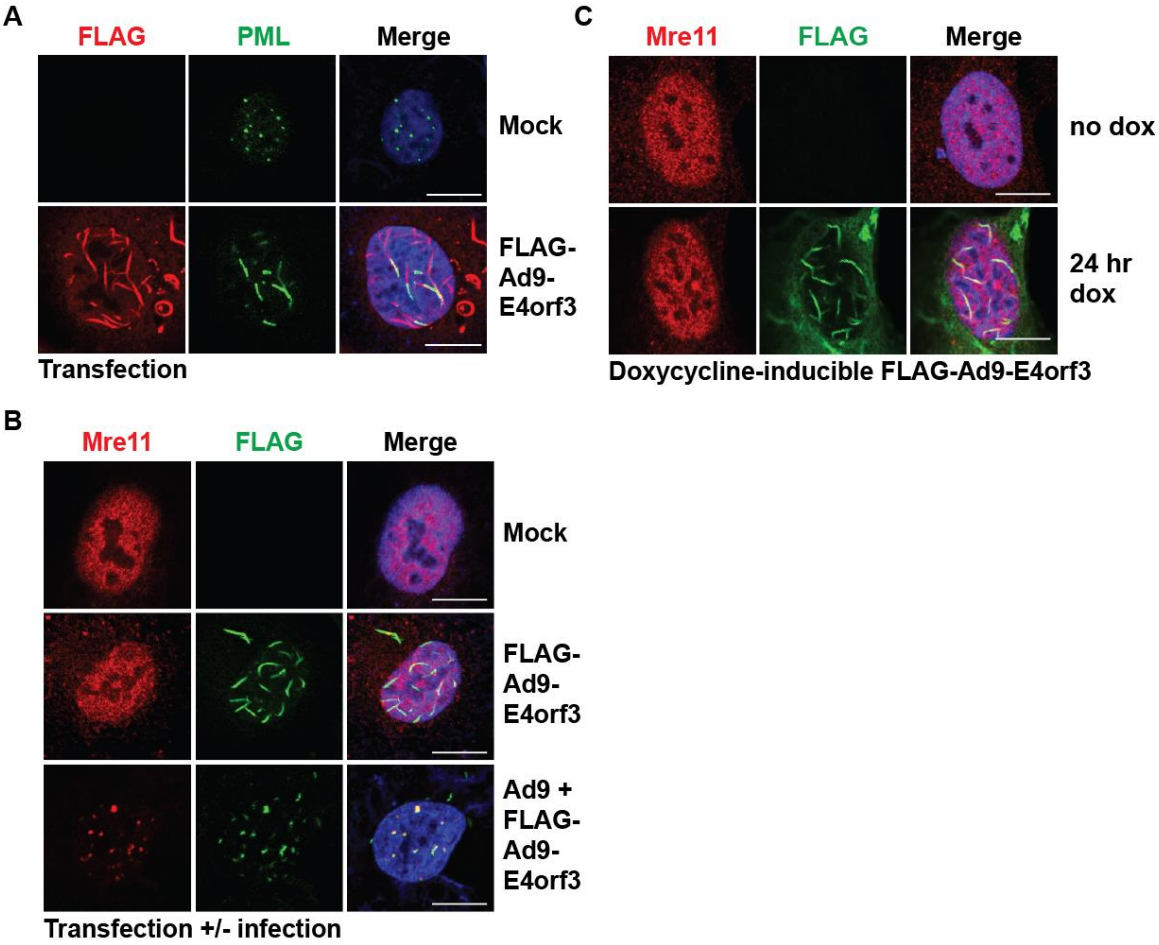

Figure 2.9: Ad9-E4orf3 is not sufficient to alter MRN localization. (A) Immunofluorescence results from U2OS cells transfected with FLAG-tagged Ad9-E4orf3 showing the effect of Ad9-E4orf3 expression on PML (green). Ad9-E4orf3 was visualized using an antibody for FLAG (red). Merged images include DAPI in blue. Scale bar = 10 μm. **(B)** Immunofluorescence of U2OS cells transfected with FLAG-tagged Ad9-E4orf3 with or without Ad9 infection. Cells were transfected 2 hpi and harvested 24 hpi. FLAG-Ad9-E4orf3 is shown in green, Mre11 in red, and merged images include DAPI in blue. Scale bar = 10 μm. **(C)** Immunofluorescence of U2OS cells with doxycycline-inducible FLAG-Ad9-E4orf3. Cells were treated with doxycycline (+dox) for 24 hours. Mre11 is

shown in red, FLAG-Ad9-E4orf3 in green, and merged images include DAPI in blue. Scale bar = 10 μm.

Figure 2.10

A

```
Ad5-E4orf3 MIRCLRLKVEGALEQIFTMAGLNIRDLLRDILRRWRDENYLGMVEGAGMFI
Ad9-E4orf3 MKVCLIMKVEGALWELFHMCGVDLHQQFVEIIQGWKNENYLGMVQECNLMI

Ad5-E4orf3 EEIHP-EGFSLYVHLDVRAVCLLEAIVQHLTNAIICSLAVEFDHATGGERV
Ad9-E4orf3 DEIDGGPAFNVILMLDVRVEPLLEATVEHLENRVGFDLAVCFHQHSGGERC

Ad5-E4orf3 HLIDLHFEVLDNLLE
Ad9-E4orf3 HLRDLHFIVLRDRLE
```

B

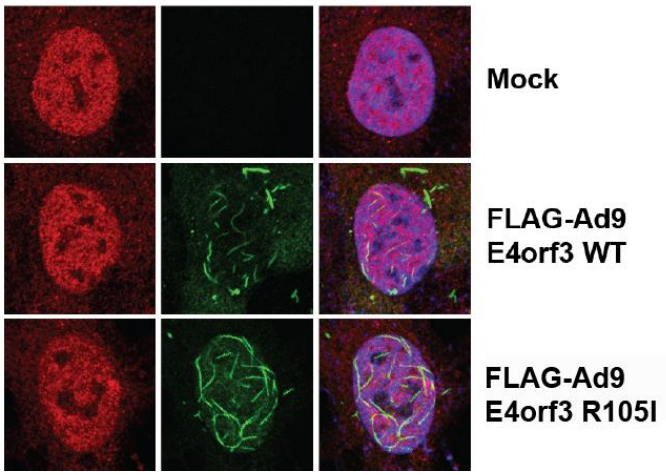

Figure 2.10: Effect of R105I mutation in Ad9-E4orf3. (A) Alignment of the Ad5-E4orf3 and Ad9-E4orf3 primary sequences. Sequences were aligned using the Geneious 6.0.6 software. I104 in Ad5-E4orf3 corresponds to R105 in Ad9-E4orf3. **(B)** Immunofluorescence of U2OS cells transfected with plasmids expressing either wild-type Ad9-E4orf3 or R105I mutant Ad9-E4orf3. Representative images show that Mre11 remains pan-nuclear in cells transfected with wild-type or R105I Ad9-E4orf3. Mre11 is shown in red, FLAG-tagged E4orf3 in green, and merged images include DAPI in blue.

Figure 2.11

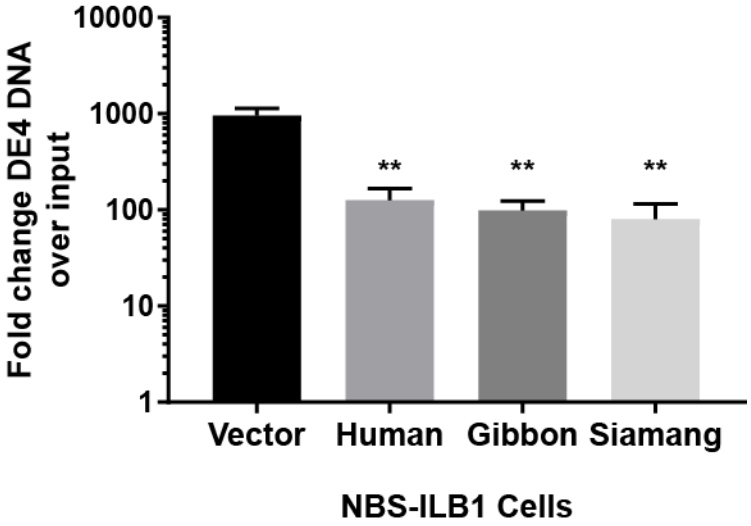

Figure 2.11: Adenovirus replication is not affected by species-specific sequence variation in Nbs1. NBS cells complemented with an empty vector, human Nbs1, siamang Nbs1, or gibbon Nbs1 were infected with the E4-deleted Ad5 mutant, *dl*1004, using MOI 20. Cells were harvested at 4 and 30 hpi. Quantitative PCR was performed using primers specific for the viral DBP gene and cellular tubulin. Values were normalized to the 4 hour time point to control for any variation in input virus. Fold increase over input is shown, and results are an average of three biological replicates. Statistical significance was determined by a student's T test, comparing NBS+Vector cells with each complemented cell type. ** = $p < 0.01$.

Discussion

Cellular proteins can serve as obstacles to virus infection, and viruses have therefore evolved strategies to overcome these intrinsic defenses. Extensive work from our lab and others has demonstrated that proteins within the DDR can inhibit adenovirus DNA replication, late protein production, and viral propagation. In particular, the MRN complex has been suggested to impair viral replication both directly and indirectly through downstream responses (Evans & Hearing, 2005; Lakdawala et al., 2008; Mathew & Bridge, 2007; Shah & O'Shea, 2015; Stracker et al., 2002). The multiple ways that wild-type Ad5 targets the MRN complex have presumably evolved to overcome this inhibition. Previous work has demonstrated that adenovirus serotypes differ in their interactions with MRN and other proteins in the DDR network (Blanchette et al., 2013; Cheng et al., 2011; Cheng et al., 2013; Forrester et al., 2011; Stracker et al., 2005). In this study, we further examined the relationship between MRN and serotypes across the adenovirus family, with representatives from different adenovirus subgroups (A-E). We found that adenovirus serotypes in different subgroups could target MRN complex proteins, suggesting that MRN is a ubiquitous obstacle to viral DNA replication across the adenovirus family. We specifically asked whether adenovirus serotypes differed in their susceptibility to MRN inhibition and found that unlike Ad5, some serotypes are unable to overcome impairment by MRN. Previous work demonstrated that MRN can impair mutants of Ad5 (subgroup C) and Ad4 (subgroup E) that cannot target MRN (Evans & Hearing, 2005; Lakdawala et al., 2008; Mathew & Bridge, 2007). Here, we demonstrate that MRN can also restrict replication of wild-type serotypes from subgroup A (Ad12) and subgroup D (Ad9) (**Figure 2.5**). We were surprised to find that even though Ad9 can redistribute MRN away from viral replication centers, wild-type Ad9 genome levels were significantly reduced in the presence of functional MRN complex (**Figure 2.5**). This

suggests that mislocalization by Ad9 is not sufficient to overcome inhibition by the MRN complex. Results with Ad12 were also unexpected, since MRN significantly impaired wild-type Ad12, despite being degraded during infection. The subgroup B serotype Ad35 did not degrade or mislocalize Mre11, similar to prior findings with other subgroup B serotypes, Ad7 and Ad11 (Forrester et al., 2011). However, another study demonstrated that transfection with E1b55K and E4orf6 from subgroup B serotypes Ad16 and Ad34 leads to a decrease in Mre11 levels (Cheng et al., 2011), raising the possibility that interactions with MRN could vary even within a subgroup. While Ad35 did not degrade or mislocalize Mre11, it did result in Rad50 degradation, demonstrating that this serotype can target a single component of the complex. Surprisingly, degradation of Rad50 did not affect Mre11 or Nbs1 levels, nor did it affect Mre11 localization to VRCs. Interestingly, wild-type Ad35 DNA replication appeared to be enhanced in the presence of MRN formation (**Figure 2.5**). It is possible that Ad35 prevents inhibition of DNA replication by MRN through its degradation of Rad50. However, this alone would not be expected to evade inhibition by Mre11, which localizes to Ad35 VRCs (**Figure 2.3**) and has been suggested to impair adenovirus replication through its nuclease activity (Stracker et al., 2002; Weiden & Ginsberg, 1994). Therefore, it is possible that Ad35 evades inhibition by Mre11 through an alternative, undefined mechanism. Results with Ad35 raise the possibility that Ad35 could even exploit Mre11 or Nbs1 to benefit viral replication, and these observations merit further investigation.

While previous studies have demonstrated that MRN can inhibit replication of mutants of Ad5 that do not manipulate MRN (Evans & Hearing, 2005; Lakdawala et al., 2008; Mathew & Bridge, 2007), we demonstrate for the first time that MRN can inhibit replication of wild-type viruses Ad9 and Ad12 despite the fact that Ad9 and Ad12 alter MRN localization or protein levels. We explored the role of ATM to determine if inhibition

could be through downstream signaling, since ATM can inhibit certain Ad5 mutants (Gautam & Bridge, 2013; Shah & O'Shea, 2015). We first investigated how infection with each of these serotypes affects ATM signaling. As previously reported (Carson et al., 2003), wild-type Ad5 limited ATM activation at VRCs, but infection with the E4-deleted Ad5 mutant dl1004 resulted in robust ATM activation at VRCs (**Figure 2.4**). ATM was activated and colocalized with VRCs during infection with all other serotypes examined (**Figure 2.4**). These data indicate that the ATM activation observed during infection with these serotypes is in response to viral DNA or replication, rather than the global ATM activation sometimes observed during Ad5 infection (Shah & O'Shea, 2015). Since all but one of the serotypes we studied can target MRN through either degradation or mislocalization, ATM activation at VRCs indicates that either (1) ATM is activated independently of MRN during these infections, or (2) there is sufficient residual MRN at VRCs to activate ATM. Pan-nuclear MRN-independent ATM activation has been observed during late stages of wild-type Ad5 infection (Shah & O'Shea, 2015), but MRN is required for ATM activation at Ad5 VRCs (Carson et al., 2003; Shah & O'Shea, 2015). Therefore, we expect that the ATM activation at VRCs is due to residual MRN at VRCs. Furthermore, since MRN inhibited wild-type Ad9 and Ad12, it is likely that there is some MRN at VRCs of these two serotypes. We found that ATM did not impair replication of Ad9 or Ad12 (**Figure 2.6**), excluding the possibility that MRN inhibition of these serotypes is through downstream ATM signaling.

Since wild-type Ad9 and Ad12 viruses did not overcome MRN inhibition of viral DNA replication, we investigated whether mislocalization or degradation by these serotypes occurred through mechanisms different than Ad5. We reasoned that different mechanisms could render these serotypes less effective at evading MRN recognition and overcoming inhibition of viral DNA replication. We found that MRN colocalizes with

Ad9-E4orf3 and PML in nuclear tracks during infection **(Figure 2.8**), similar to MRN localization during Ad5 infection (Stracker et al., 2002). However, unlike Ad5, we found that Ad9-E4orf3 alone was not able to alter MRN localization, even though it was sufficient to disrupt PML bodies (**Figure 2.9**). This difference could explain the inability of Ad9 to overcome MRN. It is possible that during Ad9 infection another viral protein is responsible for MRN mislocalization, either in conjunction with E4orf3 or by itself. The responsible Ad9 protein may only partially sequester MRN from VRCs, allowing sufficient MRN to accumulate at viral DNA and impair virus replication. Another possibility is that Ad9 infection promotes changes to the cellular environment, to MRN, or to E4orf3 that facilitate mislocalization. For example, there could be post-translational modifications to Ad9-E4orf3 or to MRN that occur during infection and promote E4orf3 interaction with MRN. Such a requirement could delay mislocalization until after some MRN had already associated with Ad9 VRCs and inhibited replication. Since Ad12 was also inhibited by MRN during infection despite degradation of MRN proteins, we further examined MRN degradation but were unable to identify any differences between Ad5 and Ad12 degradation in this study (**Figure 2.7**). Previous work has suggested that the ubiquitin ligase formed by Ad12-E1b55K and Ad12-E4orf6 utilizes Cullin 2, in contrast to the Cullin 5 used by Ad5 (Cheng et al., 2011). It is possible that this difference renders Ad12 degradation less effective at overcoming MRN, or that differences in degradation substrates between Ad12 and Ad5 (Blackford et al., 2010; Cheng et al., 2011; Forrester et al., 2011) create distinct cellular environments that influence MRN function. Together, our results demonstrate that interactions of adenovirus serotypes with the cellular MRN complex vary across the viral family. These results may lead to a better understanding of MRN targeting mechanisms, tissue tropism, or viral evolution. The broader implications of this work will be discussed in **Chapter 4**.

CHAPTER 3:

Examining the role of adenovirus core protein VII in regulating proteins associated with viral genomes

Some data from this chapter have been previously published in:

1. Reyes, E. D., Kulej, K., **Pancholi, N. J.**, Akhtar, L. N., Avgousti, D. C., Kim, E. T., . . . Weitzman, M. D. (2017). Identifying host factors associated with DNA replicated during virus infection. *Mol Cell Proteomics*. doi:10.1074/mcp.M117.067116

2. Avgousti, D. C., Herrmann, C., Kulej, K., **Pancholi, N. J.**, Sekulic, N., Petrescu, J., . . . Weitzman, M. D. (2016). A core viral protein binds host nucleosomes to sequester immune danger signals. *Nature*, 535(7610), 173-177.

This chapter incorporates several collaborative projects. As a result, some figures from this chapter were generated by others in the lab and are credited in the figure legends. Work on chromatin manipulation by protein VII was driven by Daphne Avgousti. Adaptation of iPOND to identify cellular proteins on viral genomes was driven by Emigdio Reyes. Mass spectrometry was performed by Kasia Kulej and the CHOP Proteomics Core. Proteomic analyses were performed by Kasia Kulej and Joseph Dybas.

Introduction

Successful viral replication and propagation require the careful regulation of the cellular proteins that interact with viral DNA to allow viruses to recruit beneficial host proteins, while preventing association of anti-viral factors. In this chapter, I describe how we used proteomics to identify cellular proteins associated with viral genomes and how we explored the role of a viral protein in regulating these interactions. This work began as two separate projects in the lab to which I had the opportunity to contribute. The goal of the first project was to identify the host proteins on viral genomes during infection using a technique previously used to isolate proteins interacting with cellular DNA. The second project examined how a histone-like adenovirus protein manipulates the composition of cellular chromatin. Findings from these projects suggested that this histone-like viral protein could influence the association of cellular proteins with adenoviral genomes, which I then explored using the techniques I had learned through my involvement in both projects. Here, I will briefly describe the findings of these projects and how we identified novel functions for a core viral protein.

Materials and Methods

Cell lines

A549, U2OS, 293, mouse embryonic fibroblasts (MEF), hamster kidney cels (HaK), and small airway epithelial cells (SAECs) were purchased from the American Tissue Culture Collection (ATCC). 293 cells engineered to constitutively express Cre recombinase (293-Cre) were a gift from P. Hearing. RA3331 FA-P cells (SLX4-deficient fibroblasts) and matched complemented cells have been previously described (Kim et al., 2011) and were gifts A. Smorgorzewska. HMGB1 knockout cells have been previously described (Avgousti et al., 2017). Most cells were maintained in medium supplemented with 10%

fetal bovine serum and 1% penicillin-streptomycin (Invitrogen 15140122) at 37°C in a humidified incubator with 5% CO_2. Immortalized RA3331 FA-P cells (SLX4-deficient fibroblasts) and matched cells expressing wild-type SLX4 were cultured in DMEM supplemented with 15% FBS, 100 U/ml penicillin, 100 U/ml streptomycin, and non-essential amino acids (Thermo Scientifc). Acceptor cells for the generation of doxycycline-inducible cell lines were provided by E. Makeyev and were used as previously described (Khandelia et al., 2011).

Viruses and infections

Ad5 and HSV-1 were purchased from ATCC. Flox-VII Ad5 was a gift from P. Hearing. MAV-1 was a gift from K. Spindler. Infections were carried out by standard protocols. Wild-type and flox-VII infections were carried out at multiplicity of infection 10 or 20. HSV-1 infections were carried out with an MOI of 3, and MAV-1 infections with an MOI of 1. For most infections, viruses were diluted in medium supplemented with 2% fetal bovine serum and 1% penicillin-streptomycin and added to cell monolayers. For iPOND experiments, viruses were diluted in serum-free medium containing 1% penicillin-streptomycin. Cells were incubated with virus for 2 hours at 37°C before supplementing infection medium with medium containing 10% fetal bovine serum.

Isolation of proteins on nascent DNA

Cell culture: Eight confluent 15-cm plates (approximately 1.6×10^8 cells) were used for each sample. For adenovirus infections, cells were pulsed 24 hours post-infection with 10 mM EdU for 15 minutes at 37C. At the end of the pulse, media was aspirated and cells were fixed by adding 10 mL of 1% paraformaldehyde and incubating for 20 minutes at room temperature. Crosslinking was quenched by adding 1 mL of 1.25 M glycine. Cells were harvested by scraping. Four plates per sample were combined into a single

50 mL conical tube. Cells were pelleted by centrifugation at 900xg for 5 minutes at 4C. Cell pellets were washed twice by resuspending in 20 mL PBS. After the last wash, supernatants were removed, and cell pellets were frozen in liquid nitrogen.

Permeabilization: Frozen cell pellets were thawed on ice and resuspended in 8 mL of permeabilization buffer (PBS+0.25% Triton X-100). Cells were centrifuged at 900xg for 5 minutes at 4C. Pellets were resuspended in 4 mL PBS+0.5% BSA and transferred to 15 mL conical tubes. Cell pellets were washed once more with 4 mL PBS.

Click reactions: Click reactions were prepared in the dark by adding reagents in the following order: 4.35 mL PBS, 0.05 mL Biotin Azide (stock concentration 1 mM), 0.5 mL sodium ascorbate (stock concentration 100 mM, freshly prepared), and 0.1 mL copper sulfate (stock concentration 100 mM). Volumes are per sample and were adjusted accordingly to make master mixes for multiple samples. For “no biotin” controls, 0.05 mL DMSO were added instead of biotin azide. Cells were resuspended in 4 mL click reaction (+/- biotin azide) and incubated for 2 hours by rotating in the dark at room temperature. Cells were then centrifuged for 5 minutes, 900xg, 4C. Pellets were washed once with 4 mL PBS+0.5% BSA and then once with 4 mL of PBS. Supernatants were removed by aspiration to ensure optimal removal of supernatant.

Lysis and capture: Cells were lysed by resuspending in 0.5 mL cold NLB buffer+0.5% Triton X-100 (NLB buffer: 20 mM HEPES pH 7.9, 400 mM NaCl, 1 mM EDTA, 10% glycerol) supplemented with protease inhibitors and 1 mM DTT. Cells were sonicated using a Bioruptor for 20 minutes at 4C with 30 second on/off intervals. Sonication was performed at high intensity. Sonicated samples were transferred to 1.5 mL microcentrifuge tubes and cleared by centrifuging at maximum speed (15000-18000xg), 15 minutes, 4C in a tabletop microcentrifuge. Transfer cleared lysates to fresh tubes.

Remove 50 uL of each sample for input. Add 120 uL streptavidin magnetic beads (pre-washed, 3x, 1mL NLB buffer+0.5% Triton X-100) (Dynabeads M-280, Invitrogen) to each sample. Rotate samples with beads overnight, 4C, in the dark.

Sequential wash steps: 1) Wash beads with 1 mL NLB buffer+0.5% Triton X-100, rotating for 5 minutes at room temperature. 2) Wash beads with 1 mL 1 M NaCl, rotating for 10 minutes, room temperature. 3) Wash beads 4x with 1 mL IC wash buffer (20 mM HEPES pH 7.4, 110 mM KOAc, 2 mM $MgCl_2$, 0.1% Tween-20, 0.1% Triton-X 100, 150 mM NaCl) by rotating 5 minutes each time at room temperature. Transfer beads to fresh tube after third wash step. 4) Wash beads 1x in 1 mL PBS by rotating for 5 minutes at room temperature.

Elution: Resuspend beads of one of two tubes per sample in 60 μL 1X lithium dodecyl sulfate (LDS) buffer (Invitrogen) supplemented with 10% DTT. Elute proteins by boiling at 95C for 10 minutes. Transfer supernatant to second tube of the same tube and repeat boiling step. Transfer supernatant to fresh tubes. Reverse crosslinks by incubating samples at 70C overnight.

Visualization of EdU-labeled DNA

Cells seeded on coverslips were pulsed for 15 minutes with 10 mM EdU at 37C. Pulsed cells were fixed in 4% paraformaldehyde. Cells were permeabilized by incubating in PBS+1% Triton X-100 for 30 minutes at room temperature. Click reaction mixes were prepared as follows per coverslip: 427.5 uL PBS, 12.5 uL AlexaFluor 488 azide (Thermo Scientific) (stock concentration 1 mM, 50 uL sodium ascorbate (stock concentration 100 mM), and 10 uL copper sulfate (stock concentration 100 mM). Cells were incubated with click reaction for 1 hour, rocking, room temperature, in the dark. From this point onward, all steps were performed in the dark. After click reaction incubation, cells were washed

with PBS. Cells were then blocked in 3% BSA and immunofluorescence was carried using standard protocols.

Immunoprecipitation

Anti-HA immunoprecipitation: Two 15-cm plates (approximately $4x10^7$ cells) were used per sample. VII-HA expression was induced by addition of 0.2 ug/mL doxycycline every day for 4 days. Cells were harvested after 4 complete days of induction, and cells were frozen in liquid nitrogen. Cell pellets were thawed on ice and resuspended in 500 uL IC buffer (20 mM HEPES pH 7.4, 110 mM KOAc, 2 mM $MgCl_2$, 0.1% Tween-20, 0.1% Triton-X 100, 150 mM NaCl) supplemented with protease inhibitors (Roche) and transferred to microcentrifuge tubes. Cells were incubated on ice for ten minutes, vortexing every few minutes. After incubating, 5 μL Benzonase nuclease (Novagen/Millipore) was added to each sample, and samples were incubated on ice for 1 hour. Cells were then sonicated for 5 minutes, 30 seconds on/off intervals, 4C, at the highest intensity. Samples were cleared by centrifugation at maximum speed (15000-18000xg), 4C, 15 minutes. Supernatants were transferred to fresh tubes. 50 μL were removed for input. 50 μL pre-washed anti-HA beads (Thermo Fisher) were added to each sample. Samples were incubated for 1 hour at 4C, rotating. Beads were then washed 3x, each time with 1 mL IC wash buffer supplemented with protease inhibitors by rotating for 5 minutes at 4C. Proteins were eluted by resuspending beads in 100 μL HA peptide (Thermo Fisher) and incubating at 37C with shaking for 20 minutes. Supernatants were transferred to new tubes.

Anti-VII immunoprecipitation**:** Two 15-cm plates (approximately $4x10^7$ cells) were used per sample. A549 cells were infected with wild-type Ad5 and harvested at 24 hours post-infection. Lysis and Benzonase treatment were carried out exactly as described above

for anti-HA IP. After clearing lysates and removing input, 50 μL anti-VII hybridoma supernatant (gift from H. Wodrich) were added to each sample. Samples were incubated for 2 hours, 4C, rotating. 50 μL pre-washed protein G beads (Dynabeads Thermo Scientific 10004D) were then added to samples and returned to 4C for overnight incubation with rotation. The next day, beads were washed 3x, each time with 1 mL IC wash buffer supplemented with protease inhibitors by rotating for 5 minutes at 4C. Proteins were eluted by boiling at 95C for 10 minutes in 100 μL 1X LDS sample buffer (Invitrogen) with 10% DTT. Supernatants were transferred to new tubes.

Deletion of protein VII by TAT-Cre

A549 cells were incubated with 0.5-1.5 mg/mL purified TAT-Cre in minimal volume OPTI-MEM (Thermo Scientific) for 1 hour prior to infection. Control cells were incubated with equal volume 50% glycerol in OPTI-MEM. After 1 hour, OPTI-MEM + TAT-Cre/glycerol was removed, but cells were not washed before adding infection mix. Infections were then carried out as usual with flox-VII virus at MOI 10.

Immunofluorescence, immunoblotting, and antibodies

Immunofluorescence and immunoblotting were performed as described in **Chapter 2**. Primary antibodies to cellular proteins were purchased from commercial sources: HMGB1 (Abcam), GFP (Abcam and Millipore), FMR1 (Sigma and Millipore), POLR2E (Sigma), RBM8A (Novus), RNMTL1 (Novus), SLTM (Novus), SNRPE (Abcam), SRP14 (Abcam), RecQL (Santa Cruz, H-110), FUBP1 (Abcam), SPATA5 (Abcam), Cre (Millipore), SRSF1 (Thermo), SLX4 (Novus and Abnova), Flag (Sigma), Actin (Sigma), TCOF (Sigma), GAPDH (GeneTex), TFII-I (Santa Cruz), Rad50 (GeneTex), DDX21 (Abcam), SART1 (Abcam), TRRAP (Abcam), PML (Santa Cruz, PG-M3), histone H1 (Abcam), HA (Covance and Santa Cruz), histone H3 (Millipore), Tubulin (Santa Cruz),

Emerin (Abcam), NUP160 (Abcam), IDH3A (Thermo), phospho-STAT1 (Abcam), STAT1 (Santa Cruz). Primary antibodies to viral proteins were gifts: DBP (A. Levine), protein VII (L. Gerace and H. Wodrich), late proteins (J. Wilson).

Quantitative PCR

Quantitative PCR to measure viral DNA accumulation was performed as described in **Chapter 2.** For reverse transcription quantitative PCR (RT-PCR), RNA was isolated from cells using the RNeasy Micro kit (Qiagen 74004). Reverse transcription was carried out with 0.5-1 ug of RNA using the High Capacity RNA-to-cDNA kit (Thermo Fisher Scientific 4387406). Quantitative PCR was carried out using the standard procedure for Sybr Green (Thermo). Primers: HMGB1 (5' TAACTAAACATGGGCAAAGGAG and 5' TAGCAGACATGGTCTTCCAC), protein VII (5' GCGGGTATTGTCACTGTGC and 5' CACCCAATACACGTTGCCC), ISG15 (5' CAGATCACCCAGAAGATCGG and 5' GCCCTTGTTATTCCTCACCA), MX2 (5' CACATCCATATTTCAGAGTTCTCC and 5' GGTGGCTCTCCCTTATTTGTC), NfkB (5' CTAGCACAAGGAGACATGAAACAG and 5' CCAGAGACCTCATAGTTGTCCA), and IFNβ (5' CAGCATCTGCTGGTTGAAGA and 5' CTAGCACAAGGAGACATGAAACAG).

Interferon stimulation

For stimulation by DNA, cells were transfected with 1 ug/mL poly(dA:dT)/LyoVec (Invivogen tlrl-patc) by adding to regular growth medium. Cells were collected at indicated time points (8 hours post-stimulation for RT-PCR; 6, 12, or 24 hours post-stimulation for western blot). For treatment of cells with ectopic interferon, cells were treated with 1000 units/mL universal type I interferon (PBL Assay Science) and collected 24 hours post-treatment.

Results

Identification of proteins associated with adenovirus DNA by iPOND

In order to identify novel host factors associated with viral DNA, we adapted a technique previously used to isolate and identify proteins that interact with cellular replicating DNA (Sirbu et al., 2013). This technique, called Isolation of Proteins on Nascent DNA, or iPOND, relies on the selective labeling of nascent DNA with the nucleoside analog 5-ethynyl-2'-deoxyuridine (EdU), which is incorporated into actively replicating DNA (Salic & Mitchison, 2008). Since adenovirus infection results in suppression of cellular DNA replication in favor of viral DNA replication (Halbert et al., 1985), we reasoned that pulsing infected cells with EdU would allow for selective labeling of adenoviral DNA over cellular DNA. To test this, we pulsed infected cells with EdU and visualized EdU by immunofluorescence (**Figure 3.1A**). In uninfected cells, EdU was distributed throughout the nucleus marking sites of replicated cellular DNA (**Figure 3.1A**), as has been previously reported (Leonhardt et al., 2000; Nakamura, Morita, & Sato, 1986; Salic & Mitchison, 2008). In contrast, EdU was found in distinct structures resembling viral replication centers (VRCs) when infected cells were pulsed 24 hours post-infection (**Figure 3.1A**). Colocalization of EdU with the viral DNA-binding protein, DBP, confirmed that EdU was found at VRCs (**Figure 3.1A**), demonstrating that EdU is preferentially incorporated into viral DNA during adenovirus infection. We therefore utilized the iPOND protocol in order to identify proteins associated with EdU-labeled adenoviral DNA (illustrated in **Figure 3.1B**). We pulsed infected and mock cells for 15 minutes at 24 hpi. Due to asynchronous replication origin firing and the length of the pulse, EdU was incorporated into replicated DNA throughout the viral genome, rather than strictly at replication forks. This allowed us to identify proteins associated with viral DNA at multiple stages of infection, rather than only those involved in active DNA replication.

After pulsing with EdU, samples were fixed using paraformaldehyde, and the EdU-labeled DNA was biotinylated using click chemistry (Sirbu et al., 2013). Sonication was employed to shear DNA, and the biotinylated, EdU-labeled DNA complexes were isolated using streptavidin beads. Crosslinks were reversed prior to protein elution, and isolated proteins were identified using liquid chromatography-tandem mass spectrometry. We validated our approach by examining if we isolated viral proteins known to associate with viral DNA. We identified 25 viral proteins that were uniquely found or were significantly enriched compared to “no biotin” controls (**Table 3.1**). The viral proteins identified by this approach included expected viral DNA replication proteins, such as DBP and the adenovirus DNA polymerase (Ad Pol), as well as viral proteins involved with transcription and genome packaging (**Table 3.1**). Isolation of known viral DNA-binding proteins validated the use of iPOND to identify proteins associated with viral DNA.

We next examined the host proteins isolated with adenovirus DNA. We identified 1792 host proteins associated with adenovirus DNA, and we analyzed the identified proteins in relation to the proteins identified from uninfected (“mock”) samples. We used a student’s T-test to determine if abundances of identified proteins were significantly different between mock and infected samples (p-value < 0.05). We classified proteins into three groups based on this analysis: enriched on virus, under-represented on virus, or common to virus and host. Proteins that were not significantly different between mock and infected (p-value ≥ 0.05) were considered “common” proteins. Proteins that were significantly different and more abundant ($\log_2$ fold change > 0) on DNA from infected samples were considered “enriched on virus,” and proteins that were significantly less abundant on DNA from infected samples were considered “under-represented on virus.” Of the 1792 proteins precipitated with viral DNA, 176 were enriched on virus, 311 were

under-represented on virus, and 1303 were common to virus and host (**Figure 3.1C**). In addition, two proteins were found uniquely on viral DNA (**Figure 3.1C**).

Comparison of viral and host iPOND proteomes reveals novel roles for host proteins in adenovirus replication

We demonstrated that our analysis could be used to identify novel functions for host proteins in viral replication. We reasoned that proteins “enriched on virus” or “common” could represent cellular proteins that are recruited to viral genomes to benefit viral replication, and that proteins “under-represented on virus” may be targets of inactivation by viral proteins. In support of this theory, Mre11, Rad50, and Nbs1 were under-represented on viral genomes, consistent with their known mislocalization and degradation by Ad5 early proteins (see **Chapters 1** and **2**) (Stracker et al., 2002). To determine if our analysis could be used to uncover novel functions of host proteins in the viral life cycle, we examined the impact of identified host proteins on viral replication. Our analysis identified SLX4, a multifunctional protein involved in DNA repair (Fekairi et al., 2009; Kottemann & Smogorzewska, 2013; Svendsen et al., 2009), as enriched on adenovirus genomes. Immunofluorescence of SLX4 in infected cells showed its localization at DBP-stained VRCs (**Figure 3.2A**), supporting its association with viral genomes. Since SLX4 is found at VRCs during adenovirus infection, we hypothesized that it promotes viral replication. To test this hypothesis, we examined adenovirus replication and protein production in SLX4-deficient cells complemented with empty vector (FLAG) or with SLX4 (FLAG-SLX4) (Kim et al., 2011). We measured viral DNA replication by quantitative PCR and examined viral protein production by western blot (**Figures 3.2B**). We found that SLX4 expression significantly enhances viral DNA replication and viral protein production (**Figures 3.2B**), supporting our hypothesis that SLX4 associates with viral genomes to promote viral processes. TCOF1 was another

host protein enriched on viral genomes that we found to promote viral processes. TCOF1 is a nucleolar protein that regulates ribosome biogenesis (Hayano et al., 2003; C. I. Lin & Yeh, 2009) and contributes to DNA repair (Ciccia et al., 2014). We confirmed its recruitment to VRCs by immunofluorescence (**Figure 3.2C**). Depletion of TCOF1 led to a significant reduction of viral DNA replication and viral protein production (**Figure 3.2D**). In addition to identifying host proteins that promote viral replication, we also used our iPOND analysis to identify host proteins that are inactivated by viral early proteins. We hypothesized that proteins that are under-represented on viral genomes compared to host genomes could be specifically targeted by adenovirus. We focused on under-represented proteins that had similar or lower abundance than known degradation targets, and further experimentation demonstrated that the transcription regulator TFII-I (Roy, 2012) is targeted for mislocalization and degradation by Ad5 (**Figure 3.2E-F**). Immunofluorescence confirmed that TFII-I is not found at VRCs during infection and showed that TFII-I is reorganized into distinct structures away from VRCs (**Figure 3.2E**). TFII-I protein levels were dramatically decreased during infection, and levels were rescued by treatment with a proteasome inhibitor, confirming that the decrease is due to degradation (**Figure 3.2F**). Another study also reported TFII-I as a novel degradation substrate for Ad5 (Bridges et al., 2016), supporting our data. Our findings demonstrate that our iPOND analysis not only identifies host proteins associated with viral genomes, but can also be used to identify cellular proteins inactivated or recruited by adenovirus to aid viral replication, thus uncovering novel functions for host proteins during virus infection.

Comparison of iPOND proteomes of wild-type and mutant viruses reveals targets of specific viral proteins

We also demonstrated that iPOND can be used to identify targets of specific viral proteins by comparing isolated proteins from wild-type and mutant virus infections. We compared isolated cellular proteins from wild-type Ad5 infection to those from the E4-deleted mutant. As a validation of our approach, we demonstrated that Mre11, Rad50, Nbs1, and Bloom helicase were found at higher levels on mutant genomes (**Figure 3.3A**). This is consistent with the known degradation of MRN and Bloom helicase by E4 proteins during wild-type Ad5 infection (Orazio et al., 2011; Stracker et al., 2002), which precludes their association with wild-type viral genomes.

In addition to examining mutants of adenovirus, we isolated proteins on viral genomes from wild-type and mutant herpes simplex virus type 1 (HSV-1). HSV-1 infects epithelial cells where it undergoes lytic replication, and establishes latency in neurons (Lachmann, 2003). Like adenovirus, HSV-1 is a nuclear-replicating double-stranded DNA virus. Therefore, it must also manipulate the nuclear environment to promote lytic viral replication. The immediate early viral protein ICP0 is known to promote lytic replication and has been shown to impact various cellular processes, such as the DNA damage response and interferon signaling (Smith, Boutell, & Davido, 2011). ICP0 regulates viral transcription and can target cellular proteins for degradation through its E3 ubiquitin ligase activity (Smith et al., 2011). By comparing proteins associated with DNA from wild-type and ICP0-deleted virus, we identified cellular proteins that were enriched on either wild-type or mutant genomes (**Table 3.2**). We expected that proteins inactivated by ICP0 would be under-represented on wild-type genomes and enriched on ICP0-deleted genomes. Conversely, we reasoned that proteins recruited by ICP0 would be enriched on wild-type genomes. We first verified that known ICP0 degradation targets

were identified by this strategy. As expected, the known ICP0 substrates PML, IFI16, DNA-PK, and USP7 (Smith et al., 2011) were found to be enriched on ICP0-deleted genomes compared to wild-type, validating our approach. We next identified additional cellular proteins whose association with viral genomes were significantly different between wild-type and mutant infection. These included proteins involved in transcription, mRNA splicing, and cell cycle regulation (**Table 3.2**). We demonstrated that two of these proteins, DDX21 and SART1, colocalized with ICP0 nuclear foci when ICP0 was expressed in the absence of infection (**Figure 3.3B**). Furthermore, SART1 colocalized with ICP0 in HSV-1-infected cells (**Figure 3.3C**). We showed that ICP0 affects localization but not protein levels of these proteins (**Figure 3.3D**). These data suggest that ICP0 could recruit these proteins to viral genomes.

Together, results from this project demonstrated that 1) the iPOND technique can be adapted to isolate proteins on viral DNA, 2) comparison of identified proteins between viral and cellular genomes can identify proteins that are exploited or targeted by viruses to promote viral replication, and 3) comparison of wild-type and mutant viruses can identify novel targets of specific viral proteins. We sought to utilize these resources to explore the role of other viral proteins in promoting viral replication. We were interested in examining if viral proteins found on viral genomes could regulate the host proteins on viral genomes through their interaction with viral DNA. Specifically, we asked whether the viral core protein VII regulated association of host proteins on viral genomes. Protein VII is associated with incoming viral genomes and there is evidence that it remains associated with viral DNA throughout infection. Our interest in understanding how protein VII impacts association of cellular proteins with viral DNA arose from our findings that protein VII interacts with host proteins and can impact the proteins associated with host chromatin. In the following sections, I will briefly describe these findings and then

elaborate on how we subsequently used iPOND to demonstrate that protein VII may also affect interactions of host proteins with viral genomes.

Core viral protein VII manipulates host chromatin

Protein VII is a core viral protein that condenses viral DNA and has roles in packaging, nuclear entry of viral genomes, and viral transcription (see **Chapter 1**). Protein VII has been described as “histone-like” due to its sequence similarity to cellular histones and its ability to bind and condense DNA (Johnson et al., 2004) (see **Chapter 1**). We hypothesized that protein VII could also impact host chromatin due to its DNA-binding ability and similarity to cellular histones. We first examined protein VII localization during infection by immunofluorescence to determine if protein VII localized to host chromatin (**Figure 3.4A-B**). We observed that protein VII staining overlapped with DBP-stained VRCs, DAPI, and histone H1 (**Figure 3.4A-B**), suggesting that protein VII can associate with both viral and cellular chromatin. We also observed that adenovirus infection led to manipulation of the chromatin pattern and enlargement of the nucleus. These changes correlated with infection progression and protein VII expression (**Figure 3.4B**). We therefore investigated whether protein VII causes the chromatin manipulation observed during infection. We generated an inducible A549 cell line that expresses protein VII-HA when treated with doxycycline. We examined protein VII expression in this cell line by western blot using an antibody specific to protein VII and by reverse transcription quantitative PCR (RT-PCR) using primers specific to protein VII mRNA (**Figure 3.4C**). Results confirmed protein VII expression, and comparison to infected cells demonstrated that the amount of protein VII expressed from the inducible cell line after four days of induction was less than 10 percent of the amount expressed during infection (**Figure 3.4C**). We analyzed the morphology of cellular chromatin and nuclei over a time course of induction to determine the effect of protein VII on cellular chromatin and nuclear size.

We found that protein VII expression was sufficient to induce nuclear enlargement and manipulation of DAPI-stained cellular chromatin (**Figure 3.4D**). Furthermore, these changes correlated with levels of protein VII (**Figures 3.4C-D**). We conclude that protein VII localizes to sites of viral and cellular DNA and is sufficient to disrupt the morphology of host chromatin and induce nuclear enlargement.

Protein VII sequesters HMGB proteins in cellular chromatin

We investigated whether protein VII affected the proteins associated with cellular chromatin by identifying chromatin-bound proteins in the presence and absence of protein VII expression. Because of the strong interactions between chromatin-associated proteins and DNA, these proteins are soluble only under high salt conditions (Flint & Gonzalez, 2003). We therefore utilized a gradient of salt concentration to fractionate nuclei to isolate chromatin-associated proteins (Herrmann, Avgousti, & Weitzman, 2017). Proteins isolated from the high salt fraction were identified by mass spectrometry. A student's T-test was used to identify proteins that were significantly different ($p < 0.05$) between uninduced samples and samples induced to express protein VII. The top four proteins enriched in the chromatin fraction from protein VII-expressing cells were the known VII-interacting protein SET (Haruki et al., 2003; Xue et al., 2005), and HMGB1, HMGB2, and HMGB3 (**Figure 3.5A**). HMGB proteins have roles in a variety of cellular processes, including gene expression (Agresti & Bianchi, 2003; Bianchi & Agresti, 2005), DNA and chromatin-binding and distortion (Stros, 2010), and signaling to immune cells (Yanai et al., 2009). We confirmed the mass spectrometry results by western blot with the fractionated samples (**Figure 3.5B**). Western blots demonstrated that in untreated cells that do not express protein VII, HMGB1 and HMGB2 were eluted under low salt conditions, suggesting weak interactions with DNA (**Figure 3.5B**). In protein VII-expressing cells, HMGB1 and HMGB2 both eluted only under high salt concentrations

(**Figure 3.5B**). We also fractionated Ad5-infected cells and found that HMGB1 and HMGB2 were similarly eluted only under high salt fractions during infection (**Figure 3.5B**). The HMGB1 and HMGB2 patterns are similar to that of protein VII (**Figure 3.5B**). The control for chromatin-associated proteins was histone H3, which eluted under high salt conditions in all samples, as expected (**Figure 3.5B**). These results suggested that protein VII expression leads to sequestration of HMGB proteins in cellular chromatin. However, insoluble proteins such as nucleolar proteins are also eluted only under high salt fractions, so we confirmed that HMGB proteins were in the high salt fractions due to chromatin localization (**Figure 3.5C**). Immunofluorescence demonstrates that HMGB1 and HMGB2 colocalize with protein VII and DAPI in infected cells and in cells induced to express protein VII (**Figure 3.5C**). We also showed that neither protein VII induction nor Ad5 infection led to a dramatic effect on HMGB1 expression (**Figure 3.5D**), confirming that the observed changes are not due to varying HMGB1 levels between conditions. Together, these results indicate that protein VII is sufficient to sequester HMGB proteins in cellular chromatin.

Conservation of protein VII's effect on cellular chromatin and HMGB1

We examined additional human and murine adenoviruses to determine how well conserved the effect of protein VII on chromatin and HMGB1 is. We found that infection with human serotypes Ad9 and Ad12 caused a similar reorganization of chromatin and HMGB1 (**Figure 3.6A**) and led to HMGB1 retention in high salt fractions (**Figure 3.6B**), demonstrating that protein VII's effect on host chromatin and HMGB1 is conserved across diverse human serotypes. In contrast, infection of murine embryonic fibroblasts (MEF) with murine adenovirus type 1 (MAV-1) altered chromatin morphology but did not relocalize HMGB1 or cause HMGB1 to be retained in high salt fractions (**Figures 3.6C-D**). Murine and human HMGB1 are highly conserved (98.6% protein identity), while Ad5

and MAV-1 protein VII are highly divergent (33.3% protein identity). This suggests that the inability of MAV-1 to affect HMGB1 is due to differences between protein VII expressed from human and murine adenoviruses, and not because of differences between human and murine HMGB1. We confirmed this by examining the effect of Ad5 protein VII in MEF and the effect of MAV-1 protein VII in human cells. Ad5 protein VII retained murine HMGB1 in chromatin, while MAV-1 protein VII did not affect human HMGB1 (**Figures 3.6E-F**). Furthermore, we demonstrated that expression of Ad5 protein VII and Ad5 infection of hamster kidney cells (HaK) led to relocalization of HMGB1 in chromatin (**Figure 3.6G**). We conclude that protein VII reorganization of host chromatin is conserved across human and murine adenovirus, but HMGB1 retention in chromatin is specific to human adenoviruses.

Protein VII deletion during infection

Results from our cell line demonstrated that protein VII is sufficient to induce changes to HMGB1 localization and to sequester HMGB1 in host chromatin. To determine whether protein VII is required for these effects during infection, we used a Cre-Lox system to delete protein VII during adenovirus infection (**Figure 3.7A**). We used a genetically engineered Ad5 with LoxP sites inserted on either side of the protein VII gene (Ad5-flox-VII) (Ostapchuk et al., 2017). Infection of 293 cells with constitutive expression of Cre recombinase (293-Cre) results in deletion of the protein VII gene from the viral genome and production of virions that lack protein VII (Ostapchuk et al., 2017). Although protein VII deletion does not prevent packaging of viral genomes and production of viral progeny, the resulting protein-VII deleted viruses (ΔVII-Ad5) cannot productively complete a second round of infection due to an inability to escape endosomes (Ostapchuk et al., 2017). As a result, we were unable to utilize progeny ΔVII-Ad5 viruses to determine if protein VII was necessary for HMGB1 retention. However, we determined

that we could examine the effect of protein VII during the first round of infection. Rather than infecting cells with ΔVII-Ad5, we infected 293-Cre cells with Ad5-flox-VII and found that protein VII could be successfully deleted from genomes without a substantial inhibition of viral replication (**Figures 3.7B-C**). This allowed us to examine effects of protein VII deletion without any confounding effects on viral replication. We used this system to determine the impact of protein VII deletion on HMGB1 retention in chromatin. We found that in samples where protein VII was deleted, HMGB1 eluted under low salt conditions, similar to the pattern observed in uninfected cells (**Figure 3.7D**). This demonstrated that protein VII is required for HMGB1 chromatin retention during infection.

Protein VII interacts with cellular proteins enriched on viral genomes

To determine if protein VII and HMGB1 interact, we immunoprecipitated VII-HA from induced cells under native conditions using an antibody specific to HA. Western blot analysis of HMGB1 demonstrated that protein VII and HMGB1 co-precipitate (**Figure 3.8B**). This suggests that protein VII interacts with HMGB1 and could contribute to HMGB1 sequestration. To identify additional protein VII-interacting cellular proteins, we analyzed co-precipitating proteins by mass spectrometry. Gene ontology analysis demonstrated that most identified proteins are involved in RNA and DNA-related processes, such as mRNA splicing, chromatin remodeling, and gene expression (**Figure 3.8A**). Since these are processes important for the adenovirus life cycle, we reasoned that some protein VII-interacting proteins may be involved in processes at the viral genome. Furthermore, since protein VII has been detected at viral genomes up to late time points of infection (**Table 3.1**) (Chatterjee et al., 1986), we reasoned that interaction with protein VII may recruit these proteins to viral replication centers. We compared the

167 proteins identified from the IP-MS to the 1790 cellular proteins identified in the Ad5 iPOND-MS proteome to determine if protein VII-interacting proteins were associated with Ad5 genomes (**Figure 3.8C**). This analysis revealed that 137 of the 167 protein VII-co-precipitating proteins associate with Ad5 genomes during infection (**Figure 3.8C**).

The high overlap between the datasets from the iPOND and protein VII projects led us to hypothesize that protein VII impacts the cellular proteins associated with viral genomes. Understanding how protein VII affects protein association with viral genomes could provide insight into the conflicting reports about protein VII's impact on viral transcription and replication (discussed in **Chapter 1**).

iPOND analysis of wild-type and protein VII-deleted genomes

To test our hypothesis, we took advantage of our iPOND protocol and the Cre-Lox protein VII deletion system. We performed iPOND under wild-type and protein-VII deleted conditions and compared the results to identify proteins impacted by protein VII. We have observed different growth rates and morphology between parental 293 and 293-Cre cells. Since iPOND-MS is sensitive to differences in the levels of cellular material, we decided to use only one cell type to avoid any effects of cell-type specific differences. We infected 293-Cre cells with either wild-type or flox-VII Ad5 and examined protein VII deletion by western blot and qPCR. As expected, infection of 293-Cre cells with wild-type Ad5 does not lead to deletion of protein VII, and infection with the flox-VII virus results in protein VII deletion during infection (**Figure 3.9A-B**). Since iPOND relies on EdU incorporation by replicating DNA, it was important to ensure that there were similar genome levels between wild-type and flox-VII virus at the time of the EdU pulse. We examined viral DNA levels by qPCR at 24 hours post-infection and observed only a moderate decrease in genome levels (approximately two-fold) of the flox-VII virus

compared to wild-type (**Figure 3.9B**). We therefore proceeded with iPOND using the wild-type and flox-VII viruses.

We performed three biological replicates, each of which included a mock-infected sample, wild-type infected, flox-VII infected, and a “no biotin” control. iPOND was performed as usual, and capture samples were excised from a coomassie-stained gel for mass spectrometry (**Figure 3.10A**). Visualization of proteins by coomassie stain confirmed that the “no biotin” control captured fewer proteins, as expected (**Figure 3.10A**). Proteins enriched in the “no biotin” control were considered background and removed from the analysis. Due to low quality and protein content revealed by mass spectrometry, one of the three biological replicates was excluded from the analysis. Comparison of the two remaining biological replicates demonstrated high reproducibility of the results: most isolated proteins were identified in both replicates (**Figure 3.10B**), and proteins were found at similar abundances between replicates (**Figure 3.10C**). Furthermore, principal component analysis demonstrated that the isolated proteins clustered by sample (**Figure 3.10D**). As expected, proteins isolated from the two mock samples were more similar to each other than to the infected samples, and the wild-type and mutant samples were fairly similar to each other (**Figure 3.10D**). This is consistent with the fact that cellular and viral genomes associate with different proteins.

We next compared the viral proteins isolated from wild-type and protein VII-deleted conditions. This was to ensure that protein VII deletion did not impact recruitment of viral proteins required for viral replication. We found that iPOND of wild-type and protein VII-deleted samples resulted in isolation of nearly identical lists of viral proteins (**Figure 3.11A**). Protein VII was identified only in wild-type samples, as expected. However, the E3 14.6 glycoprotein, which is normally found at the cellular membrane, was

unexpectedly isolated from protein VII-deleted samples. All other viral proteins, including the DNA replication proteins DBP, Ad Pol, and pTP, were found under both wild-type and VII-deleted conditions. Furthermore, viral proteins were found at similar abundances in both conditions (**Figure 3.11B**). We conclude that protein VII deletion does not dramatically affect the association of viral proteins. Importantly, association of viral DNA replication proteins at similar levels suggests that deletion of protein VII does not impact DNA replication, consistent with genome quantification from **Figure 3.9B**. As a result, any changes to cellular protein association with genomes can be attributed to protein VII deletion, rather than changes to DNA replication or other viral proteins.

Protein VII deletion affects association of RNA and DNA processing proteins with viral genomes

We used a student's T-test to identify cellular proteins differentially regulated between wild-type and protein VII-deleted viruses. We reasoned that proteins significantly ($p<0.05$) more enriched on wild-type virus represent proteins that could be recruited by protein VII. Conversely, proteins that are significantly ($p<0.05$) more enriched on viral DNA in the absence of protein VII represent proteins that do not associate as efficiently with viral genomes when protein VII is present. We found that 97 proteins were differentially regulated when protein VII was deleted (**Figure 3.12**). Thirty-two proteins were significantly more abundant on genomes during wild-type infection, and 65 proteins were significantly more abundant when protein VII was deleted (**Figure 3.12**). As a control, we examined the effect of protein VII deletion on SET, a cellular protein known to interact with protein VII and localize to viral genomes (Haruki et al., 2003; Haruki et al., 2006) (see **Chapter 1**). We found that SET was isolated by iPOND under wild-type conditions, but not when protein VII was deleted, validating our approach. We next examined the functions of proteins enriched on wild-type and found that several of the

proteins most upregulated on wild-type genomes (log2 fold change > 1) are involved in DNA or RNA-related processes. These processes include mRNA splicing and export, DNA replication, and transcriptional regulation. Since these processes are important for the adenovirus life cycle, our findings suggest that protein VII promotes the association of proteins that contribute to viral replication and gene expression. Functions for identified proteins are summarized in **Table 3.2**.

We examined localization of proteins enriched on wild-type genomes by immunofluorescence of infected A549 cells. Consistent with iPOND-MS results, we observed that RecQL1 and SRP14 co-localize with sites of viral DNA replication, as marked by viral DBP (**Figure 3.13**). We also found that FUBP1 and SPATA5 were found surrounding DBP-marked viral replication centers (**Figure 3.13**). This localization pattern is similar to that of viral RNA and sites of late viral transcription (Pombo et al., 1994), suggesting a role for these proteins in viral transcription. In fact, FUBP1 has been suggested to recruit E1A and promote adenovirus transcription (unpublished data presented at 2016 DNA Tumour Virus meeting, P.Pelka). Importantly, the iPOND protocol does not include an RNA digestion step. Therefore, it is possible to isolate RNA-interacting proteins through interactions of RNA with DNA. This likely explains the isolation of host proteins involved in processes such as transcription and mRNA splicing.

We next examined localization in the absence of protein VII to determine if localization to VRCs and viral transcription sites is dependent on protein VII. Immunofluorescence of 293 cells is difficult due to their small size and tendency to detach from coverslips. Therefore, we optimized a system to delete protein VII in A549 cells by treating cells with purified Cre protein prior to infection with the flox-VII virus. Cre was tagged with a fragment of the HIV-1 TAT protein, which enhances cellular uptake of Cre (Peitz,

Pfannkuche, Rajewsky, & Edenhofer, 2002). We demonstrated deletion of protein VII in infected cells pre-treated with TAT-Cre (**Figure 3.14A-B**). Similar to results in the 293 system, we found that protein VII was deleted without a substantial effect on viral replication (**Figure 3.14A-B**) or on the identified cellular proteins (**Figure 3.14C**). We next examined how protein VII deletion affects localization of FUBP1, which was enriched on wild-type viral genomes (**Figure 3.12**) and redistributed during wild-type Ad5 infection (**Figure 3.13**). We first confirmed that TAT-Cre treatment had minimal impact on infection efficiency (**Figure 3.14C, DBP panel**), and effectively deleted protein VII (**Figure 3.14C, VII panel**). Next, we quantified cells with FUBP1 relocalization in control and TAT-Cre-treated cells (**Figure 3.14C, FUBP1 panel**). We found a dramatic decrease in the proportion of cells showing changes to FUBP1 when infected cells were pre-treated with TAT-Cre. This suggests that protein VII deletion prevents the relocalization of FUBP1 observed during wild-type Ad5 infection, validating our iPOND results.

In order to gain more insight into the mechanism by which protein VII promotes the observed changes, we examined whether protein VII is sufficient to induce the localization changes to RecQL1, SRP14, FUBP1, and SPATA5 during infection. We expressed GFP-tagged protein VII from a replication incompetent adenovirus vector. Expression of protein VII was not sufficient to alter localization of these proteins (**Figure 3.15A**), indicating that additional viral proteins or processes are required. We also examined whether proteins enriched on wild-type genomes interact with protein VII during infection. We performed immunoprecipitation with wild-type Ad5-infected cells using an antibody specific to protein VII. We did not detect interaction of these proteins with protein VII during infection (**Figure 3.15B**). Together, results from **Figure 3.15** indicate that localization changes to host proteins are unlikely to be through active

recruitment by protein VII. It is possible that protein VII instead induces changes to viral DNA condensation or manipulates cellular pathways in such a way that promotes localization of host proteins with viral genomes.

Protein VII suppresses interferon signaling

We reasoned that proteins enriched on protein VII-deleted genomes could provide insight into cellular pathways targeted by protein VII. The cellular proteins TRIM25 and UBR4 were enriched on protein VII-deleted genomes and have both been implicated in the interferon response (Martin-Vicente, Medrano, Resino, Garcia-Sastre, & Martinez, 2017; Morrison et al., 2013) (**Table 3.3**). We therefore investigated whether protein VII impacts this anti-viral pathway. We hypothesized that protein VII association with cellular chromatin may affect expression of interferon stimulated genes (ISGs) through effects on transcriptional regulation or DNA accessibility. To test this hypothesis, we examined whether protein VII deletion affected ISG expression. We deleted protein VII by pre-treatment of cells with TAT-Cre, infected cells with flox-VII virus, isolated RNA, and performed RT-PCR using primers specific to ISG15 (**Figure 3.16A**). RT-PCR results demonstrate that deletion of protein VII does not affect expression of this ISG compared to wild-type infection (**Figure 3.16A**). Furthermore, we saw that infection did not lead to a dramatic increase in ISG15 expression, likely due to the actions of other viral proteins. Since multiple early viral proteins are known to suppress the interferon pathway (see **Chapter 1**), effects of protein VII could be masked due to redundancy with early proteins. Therefore, we explored the role of protein VII in the absence of infection to avoid redundancy with early viral proteins. We examined ISG expression in response to type I IFN treatment in cells expressing protein VII (**Figure 3.16B**). Again, we found that protein VII did not affect ISG expression in response to ectopic IFN treatment. This suggested that protein VII does not influence ISG expression downstream of IFN.

Recently published work led us to hypothesize that protein VII may act on steps upstream of IFN expression. Andreeva et al. suggested that murine HMGB1 contributes to activation of interferon signaling by binding foreign DNA and changing its conformation to promote binding by cGAS, a cytoplasmic DNA sensor (Andreeva et al., 2017). cGAS then signals to STING, which activates signaling to induce expression of IFNβ (see **Chapter 1** for details). Since protein VII sequesters HMGB1 in cellular chromatin (**Figure 3.5**), we hypothesized that protein VII would suppress interferon signaling by impairing recognition of foreign DNA by cellular sensors such as cGAS. As described in **Chapter 1**, detection by DNA sensors is upstream of IFN production. This could explain why we did not see an effect when we examined ISG expression downstream of IFN treatment.

To examine whether protein VII impacts the response to foreign DNA, we examined IFNβ expression after transfection of interferon stimulatory poly(dA:dT) DNA with and without protein VII expression. We observed a dramatic and significant decrease in IFNβ mRNA levels when protein VII was expressed, compared to an uninduced control (**Figure 3.16A-B**). We also observed delayed STAT1 phosphorylation in the presence of protein VII compared to the uninduced control (**Figure 3.16C**). To determine if protein VII localization to chromatin contributes to suppression of IFNβ expression, we examined the effect of a protein VII mutant that does not localize to chromatin. We have shown that post-translational modification (PTM) of protein VII is required for chromatin localization (Avgousti et al., 2016). We found that expression of ΔPTM protein VII did not affect IFNβ mRNA levels (**Figure 3.16A-B**). This suggests that protein VII suppression of IFNβ expression is dependent on chromatin localization, or another function of PTMs.

Mitotic progression is necessary for proper signaling through cGAS and STING (Harding et al., 2017). We therefore investigated whether protein VII suppression of IFN could be an indirect consequence of cell cycle effects of protein VII. We examined IFNβ expression and cell cycle distribution of protein VII-expressing cells over a time course of doxycycline induction (**Figure 3.17**). The effect of protein VII on interferon activation was observed by two days post-induction (**Figure 3.17A**), consistent with the timing for chromatin reorganization (**Figure 3.4D**). Cell cycle effects caused by protein VII did not occur until after three days of induction (**Figure 3.17C**), when G2 accumulation was observed. This suggests that protein VII-mediated suppression of IFN signaling in response to foreign DNA may occur independently of cell cycle effects.

Thus far, our data demonstrated that protein VII suppresses interferon signaling upstream of IFN expression and that localization of protein VII to host chromatin appears to be important for this suppression. We next explored the role of HMGB1 to determine if the effects of protein VII could be through HMGB1 sequestration in host chromatin. We utilized MAV-1 protein VII, which we showed could associate with cellular chromatin but could not sequester HMGB1 (**Figure 3.6**). This provided us a resource to separate the chromatin manipulation and HMGB1 sequestration functions of protein VII. We induced expression of either Ad5-protein VII or MAV-1-protein VII and examined IFNβ mRNA levels in response to stimulation with poly(dA:dT). We found that IFNβ mRNA levels were lower in cells expressing Ad5-VII than in uninduced cells, as expected (**Figure 3.18A-B**). However, there was a partial rescue of IFNβ mRNA levels when MAV-VII was expressed (**Figure 3.18A-B**). These findings are consistent with a partial role for protein VII-mediated HMGB1 sequestration in suppression of IFN signaling. However, MAV-1 protein VII expression did still suppress IFNβ levels at 4 days post-induction (**Figure**

3.18A). This could be an indirect consequence of MAV-1 protein VII-mediated effects on the cell cycle (**Figure 3.18C**), or could indicate that protein VII-mediated suppression of IFNβ is only partially dependent on HMGB1. Cell cycle effects were not observed after 2 days of dox induction of MAV-1 protein VII (**Figure 3.18C**). We therefore investigated the impact of MAV-1 protein VII on IFNβ after 2 days of induction (**Figure 3.18B**). Under these conditions, the trend of IFNβ levels suggests that MAV-1 protein VII may not suppress IFNβ (**Figure 3.18B**). The impact of MAV-1 protein VII on IFNβ will be investigated further. We also examined the effect of protein VII on IFNβ in parental and HMGB1-deficient cells (**Figure 3.18D**) Based on results from Andreeva et al., we expected decreased IFNβ levels in the absence of HMGB1. Unexpectedly, we found that IFNβ levels in response to poly(dA:dT) stimulation were not affected by the deletion of HMGB1 (**Figure 3.18D**, compare “parental, mock” to “HMGB1-KO, mock”). Results from **Figure 3.18D** suggest that the results from Andreeva et al. may not be representative of human cells or of all cell types. Intriguingly, we found that IFNβ levels were not affected by protein VII in HMGB1-deficient cells (**Figure 3.18D**, compare “parental, rAd-VII” to “HMGB1-KO, rAd-VII”), supporting a role for HMGB1 in protein VII-mediated IFN suppression. It is important to note that protein VII expression levels are decreased in HMGB1-deficient samples, thus the subdued effect on IFNβ could be due to lower protein VII levels. Together, the data from **Figure 3.18** raise the possibility that HMGB1 could contribute to protein VII-mediated IFN suppression and merit further study.

Tables and Figures

Figure 3.1

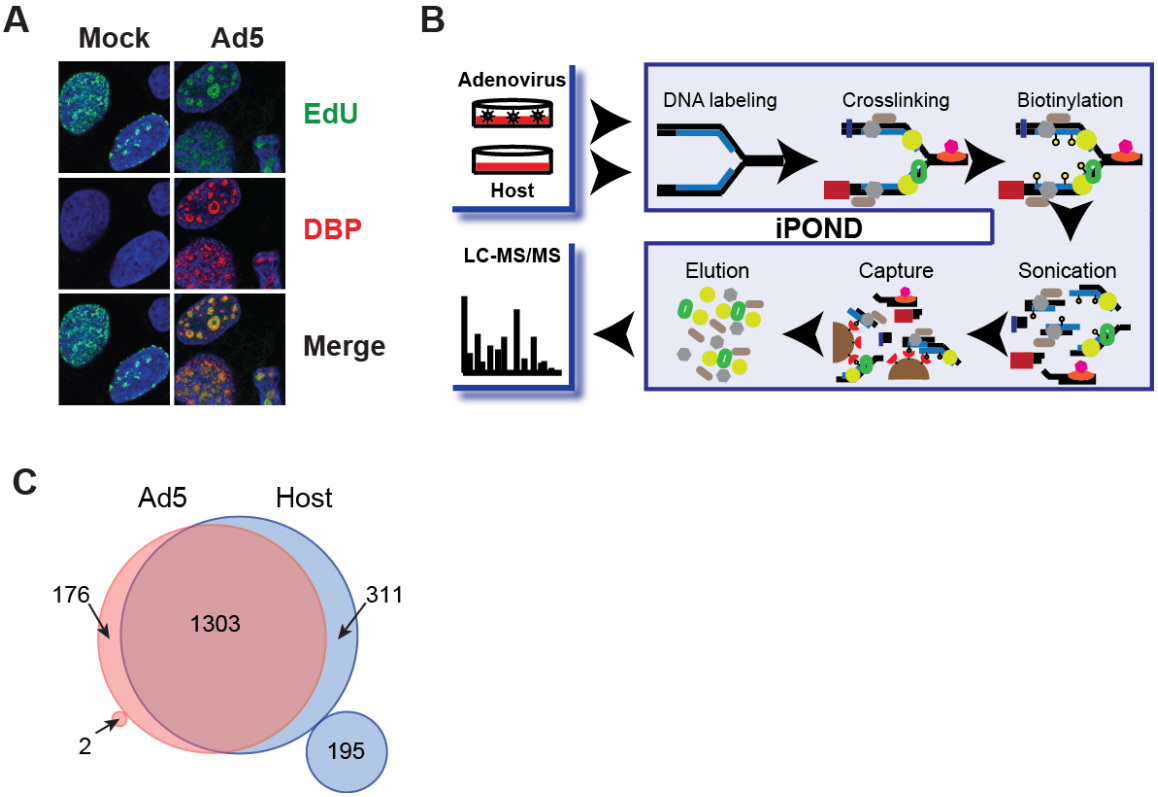

Figure 3.1: iPOND identifies proteins associated with viral genomes. (A) Visualization of EdU-labeled DNA demonstrates that EdU can be incorporated into viral DNA. Images show that EdU is found mostly at DBP-stained viral replication centers in infected cells, rather than at cellular replication sites. **(B)** Schematic of iPOND-MS protocol. **(C)** Comparison of cellular proteins identified from Ad5-infected (Ad5) and mock cells (Host). Significant changes in abundance between Ad5 and Host were identified by a student's T test (significance = $p<0.05$). 176 cellular proteins were significantly enriched in Ad5 samples, 311 were significantly enriched in Host samples, 2 cellular proteins were found only on viral genomes, and 195 proteins were found only on Host genomes. 1303 were found on both viral and cellular genomes at similar levels. *Data in Figure 1 generated by Emigdio Reyes and Kasia Kulej.*

Table 3.1

Uniprot ID	Gene Name	Protein Name/ Description	*t*-test *p*-value (+)Biotin/ (-)Biotin	log_2 Fold Change (+)Biotin/ (-)Biotin
P04496	L1	Packaging protein 3	0.00027422	3.998007776
P04133	L3	Hexon protein	0.002781689	3.650700769
P24937	L3	Pre-protein VI	0.005303297	3.455002647
P04495	E2B	**DNA polymerase (Ad Pol)**	0.006292468	3.095167706
Q2KS19		I-leader protein	0.006456385	2.670800952
P24936	L4	Pre-hexon-linking protein VIII	0.009342435	2.449544406
P03243	E1B	E1B 55 kDa protein	0.00964238	N/A
P03271	IVa2	Packaging protein 1	0.009761935	7.582386204
P11818	L5	Fiber protein	0.010417597	3.098742223
P12537	L1	Pre-hexon-linking protein IIIa	0.010428407	3.781260205
P24938	L2	Core-capsid bridging protein	0.01614357	10.09417345
P03246	E1B	E1B 19KDa protein, small T-antigen	0.020682622	2.614701953
P24933	L4	Shutoff protein	0.026250311	3.580550408
P03265	E2A	**DNA-binding protein DBP**	0.027457464	7.485553267
P04499	E2B	**Preterminal protein pTP**	0.028918193	N/A
P24940	L4	Protein 33K	0.039976253	5.585680988
P12538	L2	Penton protein	0.047079668	1.621015162
Q2KS03	L4	Packaging protein 2	0.060455869	N/A
P68951	L2	Protein VII	0.067971636	N/A
P03255	E1A	E1A protein	0.091841556	N/A
A8W995	U	U exon protein	0.097120046	N/A
P03281	IX	Hexon-interlacing protein	0.100237204	1.500316835
P04489	E4	Probable early E4 11 kDa protein (E4orf3)	0.129561159	N/A
P03253	L3	Protease	0.211324865	N/A
P04494	E3	Early E3 18.5 kDa glycoprotein	0.211324865	N/A

Table 3.1: Viral proteins identified by iPOND-MS. Proteins significantly more abundant ($p<0.05$) in Ad5 experimental samples compared to the “no biotin” controls.

Viral proteins involved in viral DNA replication are in bold. *Data in Table 3.1 generated by Emigdio Reyes.*

Figure 3.2

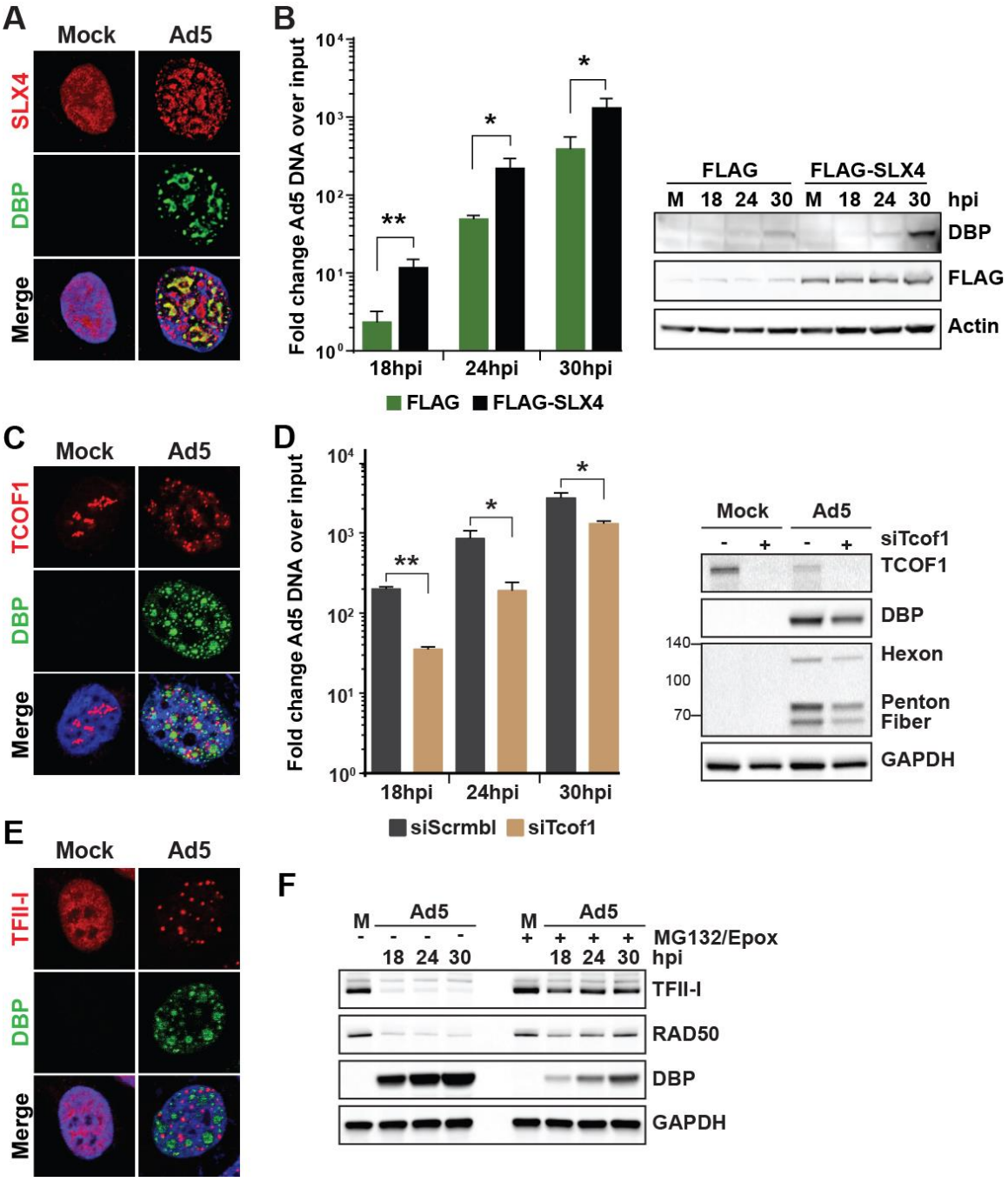

Figure 3.2: Comparison of viral and host proteomes reveals novel roles for host proteins in adenovirus replication. (A) SLX4 localization in relation to DBP-stained viral replication centers. Ad5 infection results in redistribution of SLX4 to VRCs. **(B)** Left -

Viral DNA accumulation in SLX4-deficient cells and matched cells complemented with FLAG-tagged SLX4. There is increased viral DNA accumulation in SLX4-expressing cells. Right - Western blot confirms expression of FLAG-SLX4 and demonstrates increased viral DBP levels in SLX4-expressing cells. **(C)** TCOF1 localization in relation to DBP-stained VRCs. Ad5 infection results in redistribution of TCOF1 from nucleoli to sites surrounding VRCs. **(D)** Effect of TCOF1 depletion on viral DNA accumulation. siRNA-mediated depletion of TCOF1 results in significantly decreased viral DNA levels. Western confirms TCOF1 knockdown and demonstrates decreased early (DBP) and late (hexon, penton, fiber) viral protein levels. **(E)** TFII-I localization in infected cells in relation to DBP-marked VRCs. Ad5 infection leads to redistribution of TFII-I from a pan-nuclear distribution to foci that do not colocalize with VRCs. **(F)** Western blot demonstrating proteasome-dependent decrease of TFII-I during Ad5 infection. Treatment with the proteasome inhibitors MG132 and epoxomicin rescues TFII-I levels. Rad50 is a known Ad5 degradation substrate and serves as a control for degradation. *Panels A, C, E, and F by Emigdio Reyes and Lisa Akhtar.*

Figure 3.3

A

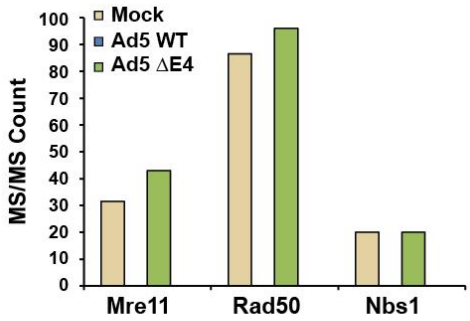

B

	Cellular Function	Enriched on
Known ICP0 targets		
PML	Transcription, apoptosis, p53 regulation	ΔICP0
IFI16	Viral DNA sensor, interferon activation	ΔICP0
Usp7	Ubiquitin specific protease	ΔICP0
DNA-PK	DNA repair	ΔICP0
Candidate ICP0 targets		
DDX21	Transcription, RNA splicing	Wild-type
MORC3	p53 regulation, RNA splicing	ΔICP0
SART1	RNA splicing	Wild-type
TRRAP	Transcription, chromatin modification	Wild-type
Nat10	Transcription, chromatin modification	Wild-type
Mybbp1a	Transcription, p53 regulation	Wild-type

C

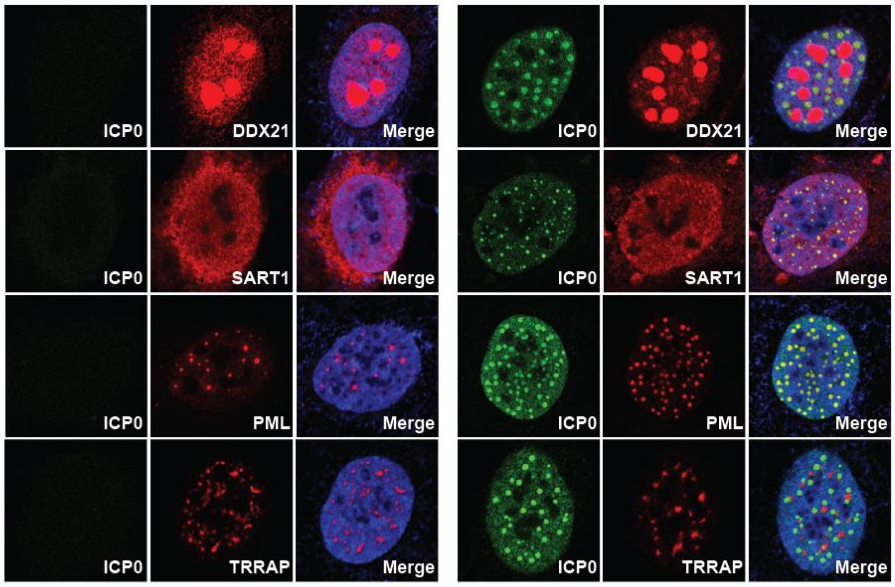

D

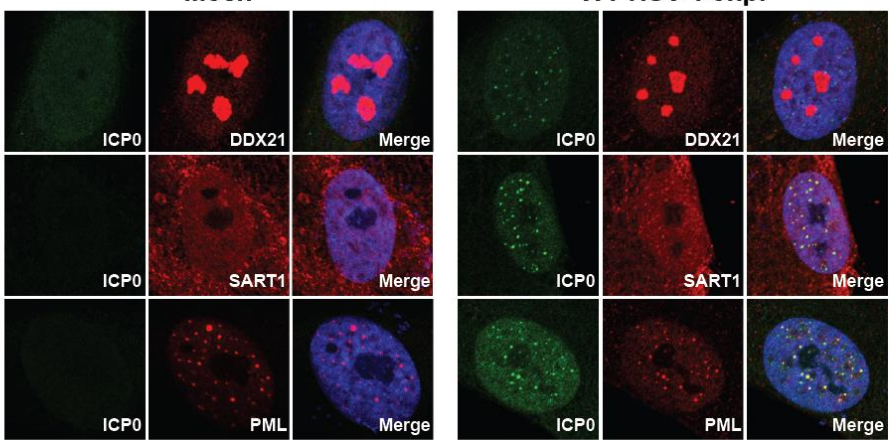

Figure 3.3: Comparison of wild-type and mutant viral proteomes reveals targets of specific viral proteins. (A) Raw spectral count data of Mre11, Rad50, and Nbs1 from iPOND-MS of mock, wild-type Ad5, and E4-deleted Ad5 samples. As expected, Mre11, Rad50, and Nbs1 are isolated with replicated DNA from mock and E4-deleted samples, but are not detected in wild-type Ad5 samples. This is consistent with the known degradation of MRN during wild-type Ad5 infection, and the known association of MRN with E4-deleted VRCs. **(B)** iPOND-MS with wild-type and ICP0-deleted HSV-1 demonstrates that known ICP0 degradation targets are enriched on ICP0-deleted genomes. Additional cellular proteins were found enriched on wild-type or ICP0-deleted genomes and represent proteins potentially regulated by ICP0. **(C)** Immunofluorescence analysis of cellular proteins identified in **B** in cells transfected with an ICP0-expression vector. DDX21, SART1, and PML colocalize with ICP0, while TRRAP does not. **(D)** Immunofluorescence analysis of cellular proteins identified in **B** in mock and HSV-1 infected cells. SART1 and PML colocalize with ICP0 during infection. Results from **C** and **D** are consistent with a role for ICP0 in affecting localization of these cellular proteins. *Data in panel B generated by Emigdio Reyes.*

Figure 3.4

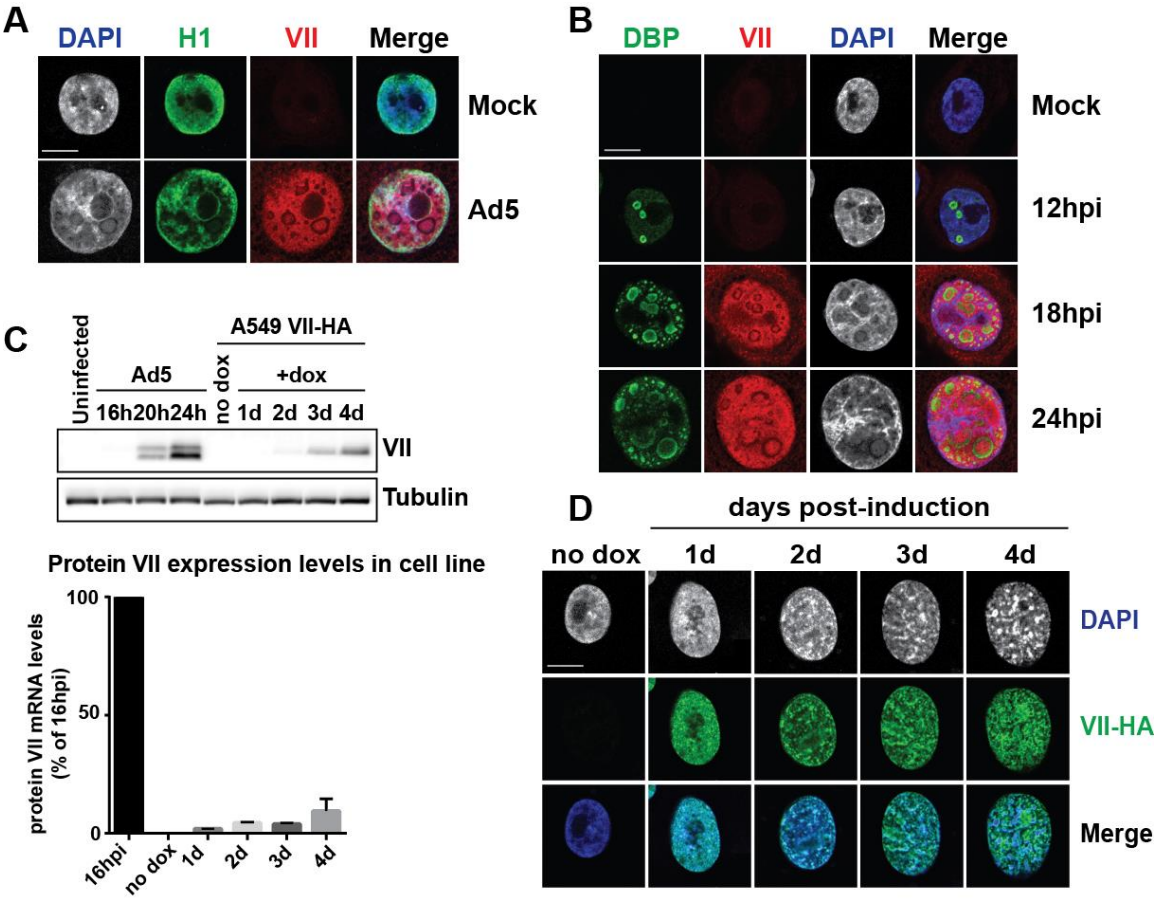

Figure 3.4: Core viral protein VII manipulates host chromatin. (A) Ad5 infection changes morphology of cellular chromatin, visualized here by DAPI and histone H1 immunofluorescence. Protein VII localizes to cellular chromatin. **(B)** Changes to chromatin during infection correlate with timing of protein VII production. Protein VII colocalizes with cellular chromatin and with DBP-marked viral replication centers. **(C)** Validation and quantification of protein VII-HA expression in inducible cell lines. Western blot and RT-PCR demonstrate that the amount of protein VII expressed from the inducible cell line is dramatically lower than during infection. Protein VII expression increases over a time course of doxycycline treatment. **(D)** Effect of protein VII expression on cellular chromatin. Protein VII is sufficient to induce changes to

appearance of host chromatin, represented by DAPI here. Changes to DAPI correlate with increasing protein VII levels (see panel **C**). *Panels A, B, and D by Daphne Avgousti.*

Figure 3.5

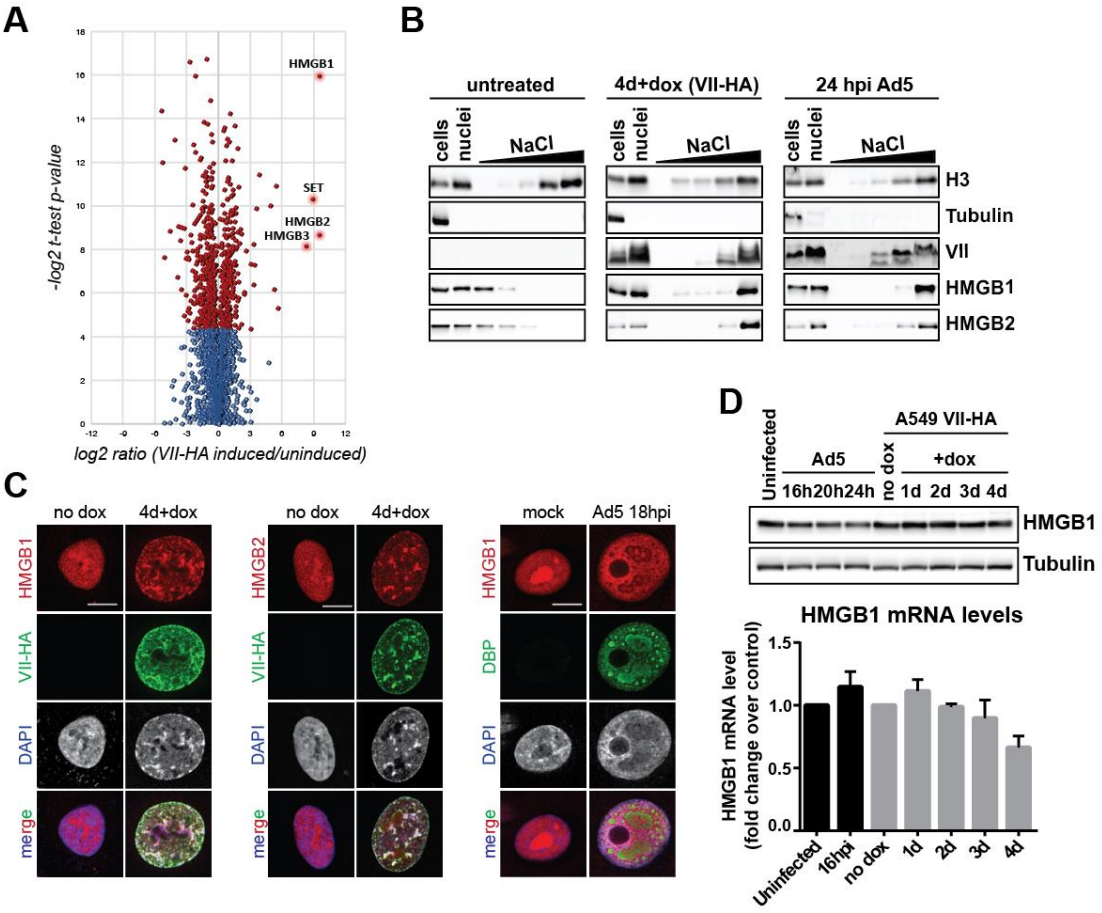

Figure 3.5: Protein VII sequesters HMGB proteins in cellular chromatin. (A) Mass spectrometry results of proteins identified in high salt fractions from induced and uninduced cells. Volcano plot demonstrates that HMGB1, HMGB2, HMGB3, and SET are significantly more abundant in the high salt fraction of cells induced to express protein VII, compared to uninduced cells. Red dots represent significantly changed proteins ($p<0.05$). **(B)** Western blot results of salt fractionation experiments. HMGB1 and HMGB2 are found in lower salt fractions in untreated cells, but are found in higher salt fractions in the protein VII cell line and in infected cells. Histone H3 is a positive control for proteins found in high salt fraction, and Tubulin is a negative control. **(C)** Immunofluorescence analysis of HMGB1 and HMGB2 localization with protein VII

expression and Ad5 infection. Expression of protein VII is sufficient to relocalize to HMGB1 and HMGB2 to DAPI-stained cellular DNA and protein VII. Ad5 infection induces reorganization of HMGB1 to cellular chromatin, similar to protein VII localization. **(D)** HMGB1 levels during infection and in the presence of protein VII. Western blot and RT-PCR analysis demonstrate that neither protein VII expression nor Ad5 infection results in dramatic changes to HMGB1 levels. *Panels A-C by Daphne Avgousti and Christin Herrmann. Proteomic analysis in panel A by Kasia Kulej.*

Figure 3.6

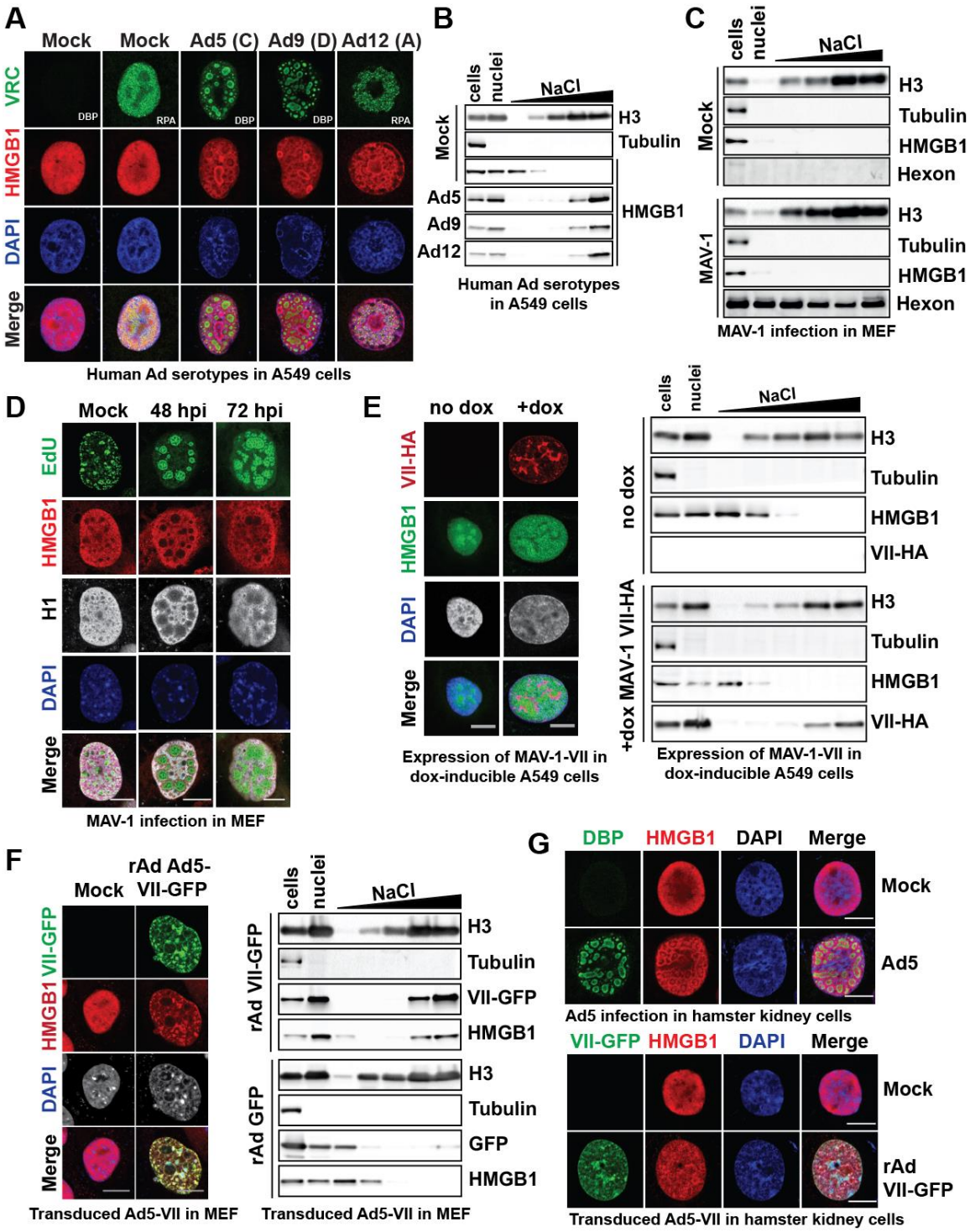
A
Mock
Mock
Ad5 (C)
Ad9 (D)
Ad12 (A)
VRC
HMGB1
DAPI
Merge
DBP
RPA
Human Ad serotypes in A549 cells
B
cells
nuclei
NaCl
Mock
Ad5
Ad9
Ad12
H3
Tubulin
HMGB1
Human Ad serotypes in A549 cells
C
cells
nuclei
NaCl
Mock
MAV-1
H3
Tubulin
HMGB1
Hexon
MAV-1 infection in MEF
D
Mock
48 hpi
72 hpi
EdU
HMGB1
H1
DAPI
Merge
MAV-1 infection in MEF
E
no dox
+dox
VII-HA
HMGB1
DAPI
Merge
Expression of MAV-1-VII in dox-inducible A549 cells
cells
nuclei
NaCl
no dox
+dox MAV-1 VII-HA
H3
Tubulin
HMGB1
VII-HA
Expression of MAV-1-VII in dox-inducible A549 cells
F
Mock
rAd Ad5-VII-GFP
VII-GFP
HMGB1
DAPI
Merge
Transduced Ad5-VII in MEF
cells
nuclei
NaCl
rAd VII-GFP
rAd GFP
H3
Tubulin
VII-GFP
HMGB1
GFP
Transduced Ad5-VII in MEF
G
DBP
HMGB1
DAPI
Merge
Mock
Ad5
Ad5 infection in hamster kidney cells
VII-GFP
HMGB1
DAPI
Merge
Mock
rAd VII-GFP
Transduced Ad5-VII in hamster kidney cells

Figure 3.6: Conservation of protein VII's effect on cellular chromatin and HMGB1. **(A)** Immunofluorescence analysis of HMGB1 and DAPI in cells infected with multiple human serotypes. Ad5, Ad9, and Ad12 alter DAPI morphology and relocalize HMGB1 to cellular chromatin. **(B)** Salt fractionation results from cells infected with diverse human serotypes. Like Ad5, Ad9 and Ad12 infections also result in retention of HMGB1 in high salt fractions. **(C)** Salt fractionation analysis of murine adenovirus type 1 (MAV-1) infection in mouse embryonic fibroblasts (MEF). MAV-1 infection does not lead to HMGB1 retention in high salt fractions. **(D)** Immunofluorescence analysis of HMGB1 and histone H1 during MAV-1 infection of MEF. Consistent with results from **C**, MAV-1 infection does not dramatically alter HMGB1 localization. However, histone H1 morphology is altered by MAV-1. **(E)** Dox-inducible expression of MAV-1 protein VII does not alter HMGB1 localization (left panel). MAV-1 protein VII is found in high salt fractions, but MAV-1 protein VII expression does not affect HMGB1. **(F)** Expression of Ad5-protein VII in murine cells is sufficient to alter HMGB1 localization and retain HMGB1 in high salt fractions. **(G)** Ad5 infection or Ad5-protein VII expression in hamster cells results in changes to HMGB1 localization. *Panels B, C, E, and F by Christin Herrmann.*

Figure 3.7

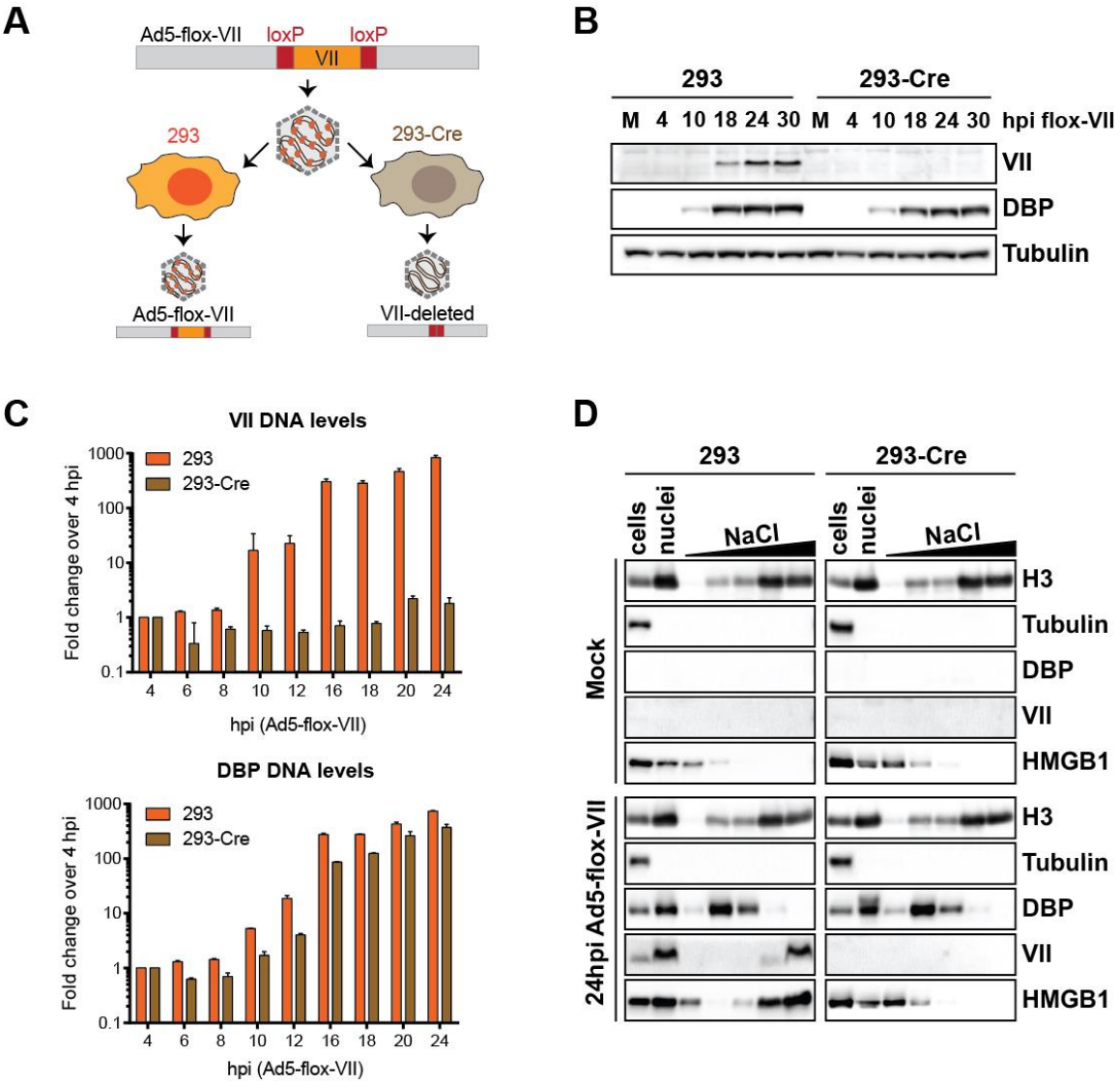

Figure 3.7: Protein VII deletion by Lox-Cre system. (A) Schematic of Lox-Cre deletion of protein VII. The protein VII gene is flanked by loxP sites in the viral genome. Infection of cells with constitutive expression of Cre recombinase results in deletion of protein VII and the generation of protein VII-deficient viral particles. Infection of cells without Cre results in production of flox-VII virus. **(B)** Western blot demonstrating deletion of protein VII by the Cre-Lox system. **(C)** Quantitative PCR demonstrates that protein VII is not found in nascent viral genomes (top graph), and protein VII deletion does not

dramatically affect viral DNA accumulation (bottom graph). **(D)** Salt fractionation of Cre cells infected with flox-VII virus to assess the effect of protein VII deletion on HMGB1 retention in high salt fraction. HMGB1 is not retained in high salt fractions when protein VII is deleted. *Panel D by Christin Herrmann.*

Figure 3.8

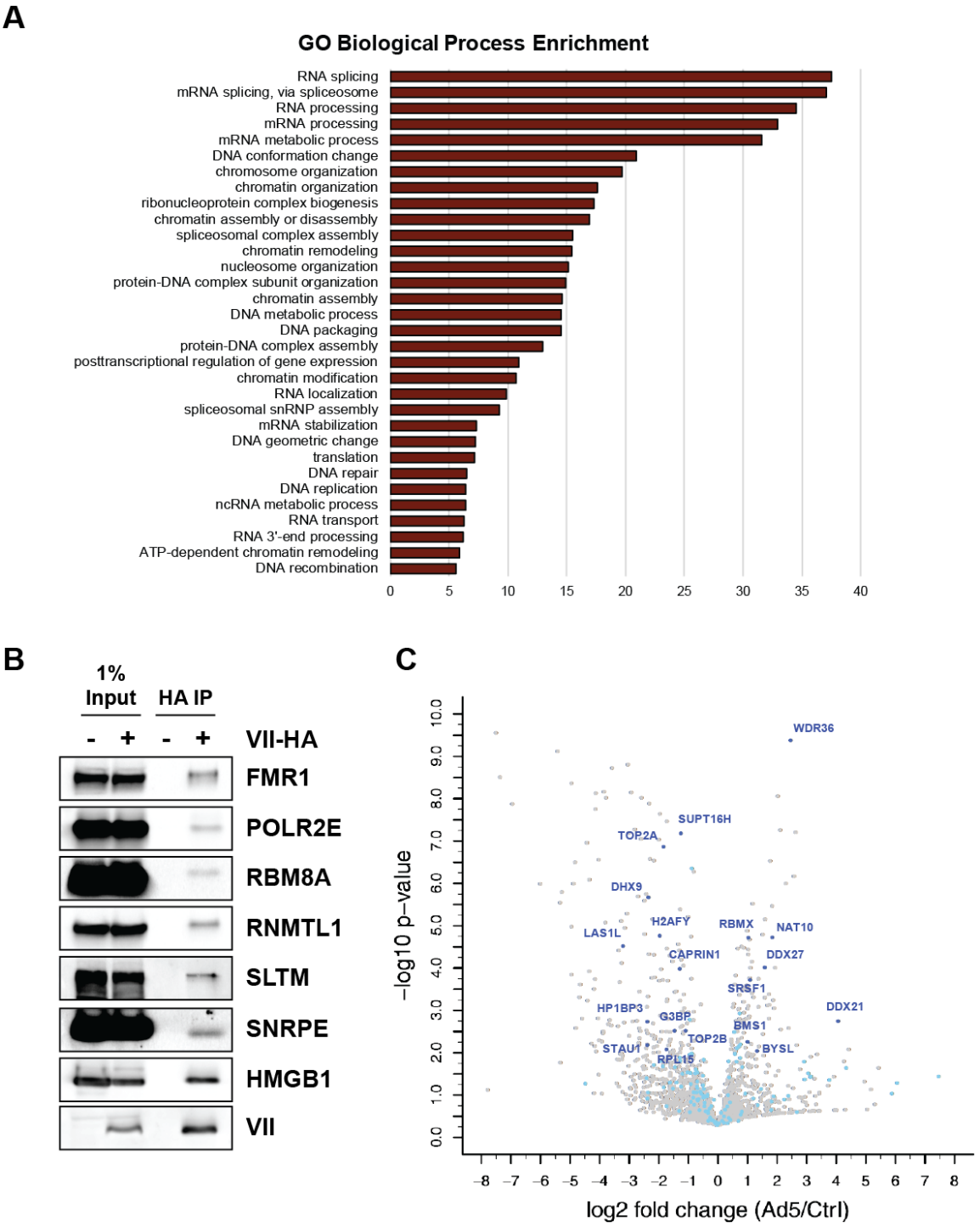
A
GO Biological Process Enrichment
RNA splicing
mRNA splicing, via spliceosome
RNA processing
mRNA processing
mRNA metabolic process
DNA conformation change
chromosome organization
chromatin organization
ribonucleoprotein complex biogenesis
chromatin assembly or disassembly
spliceosomal complex assembly
chromatin remodeling
nucleosome organization
protein-DNA complex subunit organization
chromatin assembly
DNA metabolic process
DNA packaging
protein-DNA complex assembly
posttranscriptional regulation of gene expression
chromatin modification
RNA localization
spliceosomal snRNP assembly
mRNA stabilization
DNA geometric change
translation
DNA repair
DNA replication
ncRNA metabolic process
RNA transport
RNA 3'-end processing
ATP-dependent chromatin remodeling
DNA recombination
0 5 10 15 20 25 30 35 40
B
1% Input
HA IP
- + - +
VII-HA
FMR1
POLR2E
RBM8A
RNMTL1
SLTM
SNRPE
HMGB1
VII
C
−log10 p−value
log2 fold change (Ad5/Ctrl)
WDR36
SUPT16H
TOP2A
DHX9
H2AFY
RBMX
NAT10
LAS1L
CAPRIN1
DDX27
SRSF1
DDX21
HP1BP3
G3BP
BMS1
TOP2B
STAU1
BYSL
RPL15

Figure 3.8: Protein VII interacts with HMGB1 and cellular proteins enriched on viral genomes. (A) Gene ontology analysis of cellular proteins that co-precipitate with ectopically expressed protein VII. X-axis is –log10 p-value. **(B)** Western blots confirm IP-MS results and demonstrate that several proteins with RNA and DNA-related functions co-precipitate with protein VII. IP-Western also demonstrates that HMGB1 co-precipitates with protein VII. **(C)** Volcano plot of Ad5 iPOND results with protein VII-interacting proteins highlighted. Blue dots of any shade represent proteins identified in both iPOND-MS and VII IP-MS. Dark blue dots represent proteins significantly enriched on mock or Ad5 iPOND proteomes. *Data in panels A and C generated by Daphne Avgousti and Emigdio Reyes. Proteomic analyses by Kasia Kulej and Joseph Dybas.*

Figure 3.9

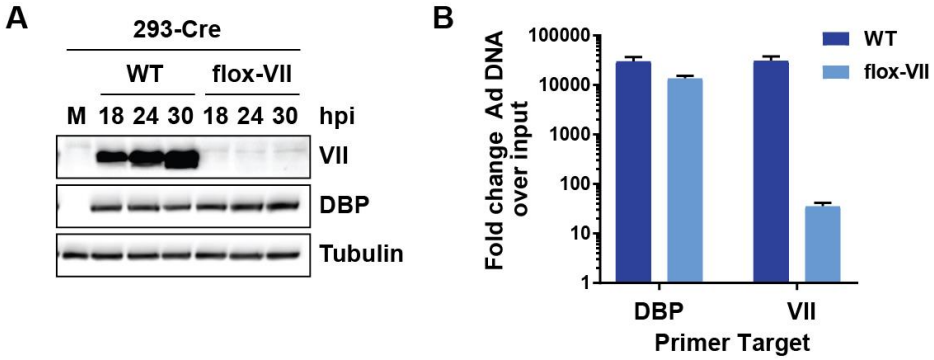

Figure 3.9: Protein VII is deleted without a dramatic effect on viral replication. (A) Western blot demonstrating protein VII is expressed when 293-Cre cells are infected with wild-type Ad5, but not when 293-Cre cells are infected with flox-VII virus. **(B)** qPCR results demonstrating similar DNA accumulation between wild-type and flox-VII viruses and decreased protein VII during infection with flox-VII.

Figure 3.10

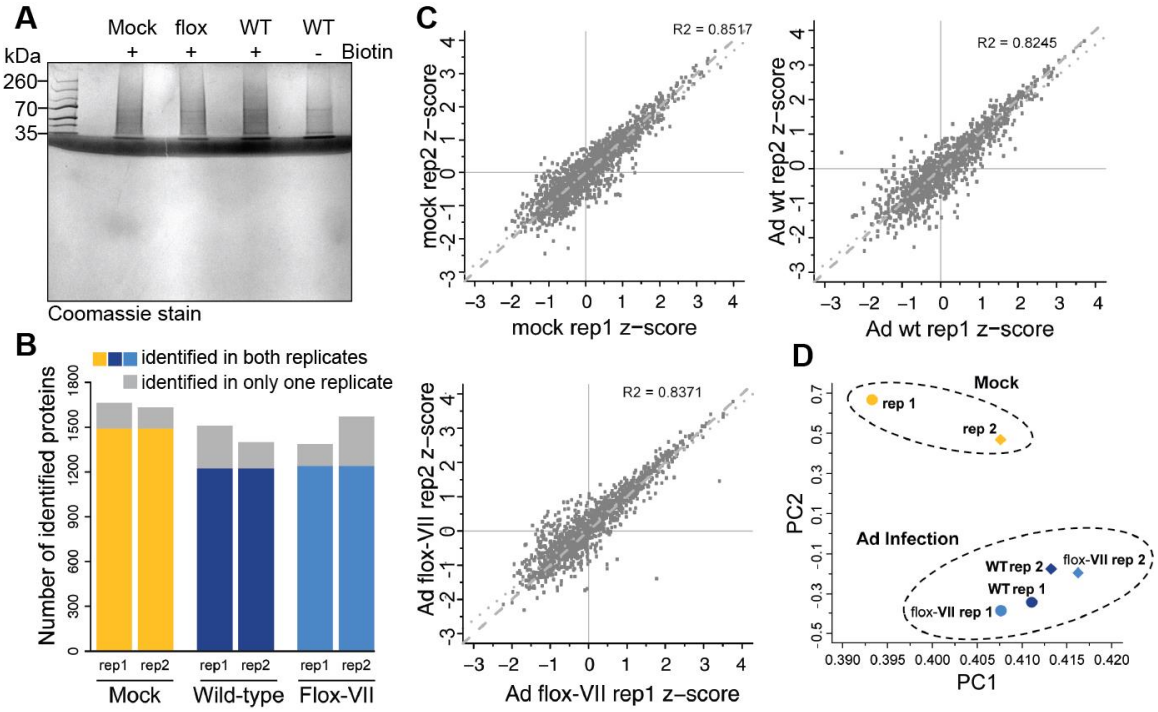

Figure 3.10: High reproducibility between iPOND replicates. (A) Coomassie stained gel of iPOND elution samples. As expected, “no biotin” negative control samples had lower protein content than “+ biotin” samples. Proteins were excised from the gel and identified by mass spectrometry. **(B)** Comparison of proteins identified in each biological replicate. The colored portion of each bar represents proteins identified in both biological replicates of each sample. The grey portion of each bar represents proteins identified in only one biological replicate. The vast majority of identified proteins were identified in both biological replicates. **(C)** Comparison of Z-score abundances of identified proteins between biological replicates. The dashed line represents perfect correlation. Proximity to the dashed line indicates that proteins identified were at similar abundances between biological replicates. **(D)** Principal component analysis. Samples cluster by condition (mock or infected). *Proteomic analyses in panels B-D by Joseph Dybas.*

Figure 3.11

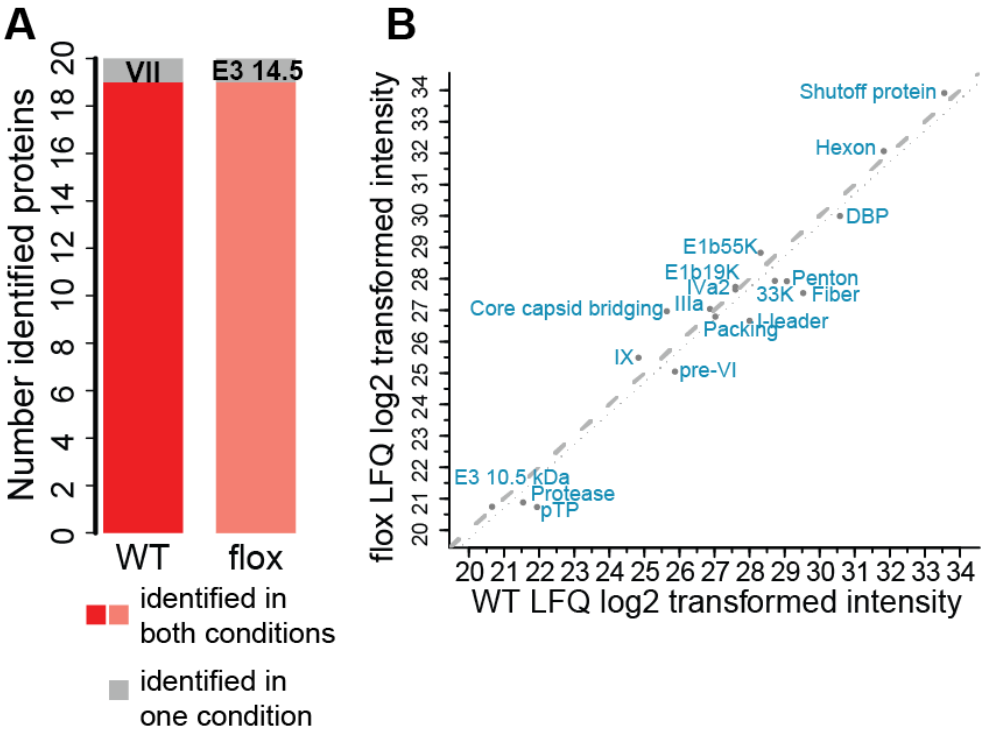

Figure 3.11: Protein VII deletion does not dramatically affect viral proteins associated with viral genomes. (A) Comparison of proteins identified between wild-type and VII-deleted (flox) samples. The colored portion of each bar represents proteins identified in both conditions. The grey portion of each bar represents a protein unique to that condition. The name of each unique protein is included. **(B)** Comparison of protein abundance between conditions. Viral proteins are found at similar abundances in wild-type and flox-VII iPOND samples. *Proteomic analyses by Joseph Dybas.*

Figure 3.12

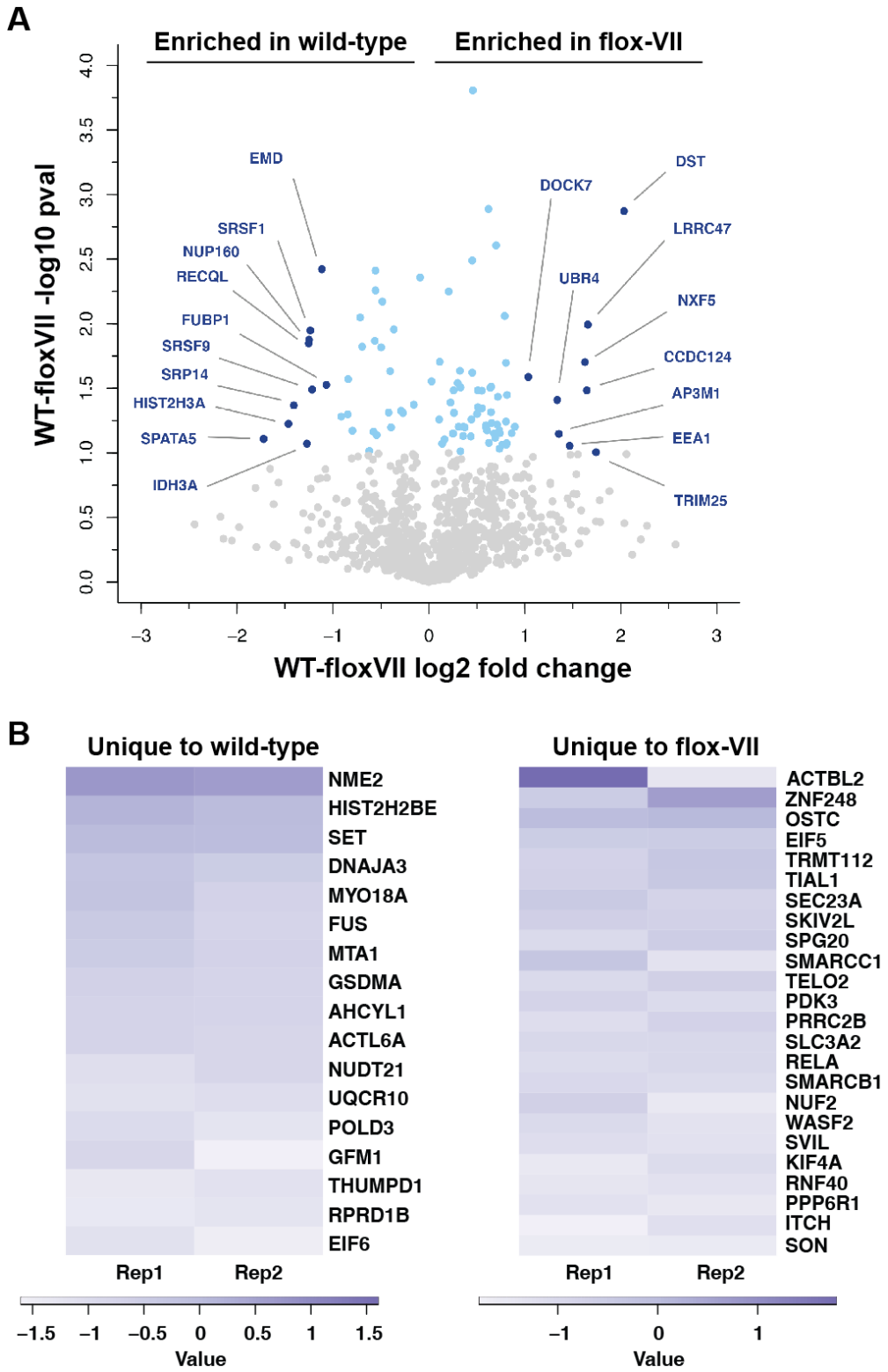
A
Enriched in wild-type
Enriched in flox-VII
WT-floxVII -log10 pval
WT-floxVII log2 fold change
EMD
SRSF1
NUP160
RECQL
FUBP1
SRSF9
SRP14
HIST2H3A
SPATA5
IDH3A
DOCK7
UBR4
DST
LRRC47
NXF5
CCDC124
AP3M1
EEA1
TRIM25
B
Unique to wild-type
NME2
HIST2H2BE
SET
DNAJA3
MYO18A
FUS
MTA1
GSDMA
AHCYL1
ACTL6A
NUDT21
UQCR10
POLD3
GFM1
THUMPD1
RPRD1B
EIF6
Rep1
Rep2
Value
Unique to flox-VII
ACTBL2
ZNF248
OSTC
EIF5
TRMT112
TIAL1
SEC23A
SKIV2L
SPG20
SMARCC1
TELO2
PDK3
PRRC2B
SLC3A2
RELA
SMARCB1
NUF2
WASF2
SVIL
KIF4A
RNF40
PPP6R1
ITCH
SON
Rep1
Rep2
Value

Figure 3.12: Protein VII deletion significantly alters cellular proteins associated with viral genomes. (A) Volcano plot demonstrates that several cellular proteins are significantly enriched on either wild-type or protein VII-deleted (flox-VII) genomes. Blue dots represent proteins significantly enriched ($p<0.05$), and dark blue dots are those proteins with fold change > 2. **(B)** Heat maps of proteins identified in only wild-type or protein VII-deleted (flox-VII) iPOND samples. SET was found on only wild-type genomes, consistent with the known role of protein VII in recruiting SET to viral genomes. *Proteomic analyses by Joseph Dybas.*

Table 3.2

UniProt ID	Gene Name	Protein Name	*t-test* *p*-value (wild-type/ flox-VII)	log_2 Fold Change (wild-type/ flox-VII)	Function
Q8NB90	SPATA5	Spermatogenesis-associated protein 5	0.078208671	1.723378674	Functions during spermatogenesis[1], and mutations in this gene are linked to encephalopathy and intellectual disability[2]; binds nucleotides and ATP[1]
Q71DI3	HIST2H3A	Histone H3.2	0.059658547	1.46571257	Core component of nucleosomes; regulates DNA accessibility
P37108	SRP14	Signal recognition particle 14 kDa protein	0.043096611	1.40764112	Together with SRP9, binds RNA and targets secretory proteins to the rough ER[3]
P50213	IDH3A	Isocitrate dehydrogenase subunit alpha	0.085079924	1.272082419	Metabolic process; converts isocitrate and NAD+ to 2-oxoglutarate, CO2, and NADH
P46063	RECQL	ATP-dependent DNA helicase Q1	0.014207372	1.252242314	3'-5' DNA helicase involved in DNA repair[4]
Q12769	NUP160	Nuclear pore complex protein Nup160	0.013324221	1.249491222	Nuclear pore protein involved in poly(A) mRNA export[5] and mitotic spindle assembly[6]
Q07955	SRSF1	Serine/arginine-rich splicing factor 1	0.011327135	1.236581772	Regulates mRNA splicing, prevents exon skipping, binds spliceosome components, and may also contribute to mRNA export[7]
Q13242	SRSF9	Serine/arginine-rich splicing factor 9	0.032430576	1.216693947	Regulates mRNA splicing[8], regulates alternative splice site selection[8], has been shown to repress splicing of MAPT/Tau[9]
P50402	EMD	Emerin	0.003789269	1.115068304	Stabilizes actin polymerization[10]; promotes beta-catenin nuclear export to inhibit its functions[11]; required for association of HIV-1 DNA with host chromatin[12]
Q96AE4	FUBP1	Far upstream element-binding protein 1	0.029789051	1.068685159	Binds upstream of *myc* promoter[13]; can activate or repress transcription[13]; binds adenovirus E1A and promotes viral replication[14]

[1] (Y. Liu, Black, Kisiel, & Kulesz-Martin, 2000) [2] (Tanaka et al., 2015) [3] (Dani, Singh, & Singh, 2003) [4] (Pike et al., 2015) [5] (Vasu et al., 2001) [6] (Orjalo et al., 2006) [7] (Das & Krainer, 2014) [8] (Graveley, 2000) [9] (Corbo, Orru, & Salvatore, 2013) [10] (Chang, Folker, Worman, & Gundersen, 2013) [11] (Markiewicz et al., 2006) [12] (Jacque & Stevenson, 2006) [13] (J. Zhang & Chen, 2013) [14] unpublished data presented at 2016 DNA Tumor Virus Meeting, P. Pelka

Table 3.2: Proteins enriched on wild-type viral genomes. A student's T test was used to identify proteins significantly more abundant on viral genomes during wild-type infection when compared to flox-VII infection. Proteins that were significant ($p<0.05$) and had a fold change in abundance > 2 are shown here.

Table 3.3

UniProt ID	Gene Name	Protein Name	*t-test* *p*-value (wild-type/ flox-VII)	log_2 Fold Change (wild-type/ flox-VII)	Function
Q03001	DST	Dystonin	0.001350666	-2.032831456	Regulates intermediate filaments, actin, and microtubule networks[1]; promotes HSV entry[2]
Q14258	TRIM25	E3 ubiquitin/ISG15 ligase TRIM25	0.099321326	-1.742417966	Ubiquitin and ISG E3 ligase, ubiquitinates DDX58 to trigger interferon signaling and production[3]
Q8N1G4	LRRC47	Leucine-rich repeat-containing protein 47	0.010231695	-1.656250822	not well characterized
Q96CT7	CCDC124	Coiled-coil domain-containing protein 124	0.032876411	-1.643837335	Regulates cytokinesis[4]
Q9H1B4	NXF5	Nuclear RNA export factor 5	0.019913025	-1.625222807	mRNA export[5]
Q15075	EEA1	Early endosome antigen 1	0.088568821	-1.465702192	Involved in endosome trafficking, binds phospholipid vesicles[6]
Q9Y2T2	AP3M1	AP-3 complex subunit mu-1	0.071661089	-1.353598547	Part of the AP-3 complex, facilitates vesicle budding from Golgi, may be involved in trafficking to lysosomes[7]
Q5T4S7	UBR4	E3 ubiquitin-protein ligase UBR4	0.038986828	-1.337716242	E3 ubiquitin ligase; co-opted by Dengue virus to degrade STAT2[8]
Q96N67	DOCK7	Dedicator of cytokinesis protein 7	0.025941548	-1.034725994	Guanine nucleotide exchange factor controlling GTPase activity[9]

[1](Ferrier, Boyer, & Kothary, 2013) [2](McElwee, Beilstein, Labetoulle, Rixon, & Pasdeloup, 2013) [3](Martin-Vicente et al., 2017) [4](Telkoparan et al., 2013) [5](Jun et al., 2001) [6](Murray et al., 2016) [7](Chapuy et al., 2008) [8](Morrison et al., 2013) [9](Majewski, Sobczak, Havrylov, Jozwiak, & Redowicz, 2012)

Table 3.3: Proteins enriched on protein VII-deleted viral genomes. A student's T test was used to identify proteins significantly more abundant on viral genomes during flox-VII infection when compared to wild-type infection. Proteins that were significant ($p<0.05$) and had a fold change in abundance > 2 are shown here.

Figure 3.13

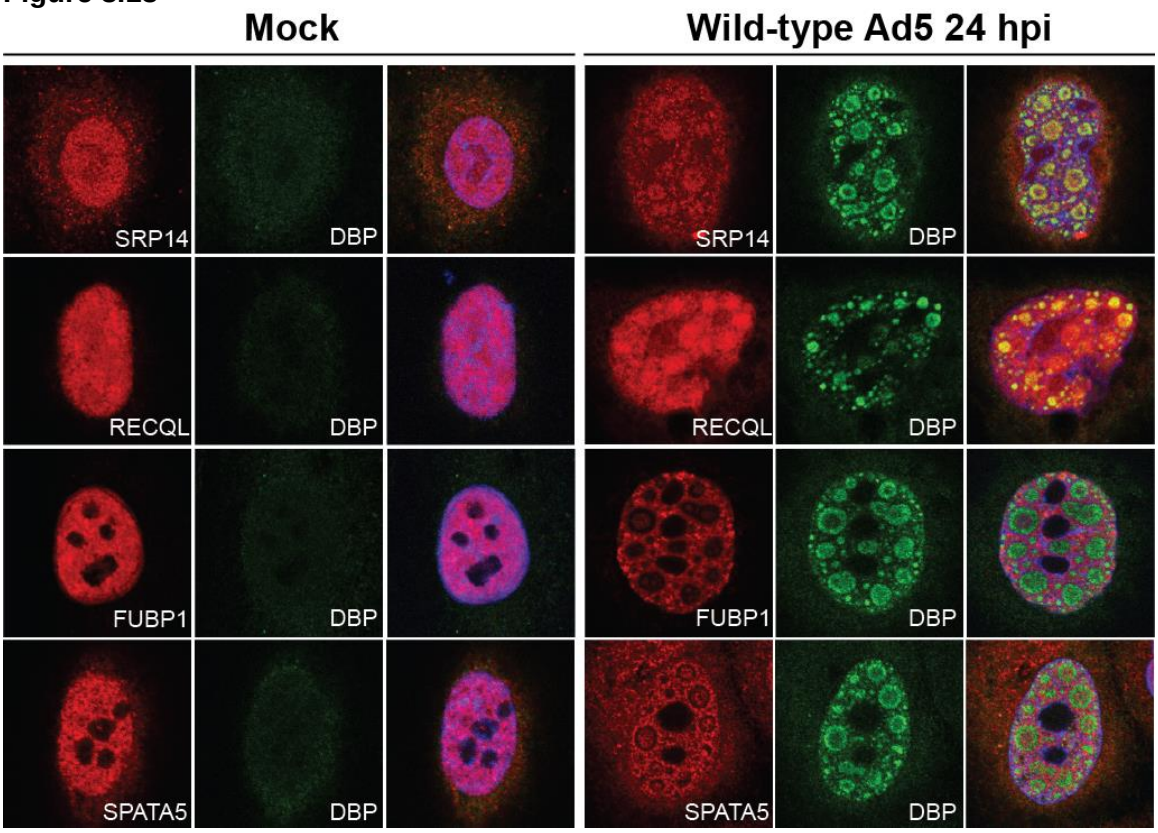

Figure 3.13: Localization of identified proteins during wild-type Ad5 infection. Immunofluorescence analysis of wild-type infected cells to determine localization of proteins enriched on wild-type genomes. A549 cells were infected with wild-type Ad5 for 24 hours. Several identified proteins are redistributed during wild-type Ad5 infection. DBP marks viral replication centers.

Figure 3.14

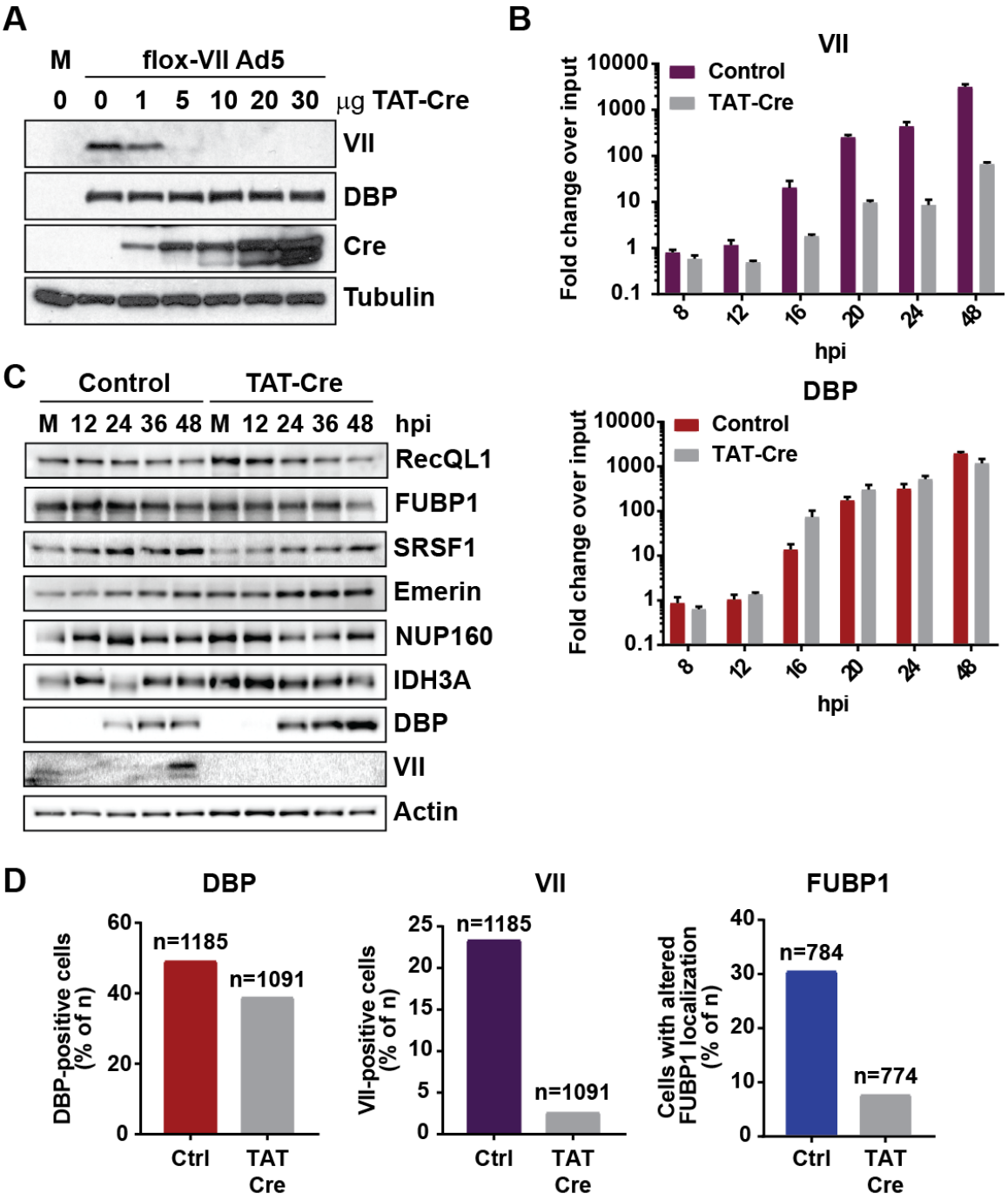

Figure 3.14: Changes to cellular protein localization are dependent on protein VII. **(A)** Western blot analysis demonstrates protein VII deletion during infection of A549 cells pre-treated with increasing amounts of TAT-Cre protein. DBP levels are unaffected by

TAT-Cre treatment or protein VII deletion. **(B)** A549 cells in 12-well plates were pre-treated with 15 μg TAT-Cre and infected with flox-VII at MOI 10. Cells were collected at the indicated time points, DNA was isolated, and qPCR was performed using primers specific to protein VII or DBP. qPCR results demonstrate a decrease in genomes containing protein VII, but no effect on total genome accumulation. **(C)** Western blot analysis of protein levels during infection in control or TAT-Cre treated cells. Cells were treated as described in **B**. TAT-Cre treatment results in protein VII deletion, but does not dramatically affect levels of cellular proteins. **(D)** Quantification of immunofluorescence results. A549 cells in 12-well plates were pre-treated with 45 μg TAT-Cre or treated with 50% glycerol as a control. Cells were infected with flox-VII virus at MOI 10 and collected for immunofluorescence after 24 hours of infection. Quantification of DBP-positive cells demonstrates that TAT-Cre treatment has only a minimal effect on infection efficiency but has a dramatic impact on protein VII expression. Quantification of FUBP1 localization pattern demonstrates an approximately 3-fold decrease in the proportion of total cells exhibiting changes to FUBP1 localization. “n” is the number of total cells counted.

Figure 3.15

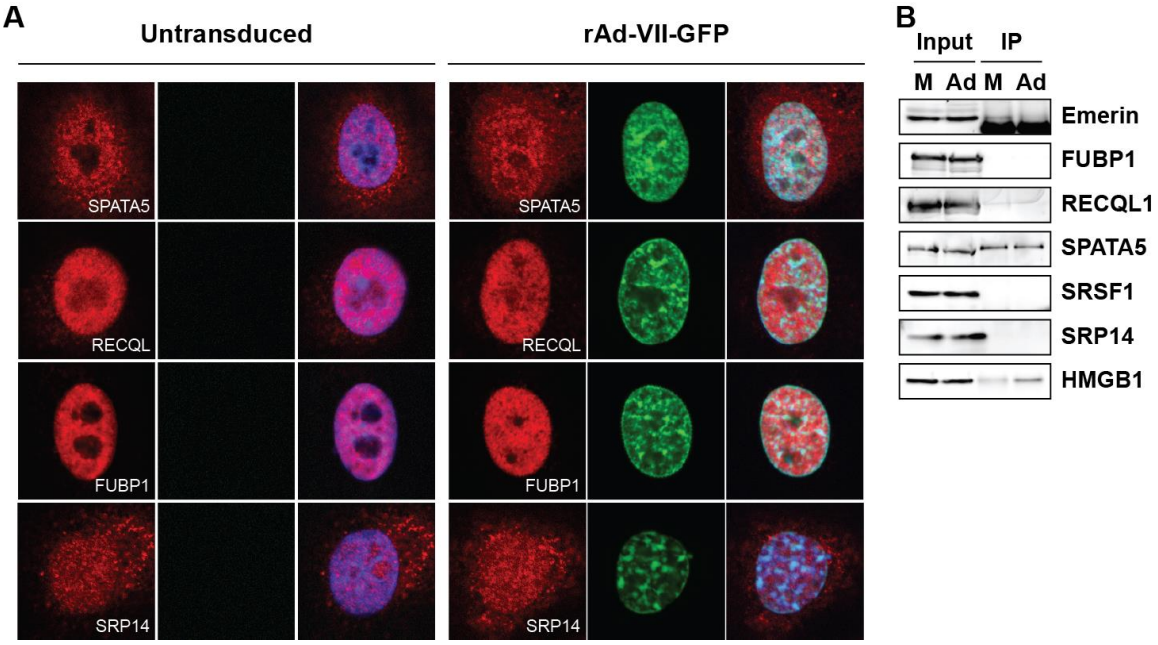

Figure 3.15: Protein VII is not sufficient to alter protein localization and does not interact with identified proteins during infection. (A) A549 cells were transduced with a recombinant Ad vector expressing GFP-tagged protein VII. Immunofluorescence of cells 24 hours post-transduction shows that protein VII expression is not sufficient to induce the localization changes observed during infection. **(B)** Immunoprecipitation of protein VII from infected A549 cells using an antibody targeting protein VII. HMGB1 is a positive control for protein VII-interacting protein. Co-immunoprecipitation of the other proteins could not be detected.

Figure 3.16

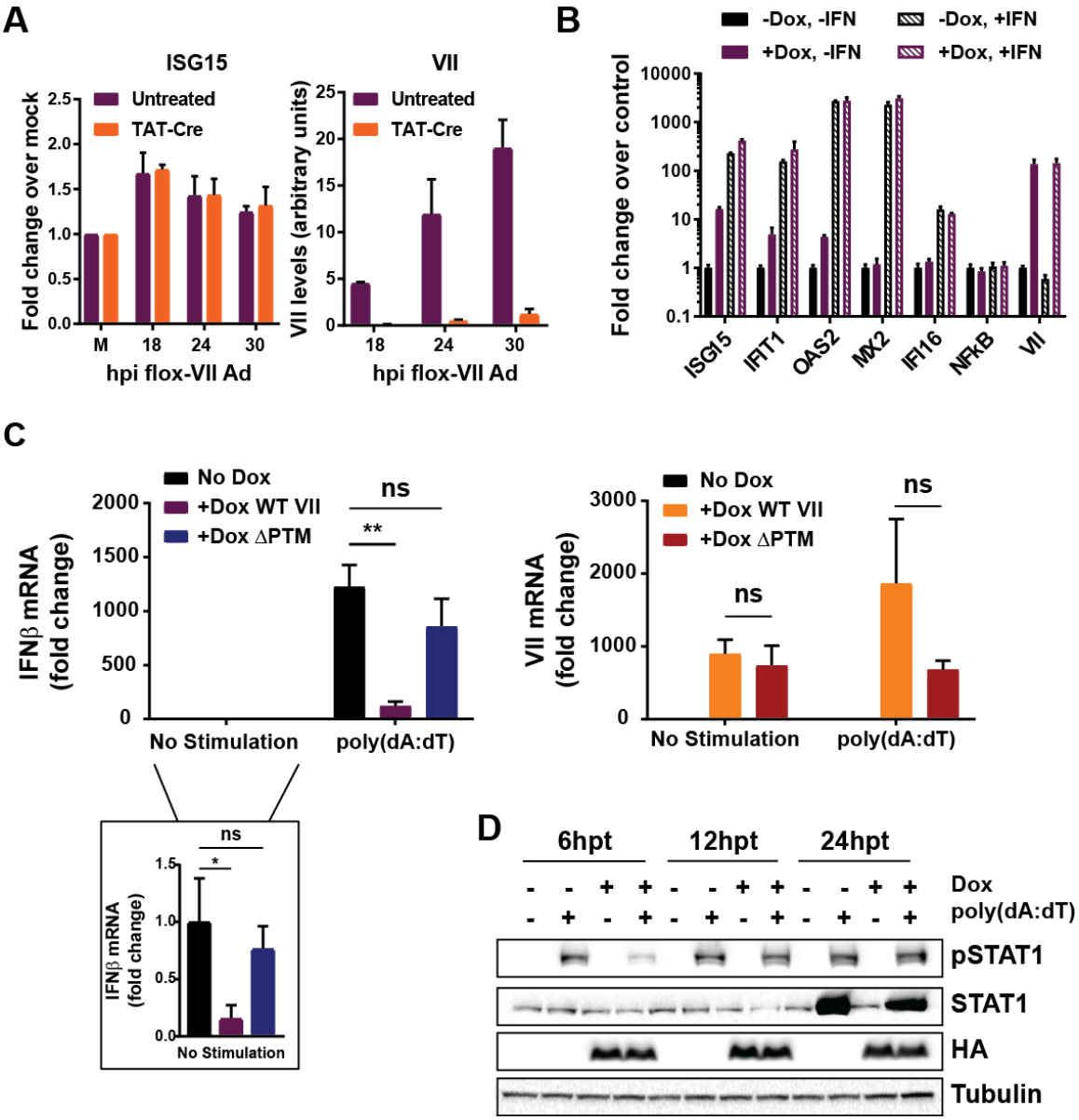

Figure 3.16: Effect of protein VII on the interferon response. (A) RT-PCR results examining mRNA levels of ISG15, an interferon stimulated gene, when protein VII is deleted during infection. Protein VII deletion does not affect expression of ISG15 (left). Right panel shows decreased protein VII expression in appropriate samples. Results are the average of three biological replicates, and error bars represent standard deviation. **(B)** RT-PCR results examining mRNA levels of interferon stimulated genes in response

to ectopic treatment with type I IFN. NfkB serves as a negative control since its expression is upstream of IFN expression, and VII verifies expression in appropriate samples. Values are normalized to the parental, untreated sample. Type I IFN treatment increases ISG expression, as expected. Protein VII expression does not impact ISG expression in response to IFN treatment. Results are the average of three biological replicates, and error bars represent standard deviation. **(C)** RT-PCR results showing the effect of protein VII expression on IFNβ mRNA levels. A549 cells were induced for 4 days to express wild-type or ΔPTM protein VII. Cells were transfected with poly(dA:dT) DNA and harvested 8 hours post-transfection. IFNβ levels were measured by RT-PCR. Wild-type protein VII expression suppresses IFNβ mRNA levels in unstimulated and poly(dA:dT) stimulated cells. Results are the average of three biological replicates, and error bars represent standard deviation. * = $p<0.05$; ** = $p < 0.01$; ns = not significant. Right panel confirms protein VII expression in appropriate samples. **(D)** Western blot analysis of STAT1 phosphorylation in response to poly(dA:dT) stimulation in uninduced and induced cells. At 6 hours post-transfection of poly(dA:dT) DNA, STAT1 phosphorylation is dramatically decreased in protein VII-expressing cells compared to uninduced controls.

Figure 3.17

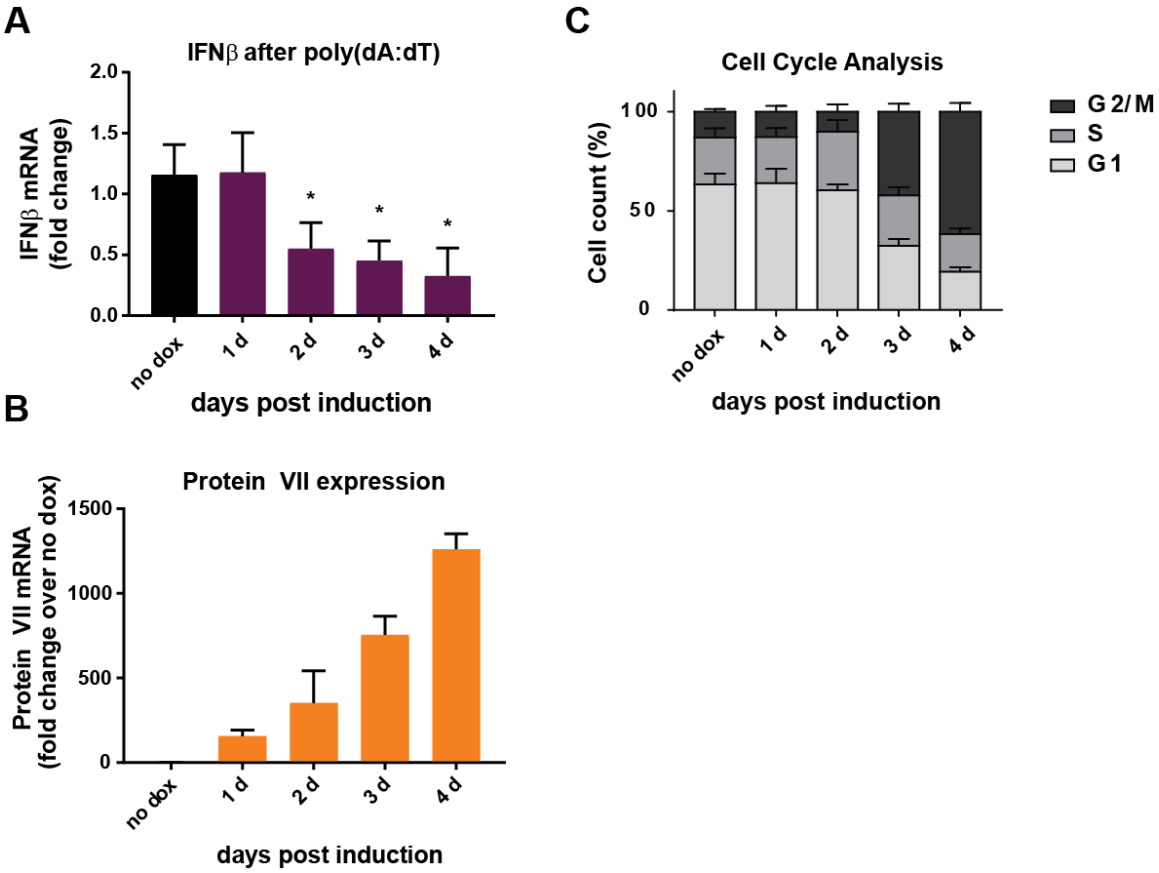

Figure 3.17: Effect of protein VII on IFNβ is independent of protein VII's effect on the cell cycle. (A) IFNβ levels were examined by RT-PCR over a time course of doxycycline induction. Values were normalized to the "no dox" sample. * = $p<0.05$. The average of three biological replicates is shown, and error bars represent standard deviation. **(B)** Protein VII levels in samples from panel **A**. The average of three biological replicates is shown. Error bars show standard deviation. **(C)** Cell cycle profile over a time course of induction. DNA content was measured by flow cytometry of propidium iodide-stained samples. The average of at least three biological replicates is shown. Error bars are standard deviation. *Panel C generated by Ashley Della Fera.*

Figure 3.18

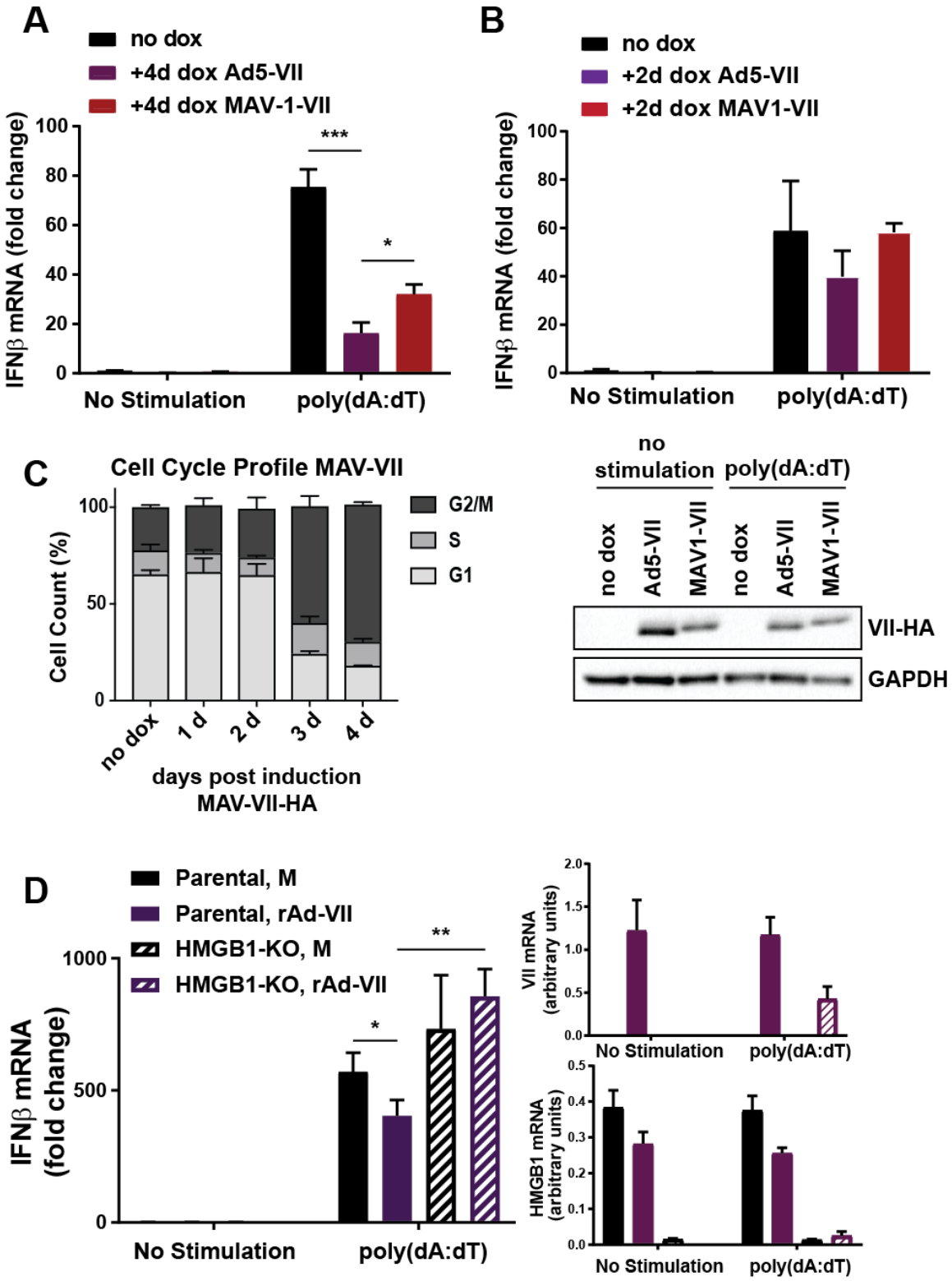
A
no dox
+4d dox Ad5-VII
+4d dox MAV-1-VII
IFNβ mRNA (fold change)
100
80
60
40
20
0
***
*
No Stimulation
poly(dA:dT)
B
no dox
+2d dox Ad5-VII
+2d dox MAV1-VII
IFNβ mRNA (fold change)
No Stimulation
poly(dA:dT)
C
Cell Cycle Profile MAV-VII
Cell Count (%)
G2/M
S
G1
no dox
1 d
2 d
3 d
4 d
days post induction
MAV-VII-HA
no stimulation
poly(dA:dT)
no dox
Ad5-VII
MAV1-VII
no dox
Ad5-VII
MAV1-VII
VII-HA
GAPDH
D
Parental, M
Parental, rAd-VII
HMGB1-KO, M
HMGB1-KO, rAd-VII
IFNβ mRNA (fold change)
1000
500
0
*
**
No Stimulation
poly(dA:dT)
VII mRNA (arbitrary units)
2.0
1.5
1.0
0.5
0.0
No Stimulation
poly(dA:dT)
HMGB1 mRNA (arbitrary units)
0.5
0.4
0.3
0.2
0.1
0.0
No Stimulation
poly(dA:dT)

Figure 3.18: HMGB1 may contribute to protein VII-mediated IFN suppression. (A) IFNβ mRNA levels in cells expressing protein VII from Ad5 or MAV-1 after 4 days of induction. The average of three biological replicates is shown, and error bars show standard deviation. * = $p<0.05$; *** = $p<0.001$. IFNβ levels are significantly higher in cells expressing MAV-1 protein VII than Ad5 protein VII. **(B)** As in **A**, but with only 2 days of dox induction. Western blot (bottom) confirms protein VII expression. **(C)** Cell cycle profile of cells expressing MAV-1 protein VII over a time course of dox induction. DNA content was measured by flow cytometry of propidium iodide stained cells. MAV-1 VII expression results in accumulation of cells in G2/M after 3 days of dox treatment. The average of three biological replicates is shown. Error bars are standard deviation. **(D)** Left - The effect of protein VII on IFNβ mRNA levels was measured in wild-type and HMGB1-deleted cells. Right – protein VII and HMGB1 expression. The average of three biological replicates is shown. Error bars show standard deviation. * = $p<0.05$; ** = $p<0.01$. *Panel C generated by Ashley Della Fera.*

Discussion

In this chapter, we demonstrate the power of a proteomics approach to identify novel host factors associated with viral genomes and to identify novel targets of specific viral proteins. We found that comparing the cellular proteins associated with viral DNA to those associated with cellular DNA can be used to identify proteins that are targeted or harnessed by viruses to promote viral processes. For example, we used this strategy to identify TCOF1 and SLX4 as cellular proteins recruited by Ad5 to enhance viral replication and TFII-I as a cellular protein that is targeted for degradation by Ad5 (**Figure 3.2**). Furthermore, we demonstrated that comparing host proteins associated with wild-type and mutant viral genomes can be used to understand how specific viral proteins manipulate or exploit cellular proteins. In **Figure 3.3A**, we demonstrated that comparison of proteins associated with wild-type and E4-deleted Ad5 identified known E4 targets, which validated our approach. We then compared wild-type and ICP0-deleted HSV-1 proteomes and identified potential ICP0 targets (**Figure 3.3B**). We conclude that iPOND-MS is a valuable resource to identify strategies used by viruses to regulate interactions of cellular proteins with viral genomes.

We also identified novel functions for a viral DNA-binding protein in influencing interactions on viral and cellular genomes. We found that this small basic core protein, called protein VII, is found at both viral and cellular genomes during infection and is sufficient to alter the proteins associated with host chromatin. We identified the HMGB family proteins as targets of protein VII and demonstrated that protein VII is necessary and sufficient to sequester HMGB proteins in cellular chromatin. These data suggested that manipulation of proteins in cellular chromatin could be a previously unexplored strategy used by adenovirus to manipulate cellular processes. Interestingly, protein VII produced by murine adenovirus localizes to chromatin and manipulates chromatin

structure, but does not sequester HMGB1. This suggests that murine HMGB1 may not impact MAV-1 replication, or MAV-1 may employ a different strategy to manipulate or harness HMGB1 function. It is possible that MAV-1 protein VII sequesters different cellular proteins in chromatin to promote viral replication. It would be interesting to identify the proteins targeted by MAV-1 protein VII to gain insight into the effects of MAV-1 protein VII localization to chromatin.

The impact of protein VII on proteins associated with cellular chromatin led us to investigate whether protein VII could also affect which cellular proteins associate with viral genomes. By comparing protein VII-interacting proteins with those identified on adenovirus genomes by iPOND, we found that several protein VII-interacting proteins are associated with viral genomes during infection (**Figure 3.8C**). We therefore hypothesized that protein VII regulates interactions of cellular proteins with viral genomes. We utilized the iPOND strategies we had optimized to test this hypothesis. Confirming our hypothesis, iPOND analysis of wild-type and protein VII-deleted viruses identified several cellular proteins that are significantly enriched on viral genomes under either wild-type or protein VII-deleted conditions. We predicted that protein VII would recruit cellular proteins that promote viral processes, while preventing association with anti-viral proteins. Consistent with this prediction, we found that proteins involved in DNA replication, transcription, RNA splicing, and mRNA export were significantly more abundant on viral genomes in the presence of protein VII. We observed that several of these proteins localize to sites of viral DNA replication or transcription (**Figure 3.13**), consistent with their association with isolated viral genomes by iPOND. Furthermore, we demonstrated that this localization was dependent on protein VII for at least one of the identified proteins (**Figure 3.14**). Future experiments will examine localization of other identified proteins when protein VII is deleted. While several of the proteins enriched on

wild-type genomes co-precipitate with ectopically expressed protein VII by IP-MS, we did not detect interaction with protein VII during Ad5 infection. Furthermore, expression of protein VII was not sufficient to alter localization of these proteins. These data suggest that the identified cellular proteins may not be actively recruited by protein VII. Instead, changes to DNA conformation or accessibility may promote association of these cellular proteins with viral genomes.

There are conflicting reports as to the effect of protein VII on viral transcription (see **Chapter 1**). While some evidence suggests that protein VII-mediated DNA condensation impairs DNA accessibility for transcription (Matsumoto et al., 1993; Okuwaki & Nagata, 1998), other reports demonstrate enhanced transcription when protein VII is added to *in vitro* transcription assays (Komatsu et al., 2011). Our results indicate that protein VII enhances the association of replication and transcription proteins with viral genomes. This would suggest that protein VII promotes viral DNA replication and transcription. It is important to note that our results do not allow us to determine where on the viral genome protein VII or cellular proteins are associated. Therefore, it is possible that protein VII and identified cellular proteins do not occupy the same regions of the genome. Protein VII could be reorganized to condense certain regions of the genome, while decondensing other regions to be more accessible to cellular proteins such as those we found to be associated with viral genomes. Thus, it is possible that protein VII inhibits transcription of some genes through DNA condensation, while promoting transcription of genes that it does not occupy by allowing association of cellular transcription proteins through an undefined mechanism. Curiously, we did not observe a dramatic effect on viral DNA replication or viral protein levels when protein VII was deleted. One possible explanation for this observation is the presence of incoming protein VII. Infection of 293-Cre cells with flox-VII virus results in deletion of the protein VII gene from viral genomes

during infection, resulting in dramatically reduced levels of protein VII. However, genomes of flox-VII virus are still packaged with protein VII, and these enter the nucleus with viral genomes. Incoming protein VII may be sufficient to promote localization of transcription and DNA replication proteins to early viral replication centers. Early localization of these proteins to viral replication centers may allow these proteins to stay in proximity to nascent viral genomes as infection progresses, even in the absence of *de novo* protein VII synthesis. In such a scenario, decreased protein VII levels would lead to significantly lower abundance of these cellular proteins on viral genomes since *de novo* protein VII would not be present to promote higher levels of these proteins at viral replication centers. However, the amount of these cellular proteins recruited early during infection may be sufficient to allow replication and transcription to occur at near wild-type levels. An alternative explanation could be that other cellular proteins that are not regulated by protein VII are redundant for the functions of those proteins that are significantly lower when protein VII is deleted.

We also examined proteins enriched on protein VII-deleted viral genomes to identify pathways potentially targeted by protein VII. UBR4 and TRIM25 were significantly enriched on protein VII-deleted genomes and are known to be involved in the interferon pathway (Martin-Vicente et al., 2017; Morrison et al., 2013). We therefore investigated whether protein VII impacted interferon signaling. We found that protein VII expression led to significantly decreased levels of IFNβ mRNA in response to stimulation by poly(dA:dT) transfection, but did not affect mRNA levels of ISGs in response to stimulation by type I interferon. The effect of protein VII, therefore, must be upstream of IFNβ production. Since HMGB1 has been suggested to promote detection of cytoplasmic DNA by cellular sensors (Andreeva et al., 2017), we hypothesized that protein VII-mediated sequestration of HMGB1 to host chromatin could prevent IFN

signaling by preventing recognition of foreign DNA. Consistent with this hypothesis, we found that HMGB1 and localization of protein VII to chromatin may contribute to suppression of IFNβ in response to poly(dA:dT) stimulation. However, we found that protein VII expression also led to decreased IFNβ mRNA in unstimulated cells. This suggests that the effect of protein VII may not be specific to poly(dA:dT) stimulation or detection of foreign DNA. The effects of protein VII could instead be through changes to the DNA conformation of the IFNβ locus, or through recruitment of transcriptional regulators such as HMGB1. It is possible that protein VII recruits HMGB1 to repress transcription of IFNβ. This is consistent with the observed increase in IFNβ levels in the absence of HMGB1 (**Figure 3.18D**). Together, our results suggest that protein VII suppresses IFNβ mRNA levels through a mechanism consistent with chromatin localization and HMGB1. The details of this mechanism require further study (see **Chapter 4**), but these data raise the possibility that protein VII could suppress host defenses by targeting the anti-viral interferon response.

Protein VII suppression of interferon signaling represents a previously unidentified mechanism used by adenovirus to evade this anti-viral pathway. As described in **Chapter 1**, several early adenovirus proteins and VA-RNA contribute to evasion of interferon-stimulated genes. This is the first demonstration of a late adenovirus protein in suppressing interferon. It is interesting to speculate on the reasons a late viral protein would need to target interferon. By the time *de novo* protein VII is expressed, viral DNA replication and transcription have already initiated. Thus, suppression of interferon at this stage would not be required for DNA replication or viral protein expression. This is consistent with our observations that viral DNA replication is not dramatically affected by protein VII deletion during infection (**Figures 3.7, 3.9,** and **3.14**). Protein VII's effect on

interferon may instead be required for proper viral spread. IFNβ is released from cells and activates interferon signaling in neighboring cells through paracrine signaling. This establishes anti-viral environments in activated cells that could prevent infection by released viral particles. During late stages of infection, the virus is preparing to be released from the cell. It would be beneficial for the virus to prevent interferon activation in neighboring cells to allow for optimal viral spread. This may be especially important at late stages of infection, when large amounts of accumulated viral DNA and protein could lead to interferon activation. Therefore, the benefit of protein VII-mediated IFN suppression may not be on viral processes within the infected cell, but rather through promoting viral spread.

For this project, we focused our experiments on the host proteins that are involved in processes known to be manipulated by adenovirus, such as transcription, splicing, and interferon signaling. However, our iPOND analysis also identified proteins involved in protein trafficking, vesicle budding, cytoskeletal organization, and metabolic processes as differentially regulated by protein VII (**Tables 3.2** and **3.3**). This raises the possibility that protein VII could manipulate these processes either directly or indirectly and could thereby regulate cellular integrity.

Together, results from this chapter demonstrate that identifying cellular proteins associated with adenovirus genomes can uncover host factors that facilitate or hinder viral replication. Furthermore, comparing proteins associated with viral genomes during infection with wild-type or mutant viruses can reveal novel targets and functions of specific viral proteins. Here, we found that protein VII deletion affects the association of cellular proteins with both viral and cellular genomes. Our data suggest that protein VII may promote association of transcription, splicing, and RNA export proteins with viral

genomes, while suppressing anti-viral responses. Results from this chapter contribute to our growing understanding of protein VII's impact on multiple viral and cellular processes, likely through regulating DNA-protein interactions.

CHAPTER 4:

Discussion

Summary

Successful viral propagation relies on manipulation of cellular proteins and pathways to establish a cellular environment conducive to viral replication. Defining the mechanisms underlying viral manipulation and understanding the outcomes of such manipulation contribute to our comprehension of viral life cycles, as well as fundamental cellular processes. Moreover, studying virus-host interactions can lead to improved strategies for anti-viral therapeutics and viral vectors for gene therapy. Viruses utilize a myriad of strategies to manipulate host cells in order to hijack cellular processes that benefit viruses, and suppress or redirect those that impair viral growth. My thesis work focused on understanding how adenovirus manipulates association of cellular proteins with viral genomes. As a nuclear replicating DNA virus, adenovirus genomes are accessible to cellular DNA-binding proteins, and adenovirus must therefore carefully regulate which cellular proteins interact with them. In each chapter of this thesis, I discussed strategies we used to understand how adenoviruses evade association of anti-viral cellular proteins with viral genomes and how they promote recruitment of beneficial cellular proteins. These approaches uncovered previously unidentified targets of viral manipulation and mechanisms used by viruses to either target or exploit cellular proteins. In **Chapter 2**, I described how comparison of evolutionary diverse adenovirus serotypes revealed differences in the ways that viruses target a previously identified intrinsic defense. In **Chapter 3**, I described how comparing the proteins associated with viral and cellular genomes identified novel targets of viral manipulation and identified cellular proteins that are exploited by adenovirus. Furthermore, we demonstrated that comparing proteins between wild-type and mutant viral genomes identifies proteins manipulated by specific

viral proteins. These projects build on our knowledge of adenovirus and contribute to understanding diverse mechanisms used by viruses to manipulate host cells. Our interpretations are summarized in the discussion section of each respective chapter. Here, I will discuss future directions to build on this work and the broader implications of these findings.

Future directions

How does Ad9 mislocalize MRN?

Are additional viral proteins required?

In **Chapter 2**, we demonstrated that Ad9 infection results in mislocalization of MRN to E4orf3-PML tracks, but expression of Ad9-E4orf3 is not sufficient to affect MRN localization. This raises the question of what exactly changes during infection to allow for MRN mislocalization. One possibility is that another viral protein contributes to mislocalization. This protein could work together with E4orf3 to target MRN, or it may be sufficient to mislocalize MRN. A potential candidate that we have begun to explore is the Ad9-E1b55K protein. Studies with Ad5 have demonstrated that E1b55K is found at several locations in the cell during Ad5 infection, including colocalized with E4orf3-PML tracks. We reasoned that Ad9-E1b55K may share this localization and could recruit MRN to these tracks. We therefore investigated the effect of Ad9-E1b55K on MRN localization. We expressed HA-tagged Ad9-E1b55K and observed localization of MRN by immunofluorescence. Unlike Ad5-E1b55K, which is cytoplasmic in the absence of E4orf3 or E4orf6, Ad9-E1b55K is found in the nucleus in track-like structures (**Figure 4.1**). Intriguingly, we found that transfection of Ad9-E1b55K was sufficient to reorganize MRN from a pan-nuclear distribution to track-like structures that colocalized with Ad9-E1b55K (**Figure 4.1**). Initially, this suggested that Ad9-E1b55K could be sufficient to mislocalize MRN to E4orf3 tracks. However, when we co-transfected Ad9-E1b55K and

Ad9-E4orf3, we found that these proteins do not colocalize (**Figure 4.1**). It appears that Ad9-E1b55K can reorganize MRN but cannot recruit it to E4orf3-PML tracks. This raises several questions about how MRN is targeted by viral proteins during Ad9 infection. Future experiments should investigate the requirements for MRN mislocalization further. For example, do Ad9-E1b55K and Ad9-E4orf3 colocalize during infection? If we find that these viral proteins co-localize during infection, this would suggest that changes induced during infection allow Ad9-E1b55K to localize with Ad9-E4orf3-PML tracks. Localization of Ad5-E1b55K to PML is regulated by SUMOylation of E1b55K. Ad9-E1b55K localization may be similarly regulated. It is possible that Ad9-E1b55K is sufficient to interact with MRN but requires SUMOylation to localize to PML tracks during infection.

The observation that Ad9-E1b55K is sufficient to alter MRN localization suggests that Ad9-E1b55K may interact with MRN. This should be determined by co-immunoprecipitation and *in vitro* studies. If Ad9-E1b55K can interact with MRN, this raises the question of why Ad9 does not degrade MRN. E1b55K has long been considered the substrate recognition component of the ubiquitin ligase formed during adenovirus infection. It is possible that interaction of Ad9-E1b55K with MRN components precludes interaction with E4orf6 or cellular components of the ubiquitin ligase due to structural changes to Ad9-E1b55K. The interaction of Ad9-E1b55K with ubiquitin ligase proteins and with MRN may be mutually exclusive. This could be investigated by sequential co-immunoprecipitation studies to determine whether the E1b55K that co-precipitates with E4orf6 is associated with MRN components.

Are post-translational modifications required?

In addition to exploring the role of additional viral proteins, we have also considered the potential role of post-translational modifications (PTMs) on E4orf3 in MRN

mislocalization. We hypothesized that PTMs could occur on Ad9-E4orf3 during Ad9 infection but not when Ad9-E4orf3 is expressed alone, and that these PTMs could enable MRN mislocalization during Ad9 infection. To test this hypothesis, we generated plasmids expressing FLAG-tagged E4orf3 from each of the serotypes in our study. We omitted Ad2-E4orf3, as it is almost identical to Ad5-E4orf3 (99.1%). We transfected the E4orf3 plasmids individually or combined with infection with each respective adenovirus serotype. Immunoblotting of transfected and/or infected samples resulted in FLAG-E4orf3 bands at the expected molecular weight of approximately 11 kDa (**Figure 4.2**). We observed higher molecular weight bands (approximately 20 kDa) for samples expressing Ad5 and Ad9-E4orf3 (**Figure 4.2**), which could represent post-translationally modified E4orf3. Intriguingly, the higher molecular weight band in samples expressing Ad9-E4orf3 intensifies during Ad9 infection (**Figure 4.2**). This may represent a post-translational modification that increases upon Ad9 infection and could explain why MRN is mislocalized during infection. Excision of these gel bands and identification of PTMs by mass spectrometry would be an interesting future direction. Identified PTMs could be tested by mutating the modified site in E4orf3 to determine if this affects its ability to alter MRN localization.

How does protein VII suppress IFNβ levels?

In **Chapter 3**, we found that ectopic expression of protein VII leads to reduced IFNβ mRNA levels and delayed downstream phosphorylation of STAT1. The mechanism by which protein VII suppresses interferon signaling remains unclear and merits further investigation. First, it should be determined whether reduced IFNβ mRNA levels are caused by suppression of transcription or by mRNA instability/degradation. To test this, luciferase assays testing activity of the IFNβ promoter in the presence and absence of

ectopic protein VII expression should be performed. In addition, the phosphorylation status of interferon regulatory factors 3 and 9 (IRF3 and IRF9) should be examined by western blot, since their activation is required for IFNβ expression. These experiments will demonstrate whether protein VII affects IFNβ transcriptional activation. To test whether protein VII affects mRNA stability, nascent IFNβ transcription should be inhibited by treating cells with the transcription inhibitor actinomycin D. The turnover rate of IFNβ transcripts should be measured and compared between control cells and cells expressing protein VII. Together, these experiments would determine whether the effect on IFNβ mRNA is upstream or downstream of transcription.

We observed that the effects of MAV-1 protein VII, which does not affect HMGB1, are less dramatic than those of Ad5 protein VII (**Figure 3.18A-B**). Furthermore, we found that ectopic protein VII expression did not affect IFNβ levels in HMGB1 knockout cells (**Figure 3.18D**), though this could be due to the decreased protein VII levels in HMGB1 knockout cells (**Figure 3.18D**). These observations indicate that HMGB1 could contribute to protein VII-mediated suppression of IFNβ. However, it remains unclear at which step of the interferon pathway protein VII and HMGB1 would be involved. Our initial hypothesis was that protein VII-mediated HMGB1 sequestration could prevent recognition of viral DNA by the cytoplasmic DNA sensor cGAS. This was based on the recently published finding that HMGB1 could promote cGAS activation in mouse cells by altering DNA conformation (Andreeva et al., 2017). Two observations from our experiments suggest this hypothesis may be incorrect. The first is that IFNβ levels are decreased in protein VII-expressing cells in the absence of stimulation by poly(dA:dT) DNA (**Figure 3.16C**). This indicates that the effect of protein VII may not be specific to detection of foreign DNA by sensors like cGAS. The second observation is that deletion

of HMGB1 leads to a rescue in IFNβ levels (**Figure 3.18D**). This demonstrates that the protein VII-mediated suppression of IFNβ is relieved in the absence of HMGB1. If HMGB1 were responsible for promoting IFN activation through cGAS detection, then HMGB1 deletion would not rescue IFN levels. Therefore, it appears that HMGB1 may actually repress IFNβ, and protein VII may harness HMGB1 function rather than inactivating it. This may represent a difference between mouse and human HMGB1, since HMGB1 was shown to promote IFN activation in mouse cells (Andreeva et al., 2017). Human HMGB1 is a known transcriptional regulator (Bianchi & Agresti, 2005); therefore, it is possible that protein VII targets HMGB1 to the IFNβ gene locus to repress transcription. To test this, chromatin immunoprecipitation studies with protein VII and HMGB1 should be performed to determine if these proteins are found at genomic regions that would regulate expression IFNβ.

Does protein VII bind RNA?

We identified several cellular proteins involved in RNA splicing and export as dependent on protein VII for association with viral genomes (**Table 3.2**). Since our iPOND protocol does not include RNA digestion, it is possible that these proteins are isolated due to interactions of RNA with EdU-labeled DNA. In addition, we found that a large portion of protein VII interacting proteins are involved in RNA processes (**Figure 3.8A-B**). This leads us to hypothesize that protein VII could bind viral RNA and influence RNA processes, such as splicing and mRNA export. Consistent with this hypothesis, we have observed that the localization pattern of protein VII resembles that of viral RNA (**Figure 4.3**). Future experiments will test this hypothesis through several experiments. First, fluorescent *in situ* hybridization (FISH) coupled with protein VII immunofluorescence would demonstrate whether protein VII localizes to sites of viral RNA. Second, we will

determine whether protein VII associates with viral RNA by performing RNA immunoprecipitation from infected samples. If protein VII co-precipitates viral RNA, this would indicate that it can associate with RNA either directly or indirectly. To determine whether protein VII can directly bind RNA, we will perform RNA electrophoretic mobility shift assay (RNA EMSA) using purified protein VII. Protein VII interaction with viral RNA would raise the possibility that protein VII can influence viral processes such as splicing and mRNA export by promoting association of relevant cellular proteins. These experiments would contribute to our growing understanding of protein VII functions.

Significance

Common cellular obstacles to adenoviruses

In each chapter of this thesis, we identified cellular proteins that are targeted by serotypes across the adenovirus family. In **Chapter 2**, we demonstrated that several serotypes target MRN by degradation, mislocalization, or by both mechanisms. In **Chapter 3**, we demonstrated that several serotypes sequester HMGB1 in cellular chromatin. Conservation across human adenovirus serotypes suggests that targeting MRN and sequestering HMGB1 to host chromatin serve important functions during human adenovirus infection. These observations also raise the possibility that MRN and HMGB1 provided selective pressure for adenovirus evolution, since diverse serotypes all evolved to target these proteins. Our finding that different adenovirus serotypes utilize distinct mechanisms to target MRN further supports the idea that MRN provided selective pressure for adenovirus evolution since this implies that serotypes separately evolved to target the same cellular complex. Consistent with these theories, we found that MRN can impair adenovirus replication and identified roles for HMGB1 in anti-viral processes. Using an *in vivo* lipopolysaccharide (LPS) lung injury model, we showed that protein VII expression in mouse lungs resulted in reduced HMGB1 secretion and

reduced neutrophil infiltration in response to LPS stimulation (data not shown) (Avgousti et al., 2016). This demonstrated that sequestration of HMGB1 by protein VII could allow adenovirus to inhibit recruitment of immune cells. In **Chapter 3**, we demonstrated that protein VII can suppress interferon signaling, through a mechanism that may be dependent on HMGB1 and localization to chromatin (**Figures 3.16-3.18**). As evasion of interferon and innate immunity is critical to viral success in an *in vivo* setting, these functions could explain the conservation of protein VII-mediated HMGB1 sequestration among human adenoviruses. Together, our findings demonstrate how studying interactions of host proteins with multiple adenoviruses can be used to identify important cellular obstacles.

Resources to define interactions with host proteins

We identified differences in the ways that viral proteins from different adenoviruses interact with cellular proteins. These proteins provide valuable resources that can be used in future studies to define the requirements for interaction with host proteins. For example, in **Chapter 3**, we demonstrated that Ad5 protein VII sequesters HMGB1 to cellular chromatin. However, protein VII expressed from murine adenovirus MAV-1 localizes to chromatin but does not sequester HMGB1 in chromatin. Comparison of protein sequences between human and murine adenoviruses would provide insight into the residues or domains required for chromatin localization, as these would be expected to be present in both human and murine adenovirus protein VII. Conversely, sequences present in human Ad protein VII but not in MAV-1 protein VII are potential HMGB1-interacting motifs. In a similar manner, results from **Chapter 2** could be used to identify requirements for interaction with MRN. We identified serotypes that cannot target MRN through either mislocalization or degradation, and comparison with serotypes that do degrade or mislocalize MRN could identify residues important for MRN targeting.

Interestingly, Ad9 mislocalizes MRN to E4orf3-PML tracks during infection, but expression of Ad9-E4orf3 is not sufficient to alter MRN localization. It is possible that another Ad9 viral protein is required to target MRN, in which case it would be interesting to determine whether this protein shares any motifs with Ad5-E4orf3 that could be required to mislocalize MRN. Another possibility is the potential role of post-translational modifications (PTMs) on E4orf3 or MRN that could be required for MRN mislocalization. Identifying PTMs on Ad9-E4orf3 and MRN components in the presence and absence of infection would reveal whether Ad9-E4orf3 or MRN is differentially modified during infection. Understanding the requirements for adenovirus proteins to target MRN or HMGB1 could provide information to identify novel MRN or HMGB1-interacting proteins. Cellular proteins or proteins expressed from other viruses could be examined to determine if they contain MRN or HMGB1-interacting sequences identified from studying adenovirus proteins.

Insights into tissue and species tropism

In **Chapter 2**, we used a single cell type in each experiment to examine serotypes with diverse tissue tropisms. This experimental design allowed us to uncover differences in interactions with MRN between these serotypes that may not be observed in their natural cell types. It is possible that Ad9 and Ad12, which respectively cause conjunctivitis and gastrointestinal disorder, are able to escape MRN inhibition in conjunctival or gastrointestinal cells but not in the fibroblasts or osteosarcoma epithelial cells used in our experiments (Cerosaletti et al., 2000; Kraakman-van der Zwet et al., 1999). This could be due to unidentified differences in MRN levels, regulation, or activity between cell types. Ad9 and Ad12 could potentially be used to uncover differences between MRN from different cell types. It is possible that MRN provided selective pressure for adenovirus evolution. Given the negative impact of MRN on adenovirus

replication, differences in tissue tropism between human adenovirus serotypes could be partially due to an inability to evade MRN-mediated restriction in certain cell types. It would also be interesting to examine the potential of HMGB1 to serve as a restriction factor determining host tropism. Murine adenoviruses do not replicate efficiently in human cells (Hartley & Rowe, 1960; Nguyen et al., 1999), indicating that murine adenoviruses may fail to overcome a cellular obstacle. Interestingly, we found that MAV-1 protein VII does not sequester HMGB1 to cellular chromatin. Since our data suggest that HMGB1 sequestration allows human adenoviruses to suppress interferon, the inability of MAV-1 protein VII to target HMGB1 could prevent or suppress the efficiency of MAV-1 infection in human cells. This could influence host tropism, promoting MAV-1 infection of murine cells over human cells. To test this hypothesis, MAV-1 replication could be examined in HMGB1-deleted human cells to determine if HMGB1 deletion enhances MAV-1 replication. It is important to note that human and murine HMGB1 have nearly identical protein sequences, so any differences in blocking viral infection would indicate different cellular regulation of HMGB1 between human and mouse cells. It would be interesting to examine whether murine HMGB1 is involved in immune signaling and if MAV-1 employs different mechanisms to target HMGB1 in mouse cells. Together, our results indicate that comparing adenoviruses with different tissue and species tropism can identify potential barriers to cross-species or cross-tissue replication. This information could be used to design adenovirus vectors for gene therapy targeted to specific tissues.

Conclusion

Together, the work from this thesis demonstrates that adenoviruses utilize several different strategies to regulate interactions of cellular proteins with viral genomes in order to promote viral processes. We conclude that studying interactions of host proteins with

viral genomes can provide insight into virus-host interactions. Defining these interactions has broader implications for understanding cellular processes, developing anti-viral therapeutics or gene therapy vectors, and in understanding viral evolution.

Figures

Figure 4.1

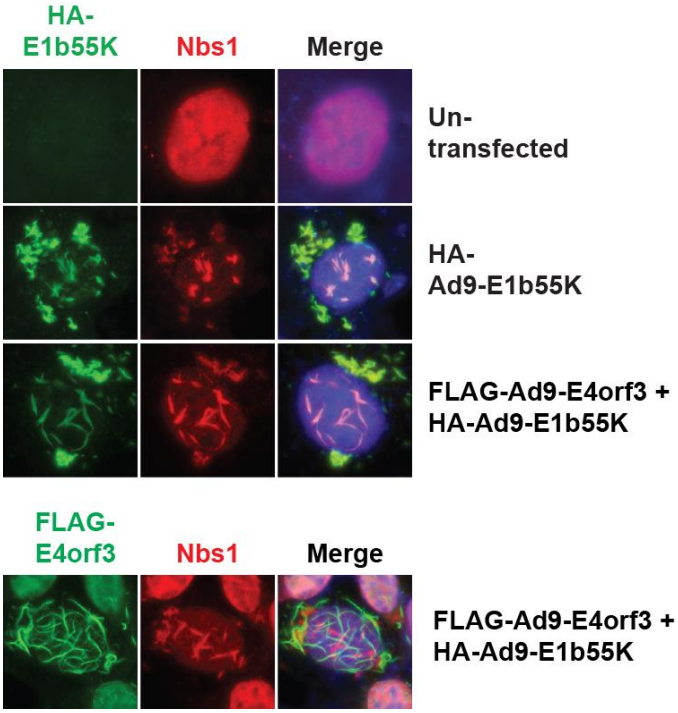

Figure 4.1: Ad9-E1b55K is sufficient to alter localization of MRN components. Immunofluorescence analysis of U2OS cells transfected with a plasmid expressing HA-tagged Ad9-E1b55K +/- Ad9-E4orf3. Transfected Ad9-E1b55K forms nuclear track-like structures and reorganizes Nbs1 into these structures. Co-transfection with Ad9-E4orf3 demonstrates that Nbs1-E1b55K track structures do not colocalize with E4orf3 tracks.

Figure 4.2

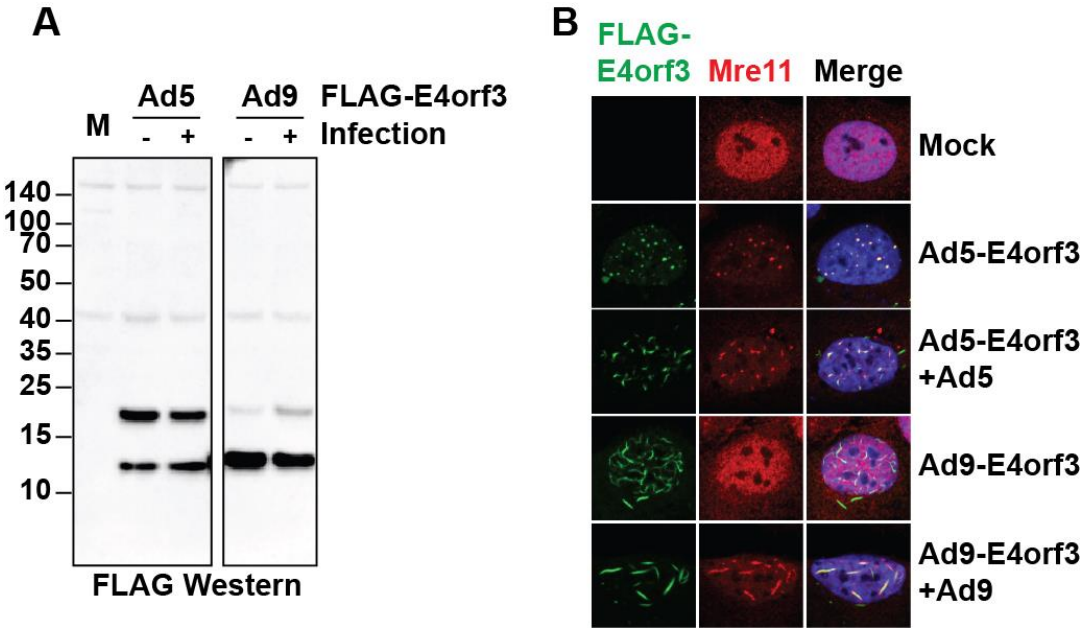

Figure 4.2: Potential post-translational modifications on E4orf3. (A) Transfection of FLAG-tagged Ad5-E4orf3 and Ad9-E4orf3 with and without infection with Ad5 or Ad9. FLAG Western blot demonstrates a higher molecular weight band that may represent a post-translational modification on E4orf3 that increases upon Ad9 infection. **(B)** Immunofluorescence of samples from **A** demonstrating that Mre11 colocalizes with Ad5-E4orf3 in the presence and absence of Ad5 infection. Mre11 does not colocalize with Ad9-E4orf3 in the absence of Ad9 infection.

Figure 4.3

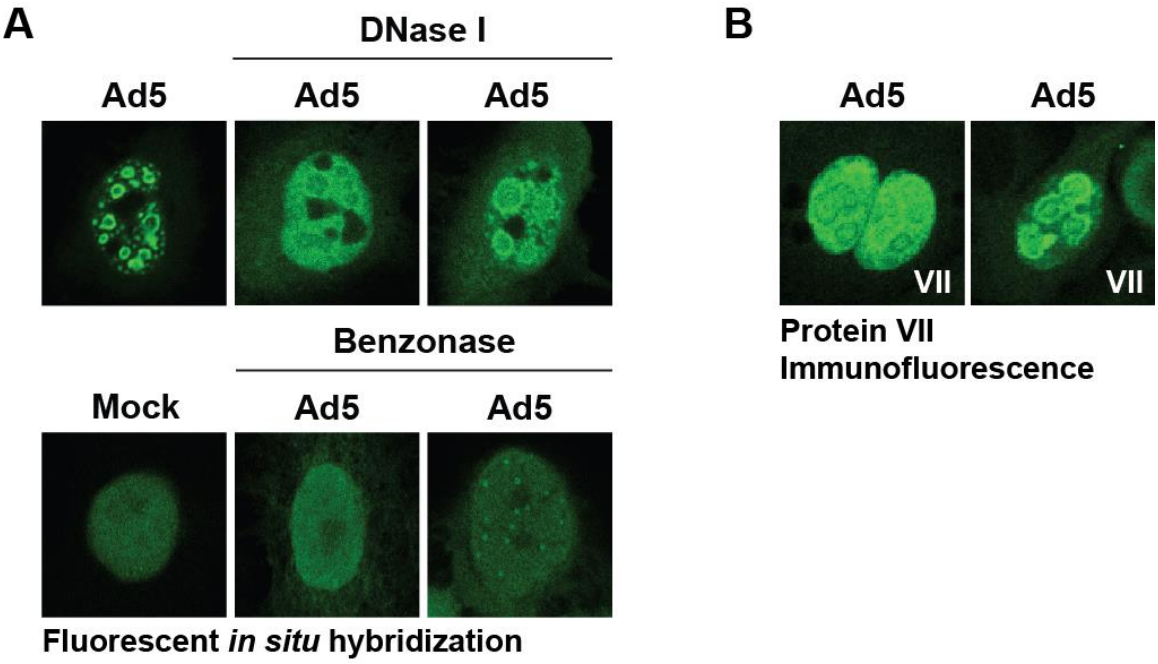

Figure 4.3: Viral RNA and protein VII have similar localization patterns.

(A) Fluorescent *in situ* hybridization with probes complementary to the Ad5 genome, performed exactly as described in (Pombo et al., 1994). DNase I treatment digests DNA, resulting in visualization of viral RNA. Benzonase treatment digests both DNA and RNA, resulting in only background fluorescence. **(B)** Immunofluorescence of protein VII in Ad5-infected cells.

BIBLIOGRAPHY

Agresti, A., & Bianchi, M. E. (2003). HMGB proteins and gene expression. *Curr Opin Genet Dev, 13*(2), 170-178.

Anacker, D. C., Gautam, D., Gillespie, K. A., Chappell, W. H., & Moody, C. A. (2014). Productive replication of human papillomavirus 31 requires DNA repair factor Nbs1. *J Virol, 88*(15), 8528-8544. doi: 10.1128/JVI.00517-14

Anderson, C. W., Baum, P. R., & Gesteland, R. F. (1973). Processing of adenovirus 2-induced proteins. *J Virol, 12*(2), 241-252.

Anderson, C. W., Young, M. E., & Flint, S. J. (1989). Characterization of the adenovirus 2 virion protein, mu. *Virology, 172*(2), 506-512.

Anderson, K. P., & Fennie, E. H. (1987). Adenovirus early region 1A modulation of interferon antiviral activity. *J Virol, 61*(3), 787-795.

Andreeva, L., Hiller, B., Kostrewa, D., Lassig, C., de Oliveira Mann, C. C., Jan Drexler, D., . . . Hopfner, K. P. (2017). cGAS senses long and HMGB/TFAM-bound U-turn DNA by forming protein-DNA ladders. *Nature, 549*(7672), 394-398. doi: 10.1038/nature23890

Araujo, F. D., Stracker, T. H., Carson, C. T., Lee, D. V., & Weitzman, M. D. (2005). Adenovirus type 5 E4orf3 protein targets the Mre11 complex to cytoplasmic aggresomes. *J Virol, 79*(17), 11382-11391. doi: 10.1128/JVI.79.17.11382-11391.2005

Avgousti, D. C., Della Fera, A. N., Otter, C. J., Herrmann, C., Pancholi, N. J., & Weitzman, M. D. (2017). Adenovirus core protein VII down-regulates the DNA damage response on the host genome. *J Virol*. doi: 10.1128/JVI.01089-17

Avgousti, D. C., Herrmann, C., Kulej, K., Pancholi, N. J., Sekulic, N., Petrescu, J., . . . Weitzman, M. D. (2016). A core viral protein binds host nucleosomes to sequester immune danger signals. *Nature, 535*(7610), 173-177. doi: 10.1038/nature18317

Babiss, L. E., & Ginsberg, H. S. (1984). Adenovirus type 5 early region 1b gene product is required for efficient shutoff of host protein synthesis. *J Virol, 50*(1), 202-212.

Bagchi, S., Raychaudhuri, P., & Nevins, J. R. (1990). Adenovirus E1A proteins can dissociate heteromeric complexes involving the E2F transcription factor: a novel mechanism for E1A trans-activation. *Cell, 62*(4), 659-669.

Baker, A., Rohleder, K. J., Hanakahi, L. A., & Ketner, G. (2007). Adenovirus E4 34k and E1b 55k oncoproteins target host DNA ligase IV for proteasomal degradation. *J Virol, 81*(13), 7034-7040. doi: 10.1128/JVI.00029-07

Bakkenist, C. J., & Kastan, M. B. (2003). DNA damage activates ATM through intermolecular autophosphorylation and dimer dissociation. *Nature, 421*(6922), 499-506. doi: 10.1038/nature01368

Bakkenist, C. J., & Kastan, M. B. (2004). Initiating cellular stress responses. *Cell, 118*(1), 9-17. doi: 10.1016/j.cell.2004.06.023

Banin, S., Moyal, L., Shieh, S., Taya, Y., Anderson, C. W., Chessa, L., . . . Ziv, Y. (1998). Enhanced phosphorylation of p53 by ATM in response to DNA damage. *Science, 281*(5383), 1674-1677.

Barbalat, R., Ewald, S. E., Mouchess, M. L., & Barton, G. M. (2011). Nucleic acid recognition by the innate immune system. *Annu Rev Immunol, 29*, 185-214. doi: 10.1146/annurev-immunol-031210-101340

Barber, G. N. (2011). Innate immune DNA sensing pathways: STING, AIMII and the regulation of interferon production and inflammatory responses. *Curr Opin Immunol, 23*(1), 10-20. doi: 10.1016/j.coi.2010.12.015

Bergelson, J. M., Cunningham, J. A., Droguett, G., Kurt-Jones, E. A., Krithivas, A., Hong, J. S., . . . Finberg, R. W. (1997). Isolation of a common receptor for Coxsackie B viruses and adenoviruses 2 and 5. *Science, 275*(5304), 1320-1323.

Berget, S. M., Moore, C., & Sharp, P. A. (1977). Spliced segments at the 5' terminus of adenovirus 2 late mRNA. *Proc Natl Acad Sci U S A, 74*(8), 3171-3175.

Berk, A. J. (2005). Recent lessons in gene expression, cell cycle control, and cell biology from adenovirus. *Oncogene, 24*(52), 7673-7685. doi: 10.1038/sj.onc.1209040

Berk, A. J. (2013). Adenoviridae. In D. M. Knipe, Howley, P.M. (Ed.), *Fields Virology* (6th ed., Vol. 2, pp. 1704-1731). Philadelphia, PA: Lippincott Williams & Wilkins.

Bianchi, M. E., & Agresti, A. (2005). HMG proteins: dynamic players in gene regulation and differentiation. *Curr Opin Genet Dev, 15*(5), 496-506. doi: 10.1016/j.gde.2005.08.007

Blackford, A. N., Bruton, R. K., Dirlik, O., Stewart, G. S., Taylor, A. M., Dobner, T., . . . Turnell, A. S. (2008). A role for E1B-AP5 in ATR signaling pathways during adenovirus infection. *J Virol, 82*(15), 7640-7652. doi: 10.1128/JVI.00170-08

Blackford, A. N., & Grand, R. J. (2009). Adenovirus E1B 55-kilodalton protein: multiple roles in viral infection and cell transformation. *J Virol, 83*(9), 4000-4012. doi: 10.1128/JVI.02417-08

Blackford, A. N., Patel, R. N., Forrester, N. A., Theil, K., Groitl, P., Stewart, G. S., . . . Turnell, A. S. (2010). Adenovirus 12 E4orf6 inhibits ATR activation by promoting TOPBP1 degradation. *Proc Natl Acad Sci U S A, 107*(27), 12251-12256. doi: 10.1073/pnas.0914605107

Blanchette, P., Kindsmuller, K., Groitl, P., Dallaire, F., Speiseder, T., Branton, P. E., & Dobner, T. (2008). Control of mRNA export by adenovirus E4orf6 and E1B55K proteins during productive infection requires E4orf6 ubiquitin ligase activity. *J Virol, 82*(6), 2642-2651. doi: 10.1128/JVI.02309-07

Blanchette, P., Wimmer, P., Dallaire, F., Cheng, C. Y., & Branton, P. E. (2013). Aggresome formation by the adenoviral protein E1B55K is not conserved among adenovirus species and is not required for efficient degradation of nuclear substrates. *J Virol, 87*(9), 4872-4881. doi: 10.1128/JVI.03272-12

Boyer, J., Rohleder, K., & Ketner, G. (1999). Adenovirus E4 34k and E4 11k inhibit double strand break repair and are physically associated with the cellular DNA-dependent protein kinase. *Virology, 263*(2), 307-312. doi: 10.1006/viro.1999.9866

Bridge, E., & Ketner, G. (1989). Redundant control of adenovirus late gene expression by early region 4. *J Virol, 63*(2), 631-638.

Bridges, R. G., Sohn, S. Y., Wright, J., Leppard, K. N., & Hearing, P. (2016). The Adenovirus E4-ORF3 Protein Stimulates SUMOylation of General Transcription Factor TFII-I to Direct Proteasomal Degradation. *MBio, 7*(1), e02184-02115. doi: 10.1128/mBio.02184-15

Burma, S., Chen, B. P., Murphy, M., Kurimasa, A., & Chen, D. J. (2001). ATM phosphorylates histone H2AX in response to DNA double-strand breaks. *J Biol Chem, 276*(45), 42462-42467. doi: 10.1074/jbc.C100466200

Carson, C. T., Orazio, N. I., Lee, D. V., Suh, J., Bekker-Jensen, S., Araujo, F. D., . . . Weitzman, M. D. (2009). Mislocalization of the MRN complex prevents ATR signaling during adenovirus infection. *EMBO J, 28*(6), 652-662. doi: 10.1038/emboj.2009.15

Carson, C. T., Schwartz, R. A., Stracker, T. H., Lilley, C. E., Lee, D. V., & Weitzman, M. D. (2003). The Mre11 complex is required for ATM activation and the G2/M checkpoint. *EMBO J, 22*(24), 6610-6620. doi: 10.1093/emboj/cdg630

Carvalho, T., Seeler, J. S., Ohman, K., Jordan, P., Pettersson, U., Akusjarvi, G., . . . Dejean, A. (1995). Targeting of adenovirus E1A and E4-ORF3 proteins to nuclear matrix-associated PML bodies. *J Cell Biol, 131*(1), 45-56.

Cerosaletti, K. M., Desai-Mehta, A., Yeo, T. C., Kraakman-Van Der Zwet, M., Zdzienicka, M. Z., & Concannon, P. (2000). Retroviral expression of the NBS1 gene in cultured Nijmegen breakage syndrome cells restores normal radiation sensitivity and nuclear focus formation. *Mutagenesis, 15*(3), 281-286.

Chahal, J. S., Qi, J., & Flint, S. J. (2012). The human adenovirus type 5 E1B 55 kDa protein obstructs inhibition of viral replication by type I interferon in normal human cells. *PLoS Pathog, 8*(8), e1002853. doi: 10.1371/journal.ppat.1002853

Chang, W., Folker, E. S., Worman, H. J., & Gundersen, G. G. (2013). Emerin organizes actin flow for nuclear movement and centrosome orientation in migrating fibroblasts. *Mol Biol Cell, 24*(24), 3869-3880. doi: 10.1091/mbc.E13-06-0307

Chapuy, B., Tikkanen, R., Muhlhausen, C., Wenzel, D., von Figura, K., & Honing, S. (2008). AP-1 and AP-3 mediate sorting of melanosomal and lysosomal membrane proteins into distinct post-Golgi trafficking pathways. *Traffic, 9*(7), 1157-1172. doi: 10.1111/j.1600-0854.2008.00745.x

Chardonnet, Y., & Dales, S. (1970). Early events in the interaction of adenoviruses with HeLa cells. I. Penetration of type 5 and intracellular release of the DNA genome. *Virology, 40*(3), 462-477.

Chatterjee, P. K., Vayda, M. E., & Flint, S. J. (1986). Identification of proteins and protein domains that contact DNA within adenovirus nucleoprotein cores by ultraviolet light crosslinking of oligonucleotides 32P-labelled in vivo. *J Mol Biol, 188*(1), 23-37.

Chelius, D., Huhmer, A. F., Shieh, C. H., Lehmberg, E., Traina, J. A., Slattery, T. K., & Pungor, E., Jr. (2002). Analysis of the adenovirus type 5 proteome by liquid chromatography and tandem mass spectrometry methods. *J Proteome Res, 1*(6), 501-513.

Chen, J., Morral, N., & Engel, D. A. (2007). Transcription releases protein VII from adenovirus chromatin. *Virology, 369*(2), 411-422. doi: 10.1016/j.virol.2007.08.012

Chen, P. H., Ornelles, D. A., & Shenk, T. (1993). The adenovirus L3 23-kilodalton proteinase cleaves the amino-terminal head domain from cytokeratin 18 and disrupts the cytokeratin network of HeLa cells. *J Virol, 67*(6), 3507-3514.

Cheng, C. Y., Gilson, T., Dallaire, F., Ketner, G., Branton, P. E., & Blanchette, P. (2011). The E4orf6/E1B55K E3 ubiquitin ligase complexes of human adenoviruses exhibit heterogeneity in composition and substrate specificity. *J Virol, 85*(2), 765-775. doi: 10.1128/JVI.01890-10

Cheng, C. Y., Gilson, T., Wimmer, P., Schreiner, S., Ketner, G., Dobner, T., . . . Blanchette, P. (2013). Role of E1B55K in E4orf6/E1B55K E3 ligase complexes formed by different human adenovirus serotypes. *J Virol, 87*(11), 6232-6245. doi: 10.1128/JVI.00384-13

Christensen, J. B., Byrd, S. A., Walker, A. K., Strahler, J. R., Andrews, P. C., & Imperiale, M. J. (2008). Presence of the adenovirus IVa2 protein at a single vertex of the mature virion. *J Virol, 82*(18), 9086-9093. doi: 10.1128/JVI.01024-08

Ciccia, A., & Elledge, S. J. (2010). The DNA damage response: making it safe to play with knives. *Mol Cell, 40*(2), 179-204. doi: 10.1016/j.molcel.2010.09.019

Ciccia, A., Huang, J. W., Izhar, L., Sowa, M. E., Harper, J. W., & Elledge, S. J. (2014). Treacher Collins syndrome TCOF1 protein cooperates with NBS1 in the DNA

damage response. *Proc Natl Acad Sci U S A, 111*(52), 18631-18636. doi: 10.1073/pnas.1422488112

Cole, J. L. (2007). Activation of PKR: an open and shut case? *Trends Biochem Sci, 32*(2), 57-62. doi: 10.1016/j.tibs.2006.12.003

Corbo, C., Orru, S., & Salvatore, F. (2013). SRp20: an overview of its role in human diseases. *Biochem Biophys Res Commun, 436*(1), 1-5. doi: 10.1016/j.bbrc.2013.05.027

Cortez, D., Wang, Y., Qin, J., & Elledge, S. J. (1999). Requirement of ATM-dependent phosphorylation of brca1 in the DNA damage response to double-strand breaks. *Science, 286*(5442), 1162-1166.

Cotten, M., & Weber, J. M. (1995). The adenovirus protease is required for virus entry into host cells. *Virology, 213*(2), 494-502. doi: 10.1006/viro.1995.0022

Cuconati, A., & White, E. (2002). Viral homologs of BCL-2: role of apoptosis in the regulation of virus infection. *Genes Dev, 16*(19), 2465-2478. doi: 10.1101/gad.1012702

Dales, S., & Chardonnet, Y. (1973). Early events in the interaction of adenoviruses with HeLa cells. IV. Association with microtubules and the nuclear pore complex during vectorial movement of the inoculum. *Virology, 56*(2), 465-483.

Dallaire, F., Blanchette, P., Groitl, P., Dobner, T., & Branton, P. E. (2009). Identification of integrin alpha3 as a new substrate of the adenovirus E4orf6/E1B 55-kilodalton E3 ubiquitin ligase complex. *J Virol, 83*(11), 5329-5338. doi: 10.1128/JVI.00089-09

Dani, H. M., Singh, J., & Singh, S. (2003). Advances in the structure and functions of signal recognition particle in protein targeting. *J Biol Regul Homeost Agents, 17*(4), 303-307.

Das, S., & Krainer, A. R. (2014). Emerging functions of SRSF1, splicing factor and oncoprotein, in RNA metabolism and cancer. *Mol Cancer Res, 12*(9), 1195-1204. doi: 10.1158/1541-7786.MCR-14-0131

Daugherty, M. D., & Malik, H. S. (2012). Rules of engagement: molecular insights from host-virus arms races. *Annu Rev Genet, 46*, 677-700. doi: 10.1146/annurev-genet-110711-155522

Davison, A. J., Benko, M., & Harrach, B. (2003). Genetic content and evolution of adenoviruses. *J Gen Virol, 84*(Pt 11), 2895-2908. doi: 10.1099/vir.0.19497-0

De Andrea, M., Ravera, R., Gioia, D., Gariglio, M., & Landolfo, S. (2002). The interferon system: an overview. *Eur J Paediatr Neurol, 6 Suppl A*, A41-46; discussion A55-48.

Dekker, J., Kanellopoulos, P. N., Loonstra, A. K., van Oosterhout, J. A., Leonard, K., Tucker, P. A., & van der Vliet, P. C. (1997). Multimerization of the adenovirus DNA-binding protein is the driving force for ATP-independent DNA unwinding during strand displacement synthesis. *EMBO J, 16*(6), 1455-1463. doi: 10.1093/emboj/16.6.1455

Dekker, J., Kanellopoulos, P. N., van Oosterhout, J. A., Stier, G., Tucker, P. A., & van der Vliet, P. C. (1998). ATP-independent DNA unwinding by the adenovirus single-stranded DNA binding protein requires a flexible DNA binding loop. *J Mol Biol, 277*(4), 825-838. doi: 10.1006/jmbi.1998.1652

Delacroix, S., Wagner, J. M., Kobayashi, M., Yamamoto, K., & Karnitz, L. M. (2007). The Rad9-Hus1-Rad1 (9-1-1) clamp activates checkpoint signaling via TopBP1. *Genes Dev, 21*(12), 1472-1477. doi: 10.1101/gad.1547007

Dey, M., Cao, C., Dar, A. C., Tamura, T., Ozato, K., Sicheri, F., & Dever, T. E. (2005). Mechanistic link between PKR dimerization, autophosphorylation, and eIF2alpha substrate recognition. *Cell, 122*(6), 901-913. doi: 10.1016/j.cell.2005.06.041

Dobner, T., Horikoshi, N., Rubenwolf, S., & Shenk, T. (1996). Blockage by adenovirus E4orf6 of transcriptional activation by the p53 tumor suppressor. *Science, 272*(5267), 1470-1473.

Doucas, V., Ishov, A. M., Romo, A., Juguilon, H., Weitzman, M. D., Evans, R. M., & Maul, G. G. (1996). Adenovirus replication is coupled with the dynamic properties of the PML nuclear structure. *Genes Dev, 10*(2), 196-207.

Endter, C., & Dobner, T. (2004). Cell transformation by human adenoviruses. *Curr Top Microbiol Immunol, 273*, 163-214.

Evans, J. D., & Hearing, P. (2003). Distinct roles of the Adenovirus E4 ORF3 protein in viral DNA replication and inhibition of genome concatenation. *J Virol, 77*(9), 5295-5304.

Evans, J. D., & Hearing, P. (2005). Relocalization of the Mre11-Rad50-Nbs1 complex by the adenovirus E4 ORF3 protein is required for viral replication. *J Virol, 79*(10), 6207-6215. doi: 10.1128/JVI.79.10.6207-6215.2005

Fekairi, S., Scaglione, S., Chahwan, C., Taylor, E. R., Tissier, A., Coulon, S., . . . Gaillard, P. H. (2009). Human SLX4 is a Holliday junction resolvase subunit that binds multiple DNA repair/recombination endonucleases. *Cell, 138*(1), 78-89. doi: 10.1016/j.cell.2009.06.029

Ferrier, A., Boyer, J. G., & Kothary, R. (2013). Cellular and molecular biology of neuronal dystonin. *Int Rev Cell Mol Biol, 300*, 85-120. doi: 10.1016/B978-0-12-405210-9.00003-5

Fitzgerald, K. A., McWhirter, S. M., Faia, K. L., Rowe, D. C., Latz, E., Golenbock, D. T., . . . Maniatis, T. (2003). IKKepsilon and TBK1 are essential components of the IRF3 signaling pathway. *Nat Immunol, 4*(5), 491-496. doi: 10.1038/ni921

Flint, S. J., & Gonzalez, R. A. (2003). Regulation of mRNA production by the adenoviral E1B 55-kDa and E4 Orf6 proteins. *Curr Top Microbiol Immunol, 272*, 287-330.

Fonseca, G. J., Thillainadesan, G., Yousef, A. F., Ablack, J. N., Mossman, K. L., Torchia, J., & Mymryk, J. S. (2012). Adenovirus evasion of interferon-mediated innate immunity by direct antagonism of a cellular histone posttranslational modification. *Cell Host Microbe, 11*(6), 597-606. doi: 10.1016/j.chom.2012.05.005

Forrester, N. A., Sedgwick, G. G., Thomas, A., Blackford, A. N., Speiseder, T., Dobner, T., . . . Grand, R. J. (2011). Serotype-specific inactivation of the cellular DNA damage response during adenovirus infection. *J Virol, 85*(5), 2201-2211. doi: 10.1128/JVI.01748-10

Freimuth, P., & Anderson, C. W. (1993). Human adenovirus serotype 12 virion precursors pMu and pVI are cleaved at amino-terminal and carboxy-terminal sites that conform to the adenovirus 2 endoproteinase cleavage consensus sequence. *Virology, 193*(1), 348-355. doi: 10.1006/viro.1993.1131

Gaggar, A., Shayakhmetov, D. M., & Lieber, A. (2003). CD46 is a cellular receptor for group B adenoviruses. *Nat Med, 9*(11), 1408-1412. doi: 10.1038/nm952

Gautam, D., & Bridge, E. (2013). The kinase activity of ataxia-telangiectasia mutated interferes with adenovirus E4 mutant DNA replication. *J Virol, 87*(15), 8687-8696. doi: 10.1128/JVI.00376-13

Giberson, A. N., Davidson, A. R., & Parks, R. J. (2012). Chromatin structure of adenovirus DNA throughout infection. *Nucleic Acids Res, 40*(6), 2369-2376. doi: 10.1093/nar/gkr1076

Graveley, B. R. (2000). Sorting out the complexity of SR protein functions. *RNA, 6*(9), 1197-1211.

Greber, U. F., Suomalainen, M., Stidwill, R. P., Boucke, K., Ebersold, M. W., & Helenius, A. (1997). The role of the nuclear pore complex in adenovirus DNA entry. *EMBO J, 16*(19), 5998-6007. doi: 10.1093/emboj/16.19.5998

Greber, U. F., Webster, P., Weber, J., & Helenius, A. (1996). The role of the adenovirus protease on virus entry into cells. *EMBO J, 15*(8), 1766-1777.

Greber, U. F., Willetts, M., Webster, P., & Helenius, A. (1993). Stepwise dismantling of adenovirus 2 during entry into cells. *Cell, 75*(3), 477-486.

Greer, A. E., Hearing, P., & Ketner, G. (2011). The adenovirus E4 11 k protein binds and relocalizes the cytoplasmic P-body component Ddx6 to aggresomes. *Virology, 417*(1), 161-168. doi: 10.1016/j.virol.2011.05.017

Gupta, A., Jha, S., Engel, D. A., Ornelles, D. A., & Dutta, A. (2013). Tip60 degradation by adenovirus relieves transcriptional repression of viral transcriptional activator EIA. *Oncogene, 32*(42), 5017-5025. doi: 10.1038/onc.2012.534

Halbert, D. N., Cutt, J. R., & Shenk, T. (1985). Adenovirus early region 4 encodes functions required for efficient DNA replication, late gene expression, and host cell shutoff. *J Virol, 56*(1), 250-257.

Haller, O., Kochs, G., & Weber, F. (2006). The interferon response circuit: induction and suppression by pathogenic viruses. *Virology, 344*(1), 119-130. doi: 10.1016/j.virol.2005.09.024

Harada, J. N., Shevchenko, A., Shevchenko, A., Pallas, D. C., & Berk, A. J. (2002). Analysis of the adenovirus E1B-55K-anchored proteome reveals its link to ubiquitination machinery. *J Virol, 76*(18), 9194-9206.

Harding, S. M., Benci, J. L., Irianto, J., Discher, D. E., Minn, A. J., & Greenberg, R. A. (2017). Mitotic progression following DNA damage enables pattern recognition within micronuclei. *Nature, 548*(7668), 466-470. doi: 10.1038/nature23470

Harper, J. W., & Elledge, S. J. (2007). The DNA damage response: ten years after. *Mol Cell, 28*(5), 739-745. doi: 10.1016/j.molcel.2007.11.015

Hartley, J. W., & Rowe, W. P. (1960). A new mouse virus apparently related to the adenovirus group. *Virology, 11*, 645-647.

Haruki, H., Gyurcsik, B., Okuwaki, M., & Nagata, K. (2003). Ternary complex formation between DNA-adenovirus core protein VII and TAF-Ibeta/SET, an acidic molecular chaperone. *FEBS Lett, 555*(3), 521-527.

Haruki, H., Okuwaki, M., Miyagishi, M., Taira, K., & Nagata, K. (2006). Involvement of template-activating factor I/SET in transcription of adenovirus early genes as a positive-acting factor. *J Virol, 80*(2), 794-801. doi: 10.1128/JVI.80.2.794-801.2006

Hayano, T., Yanagida, M., Yamauchi, Y., Shinkawa, T., Isobe, T., & Takahashi, N. (2003). Proteomic analysis of human Nop56p-associated pre-ribosomal ribonucleoprotein complexes. Possible link between Nop56p and the nucleolar protein treacle responsible for Treacher Collins syndrome. *J Biol Chem, 278*(36), 34309-34319. doi: 10.1074/jbc.M304304200

Hearing, P., Samulski, R. J., Wishart, W. L., & Shenk, T. (1987). Identification of a repeated sequence element required for efficient encapsidation of the adenovirus type 5 chromosome. *J Virol, 61*(8), 2555-2558.

Hearing, P., & Shenk, T. (1983). The adenovirus type 5 E1A transcriptional control region contains a duplicated enhancer element. *Cell, 33*(3), 695-703.

Herrmann, C., Avgousti, D. C., & Weitzman, M. D. (2017). Differential Salt Fractionation of Nuclei to Analyze Chromatin-associated Proteins from Cultured Mammalian Cells. *Bio Protoc, 7*(6).

Hickson, I., Zhao, Y., Richardson, C. J., Green, S. J., Martin, N. M., Orr, A. I., . . . Smith, G. C. (2004). Identification and characterization of a novel and specific inhibitor

of the ataxia-telangiectasia mutated kinase ATM. *Cancer Res, 64*(24), 9152-9159. doi: 10.1158/0008-5472.CAN-04-2727

Higashino, F., Pipas, J. M., & Shenk, T. (1998). Adenovirus E4orf6 oncoprotein modulates the function of the p53-related protein, p73. *Proc Natl Acad Sci U S A, 95*(26), 15683-15687.

Hindley, C. E., Lawrence, F. J., & Matthews, D. A. (2007). A role for transportin in the nuclear import of adenovirus core proteins and DNA. *Traffic, 8*(10), 1313-1322. doi: 10.1111/j.1600-0854.2007.00618.x

Hirao, A., Kong, Y. Y., Matsuoka, S., Wakeham, A., Ruland, J., Yoshida, H., . . . Mak, T. W. (2000). DNA damage-induced activation of p53 by the checkpoint kinase Chk2. *Science, 287*(5459), 1824-1827.

Hollingworth, R., & Grand, R. J. (2015). Modulation of DNA damage and repair pathways by human tumour viruses. *Viruses, 7*(5), 2542-2591. doi: 10.3390/v7052542

Horwitz, M. S., Scharff, M. D., & Maizel, J. V., Jr. (1969). Synthesis and assembly of adenovirus 2. I. Polypeptide synthesis, assembly of capsomeres, and morphogenesis of the virion. *Virology, 39*(4), 682-694.

Howley, P. M., & Livingston, D. M. (2009). Small DNA tumor viruses: large contributors to biomedical sciences. *Virology, 384*(2), 256-259. doi: 10.1016/j.virol.2008.12.006

Huang, M. M., & Hearing, P. (1989). Adenovirus early region 4 encodes two gene products with redundant effects in lytic infection. *J Virol, 63*(6), 2605-2615.

Ishikawa, H., & Barber, G. N. (2008). STING is an endoplasmic reticulum adaptor that facilitates innate immune signalling. *Nature, 455*(7213), 674-678. doi: 10.1038/nature07317

Ishikawa, H., Ma, Z., & Barber, G. N. (2009). STING regulates intracellular DNA-mediated, type I interferon-dependent innate immunity. *Nature, 461*(7265), 788-792. doi: 10.1038/nature08476

Jackson, S. P., & Bartek, J. (2009). The DNA-damage response in human biology and disease. *Nature, 461*(7267), 1071-1078. doi: 10.1038/nature08467

Jacque, J. M., & Stevenson, M. (2006). The inner-nuclear-envelope protein emerin regulates HIV-1 infectivity. *Nature, 441*(7093), 641-645. doi: 10.1038/nature04682

Jayaram, S., & Bridge, E. (2005). Genome concatenation contributes to the late gene expression defect of an adenovirus E4 mutant. *Virology, 342*(2), 286-296. doi: 10.1016/j.virol.2005.08.004

Jazayeri, A., Falck, J., Lukas, C., Bartek, J., Smith, G. C., Lukas, J., & Jackson, S. P. (2006). ATM- and cell cycle-dependent regulation of ATR in response to DNA double-strand breaks. *Nat Cell Biol, 8*(1), 37-45. doi: 10.1038/ncb1337

Jha, H. C., Banerjee, S., & Robertson, E. S. (2016). The Role of Gammaherpesviruses in Cancer Pathogenesis. *Pathogens, 5*(1). doi: 10.3390/pathogens5010018

Jin, L., Waterman, P. M., Jonscher, K. R., Short, C. M., Reisdorph, N. A., & Cambier, J. C. (2008). MPYS, a novel membrane tetraspanner, is associated with major histocompatibility complex class II and mediates transduction of apoptotic signals. *Mol Cell Biol, 28*(16), 5014-5026. doi: 10.1128/MCB.00640-08

Johnson, J. S., Osheim, Y. N., Xue, Y., Emanuel, M. R., Lewis, P. W., Bankovich, A., . . . Engel, D. A. (2004). Adenovirus protein VII condenses DNA, represses transcription, and associates with transcriptional activator E1A. *J Virol, 78*(12), 6459-6468. doi: 10.1128/JVI.78.12.6459-6468.2004

Jun, L., Frints, S., Duhamel, H., Herold, A., Abad-Rodrigues, J., Dotti, C., . . . Froyen, G. (2001). NXF5, a novel member of the nuclear RNA export factor family, is lost in a male patient with a syndromic form of mental retardation. *Curr Biol, 11*(18), 1381-1391.

Karen, K. A., & Hearing, P. (2011). Adenovirus core protein VII protects the viral genome from a DNA damage response at early times after infection. *J Virol, 85*(9), 4135-4142. doi: 10.1128/JVI.02540-10

Karen, K. A., Hoey, P. J., Young, C. S., & Hearing, P. (2009). Temporal regulation of the Mre11-Rad50-Nbs1 complex during adenovirus infection. *J Virol, 83*(9), 4565-4573. doi: 10.1128/JVI.00042-09

Kastan, M. B., & Bartek, J. (2004). Cell-cycle checkpoints and cancer. *Nature, 432*(7015), 316-323. doi: 10.1038/nature03097

Keating, S. E., Baran, M., & Bowie, A. G. (2011). Cytosolic DNA sensors regulating type I interferon induction. *Trends Immunol, 32*(12), 574-581. doi: 10.1016/j.it.2011.08.004

Khandelia, P., Yap, K., & Makeyev, E. V. (2011). Streamlined platform for short hairpin RNA interference and transgenesis in cultured mammalian cells. *Proc Natl Acad Sci U S A, 108*(31), 12799-12804. doi: 10.1073/pnas.1103532108

Kim, Y., Lach, F. P., Desetty, R., Hanenberg, H., Auerbach, A. D., & Smogorzewska, A. (2011). Mutations of the SLX4 gene in Fanconi anemia. *Nat Genet, 43*(2), 142-146. doi: 10.1038/ng.750

Kitajewski, J., Schneider, R. J., Safer, B., Munemitsu, S. M., Samuel, C. E., Thimmappaya, B., & Shenk, T. (1986). Adenovirus VAI RNA antagonizes the antiviral action of interferon by preventing activation of the interferon-induced eIF-2 alpha kinase. *Cell, 45*(2), 195-200.

Kitajewski, J., Schneider, R. J., Safer, B., & Shenk, T. (1986). An adenovirus mutant unable to express VAI RNA displays different growth responses and sensitivity to interferon in various host cell lines. *Mol Cell Biol, 6*(12), 4493-4498.

Komatsu, T., Haruki, H., & Nagata, K. (2011). Cellular and viral chromatin proteins are positive factors in the regulation of adenovirus gene expression. *Nucleic Acids Res, 39*(3), 889-901. doi: 10.1093/nar/gkq783

Komatsu, T., & Nagata, K. (2012). Replication-uncoupled histone deposition during adenovirus DNA replication. *J Virol, 86*(12), 6701-6711. doi: 10.1128/JVI.00380-12

Koonin, E. V., Senkevich, T. G., & Chernos, V. I. (1993). Gene A32 product of vaccinia virus may be an ATPase involved in viral DNA packaging as indicated by sequence comparisons with other putative viral ATPases. *Virus Genes, 7*(1), 89-94.

Kottemann, M. C., & Smogorzewska, A. (2013). Fanconi anaemia and the repair of Watson and Crick DNA crosslinks. *Nature, 493*(7432), 356-363. doi: 10.1038/nature11863

Kraakman-van der Zwet, M., Overkamp, W. J., Friedl, A. A., Klein, B., Verhaegh, G. W., Jaspers, N. G., . . . Zdzienicka, M. Z. (1999). Immortalization and characterization of Nijmegen Breakage syndrome fibroblasts. *Mutat Res, 434*(1), 17-27.

Lachmann, R. (2003). Herpes simplex virus latency. *Expert Rev Mol Med, 5*(29), 1-14. doi: doi:10.1017/S1462399403006975

Lakdawala, S. S., Schwartz, R. A., Ferenchak, K., Carson, C. T., McSharry, B. P., Wilkinson, G. W., & Weitzman, M. D. (2008). Differential requirements of the C terminus of Nbs1 in suppressing adenovirus DNA replication and promoting concatemer formation. *J Virol, 82*(17), 8362-8372. doi: 10.1128/JVI.00900-08

Latorre, I. J., Roh, M. H., Frese, K. K., Weiss, R. S., Margolis, B., & Javier, R. T. (2005). Viral oncoprotein-induced mislocalization of select PDZ proteins disrupts tight junctions and causes polarity defects in epithelial cells. *J Cell Sci, 118*(Pt 18), 4283-4293. doi: 10.1242/jcs.02560

Lee, J. H., & Paull, T. T. (2005). ATM activation by DNA double-strand breaks through the Mre11-Rad50-Nbs1 complex. *Science, 308*(5721), 551-554. doi: 10.1126/science.1108297

Leonhardt, H., Rahn, H. P., Weinzierl, P., Sporbert, A., Cremer, T., Zink, D., & Cardoso, M. C. (2000). Dynamics of DNA replication factories in living cells. *J Cell Biol, 149*(2), 271-280.

Lilley, C. E., Carson, C. T., Muotri, A. R., Gage, F. H., & Weitzman, M. D. (2005). DNA repair proteins affect the lifecycle of herpes simplex virus 1. *Proc Natl Acad Sci U S A, 102*(16), 5844-5849. doi: 10.1073/pnas.0501916102

Lilley, C. E., Schwartz, R. A., & Weitzman, M. D. (2007). Using or abusing: viruses and the cellular DNA damage response. *Trends Microbiol, 15*(3), 119-126. doi: 10.1016/j.tim.2007.01.003

Lim, D. S., Kim, S. T., Xu, B., Maser, R. S., Lin, J., Petrini, J. H., & Kastan, M. B. (2000). ATM phosphorylates p95/nbs1 in an S-phase checkpoint pathway. *Nature, 404*(6778), 613-617. doi: 10.1038/35007091

Lin, C. I., & Yeh, N. H. (2009). Treacle recruits RNA polymerase I complex to the nucleolus that is independent of UBF. *Biochem Biophys Res Commun, 386*(2), 396-401. doi: 10.1016/j.bbrc.2009.06.050

Lin, R., Heylbroeck, C., Pitha, P. M., & Hiscott, J. (1998). Virus-dependent phosphorylation of the IRF-3 transcription factor regulates nuclear translocation, transactivation potential, and proteasome-mediated degradation. *Mol Cell Biol, 18*(5), 2986-2996.

Liu, H., Jin, L., Koh, S. B., Atanasov, I., Schein, S., Wu, L., & Zhou, Z. H. (2010). Atomic structure of human adenovirus by cryo-EM reveals interactions among protein networks. *Science, 329*(5995), 1038-1043. doi: 10.1126/science.1187433

Liu, S., Cai, X., Wu, J., Cong, Q., Chen, X., Li, T., . . . Chen, Z. J. (2015). Phosphorylation of innate immune adaptor proteins MAVS, STING, and TRIF induces IRF3 activation. *Science, 347*(6227), aaa2630. doi: 10.1126/science.aaa2630

Liu, Y., Black, J., Kisiel, N., & Kulesz-Martin, M. F. (2000). SPAF, a new AAA-protein specific to early spermatogenesis and malignant conversion. *Oncogene, 19*(12), 1579-1588. doi: 10.1038/sj.onc.1203442

Lou, D. I., Kim, E. T., Meyerson, N. R., Pancholi, N. J., Mohni, K. N., Enard, D., . . . Sawyer, S. L. (2016). An Intrinsically Disordered Region of the DNA Repair Protein Nbs1 Is a Species-Specific Barrier to Herpes Simplex Virus 1 in Primates. *Cell Host Microbe, 20*(2), 178-188. doi: 10.1016/j.chom.2016.07.003

Lovejoy, C. A., & Cortez, D. (2009). Common mechanisms of PIKK regulation. *DNA Repair (Amst), 8*(9), 1004-1008. doi: 10.1016/j.dnarep.2009.04.006

Luftig, M. A. (2014). Viruses and the DNA Damage Response: Activation and Antagonism. *Annu Rev Virol, 1*(1), 605-625. doi: 10.1146/annurev-virology-031413-085548

Maizel, J. V., Jr., White, D. O., & Scharff, M. D. (1968). The polypeptides of adenovirus. II. Soluble proteins, cores, top components and the structure of the virion. *Virology, 36*(1), 126-136.

Majewski, L., Sobczak, M., Havrylov, S., Jozwiak, J., & Redowicz, M. J. (2012). Dock7: a GEF for Rho-family GTPases and a novel myosin VI-binding partner in neuronal PC12 cells. *Biochem Cell Biol, 90*(4), 565-574. doi: 10.1139/o2012-009

Markiewicz, E., Tilgner, K., Barker, N., van de Wetering, M., Clevers, H., Dorobek, M., . . . Hutchison, C. J. (2006). The inner nuclear membrane protein emerin regulates beta-catenin activity by restricting its accumulation in the nucleus. *EMBO J, 25*(14), 3275-3285. doi: 10.1038/sj.emboj.7601230

Martin-Vicente, M., Medrano, L. M., Resino, S., Garcia-Sastre, A., & Martinez, I. (2017). TRIM25 in the Regulation of the Antiviral Innate Immunity. *Front Immunol, 8*, 1187. doi: 10.3389/fimmu.2017.01187

Mathew, S. S., & Bridge, E. (2007). The cellular Mre11 protein interferes with adenovirus E4 mutant DNA replication. *Virology, 365*(2), 346-355. doi: 10.1016/j.virol.2007.03.049

Mathew, S. S., & Bridge, E. (2008). Nbs1-dependent binding of Mre11 to adenovirus E4 mutant viral DNA is important for inhibiting DNA replication. *Virology, 374*(1), 11-22. doi: 10.1016/j.virol.2007.12.034

Mathews, M. B., & Shenk, T. (1991). Adenovirus virus-associated RNA and translation control. *J Virol, 65*(11), 5657-5662.

Matsumoto, K., Nagata, K., Ui, M., & Hanaoka, F. (1993). Template activating factor I, a novel host factor required to stimulate the adenovirus core DNA replication. *J Biol Chem, 268*(14), 10582-10587.

Matsuoka, S., Huang, M., & Elledge, S. J. (1998). Linkage of ATM to cell cycle regulation by the Chk2 protein kinase. *Science, 282*(5395), 1893-1897.

McElwee, M., Beilstein, F., Labetoulle, M., Rixon, F. J., & Pasdeloup, D. (2013). Dystonin/BPAG1 promotes plus-end-directed transport of herpes simplex virus 1 capsids on microtubules during entry. *J Virol, 87*(20), 11008-11018. doi: 10.1128/JVI.01633-13

Miller, D. L., Rickards, B., Mashiba, M., Huang, W., & Flint, S. J. (2009). The adenoviral E1B 55-kilodalton protein controls expression of immune response genes but not p53-dependent transcription. *J Virol, 83*(8), 3591-3603. doi: 10.1128/JVI.02269-08

Moody, C. A., & Laimins, L. A. (2010). Human papillomavirus oncoproteins: pathways to transformation. *Nat Rev Cancer, 10*(8), 550-560. doi: 10.1038/nrc2886

Morrison, J., Laurent-Rolle, M., Maestre, A. M., Rajsbaum, R., Pisanelli, G., Simon, V., . . . Garcia-Sastre, A. (2013). Dengue virus co-opts UBR4 to degrade STAT2 and antagonize type I interferon signaling. *PLoS Pathog, 9*(3), e1003265. doi: 10.1371/journal.ppat.1003265

Murray, D. H., Jahnel, M., Lauer, J., Avellaneda, M. J., Brouilly, N., Cezanne, A., . . . Zerial, M. (2016). An endosomal tether undergoes an entropic collapse to bring vesicles together. *Nature, 537*(7618), 107-111. doi: 10.1038/nature19326

Nakamura, H., Morita, T., & Sato, C. (1986). Structural organizations of replicon domains during DNA synthetic phase in the mammalian nucleus. *Exp Cell Res, 165*(2), 291-297.

Nevins, J. R., Ginsberg, H. S., Blanchard, J. M., Wilson, M. C., & Darnell, J. E., Jr. (1979). Regulation of the primary expression of the early adenovirus transcription units. *J Virol, 32*(3), 727-733.

Nguyen, T., Nery, J., Joseph, S., Rocha, C., Carney, G., Spindler, K., & Villarreal, L. (1999). Mouse adenovirus (MAV-1) expression in primary human endothelial cells and generation of a full-length infectious plasmid. *Gene Ther, 6*(7), 1291-1297. doi: 10.1038/sj.gt.3300949

Nichols, G. J., Schaack, J., & Ornelles, D. A. (2009). Widespread phosphorylation of histone H2AX by species C adenovirus infection requires viral DNA replication. *J Virol, 83*(12), 5987-5998. doi: 10.1128/JVI.00091-09

Nick McElhinny, S. A., Snowden, C. M., McCarville, J., & Ramsden, D. A. (2000). Ku recruits the XRCC4-ligase IV complex to DNA ends. *Mol Cell Biol, 20*(9), 2996-3003.

Okuwaki, M., & Nagata, K. (1998). Template activating factor-I remodels the chromatin structure and stimulates transcription from the chromatin template. *J Biol Chem, 273*(51), 34511-34518.

Orazio, N. I., Naeger, C. M., Karlseder, J., & Weitzman, M. D. (2011). The adenovirus E1b55K/E4orf6 complex induces degradation of the Bloom helicase during infection. *J Virol, 85*(4), 1887-1892. doi: 10.1128/JVI.02134-10

Orjalo, A. V., Arnaoutov, A., Shen, Z., Boyarchuk, Y., Zeitlin, S. G., Fontoura, B., . . . Forbes, D. J. (2006). The Nup107-160 nucleoporin complex is required for correct bipolar spindle assembly. *Mol Biol Cell, 17*(9), 3806-3818. doi: 10.1091/mbc.E05-11-1061

Ostapchuk, P., & Hearing, P. (2005). Control of adenovirus packaging. *J Cell Biochem, 96*(1), 25-35. doi: 10.1002/jcb.20523

Ostapchuk, P., Suomalainen, M., Zheng, Y., Boucke, K., Greber, U. F., & Hearing, P. (2017). The adenovirus major core protein VII is dispensable for virion assembly but is essential for lytic infection. *PLoS Pathog, 13*(6), e1006455. doi: 10.1371/journal.ppat.1006455

Ostapchuk, P., Yang, J., Auffarth, E., & Hearing, P. (2005). Functional interaction of the adenovirus IVa2 protein with adenovirus type 5 packaging sequences. *J Virol, 79*(5), 2831-2838. doi: 10.1128/JVI.79.5.2831-2838.2005

Ou, H. D., Kwiatkowski, W., Deerinck, T. J., Noske, A., Blain, K. Y., Land, H. S., . . . O'Shea, C. C. (2012). A structural basis for the assembly and functions of a viral polymer that inactivates multiple tumor suppressors. *Cell, 151*(2), 304-319. doi: 10.1016/j.cell.2012.08.035

Paull, T. T., & Lee, J. H. (2005). The Mre11/Rad50/Nbs1 complex and its role as a DNA double-strand break sensor for ATM. *Cell Cycle, 4*(6), 737-740. doi: 10.4161/cc.4.6.1715

Peitz, M., Pfannkuche, K., Rajewsky, K., & Edenhofer, F. (2002). Ability of the hydrophobic FGF and basic TAT peptides to promote cellular uptake of recombinant Cre recombinase: a tool for efficient genetic engineering of mammalian genomes. *Proc Natl Acad Sci U S A, 99*(7), 4489-4494. doi: 10.1073/pnas.032068699

Pelka, P., Ablack, J. N., Torchia, J., Turnell, A. S., Grand, R. J., & Mymryk, J. S. (2009). Transcriptional control by adenovirus E1A conserved region 3 via p300/CBP. *Nucleic Acids Res, 37*(4), 1095-1106. doi: 10.1093/nar/gkn1057

Philipson, L., Lonberg-Holm, K., & Pettersson, U. (1968). Virus-receptor interaction in an adenovirus system. *J Virol, 2*(10), 1064-1075.

Pike, A. C., Gomathinayagam, S., Swuec, P., Berti, M., Zhang, Y., Schnecke, C., . . . Vindigni, A. (2015). Human RECQ1 helicase-driven DNA unwinding, annealing, and branch migration: insights from DNA complex structures. *Proc Natl Acad Sci U S A, 112*(14), 4286-4291. doi: 10.1073/pnas.1417594112

Pipas, J. M. (2009). SV40: Cell transformation and tumorigenesis. *Virology, 384*(2), 294-303. doi: 10.1016/j.virol.2008.11.024

Polo, S. E., & Jackson, S. P. (2011). Dynamics of DNA damage response proteins at DNA breaks: a focus on protein modifications. *Genes Dev, 25*(5), 409-433. doi: 10.1101/gad.2021311

Pombo, A., Ferreira, J., Bridge, E., & Carmo-Fonseca, M. (1994). Adenovirus replication and transcription sites are spatially separated in the nucleus of infected cells. *EMBO J, 13*(21), 5075-5085.

Puvion-Dutilleul, F., & Puvion, E. (1990a). Analysis by in situ hybridization and autoradiography of sites of replication and storage of single- and double-stranded adenovirus type 5 DNA in lytically infected HeLa cells. *J Struct Biol, 103*(3), 280-289.

Puvion-Dutilleul, F., & Puvion, E. (1990b). Replicating single-stranded adenovirus type 5 DNA molecules accumulate within well-delimited intranuclear areas of lytically infected HeLa cells. *Eur J Cell Biol, 52*(2), 379-388.

Querido, E., Blanchette, P., Yan, Q., Kamura, T., Morrison, M., Boivin, D., . . . Branton, P. E. (2001). Degradation of p53 by adenovirus E4orf6 and E1B55K proteins occurs via a novel mechanism involving a Cullin-containing complex. *Genes Dev, 15*(23), 3104-3117. doi: 10.1101/gad.926401

Querido, E., Marcellus, R. C., Lai, A., Charbonneau, R., Teodoro, J. G., Ketner, G., & Branton, P. E. (1997). Regulation of p53 levels by the E1B 55-kilodalton protein and E4orf6 in adenovirus-infected cells. *J Virol, 71*(5), 3788-3798.

Querido, E., Morrison, M. R., Chu-Pham-Dang, H., Thirlwell, S. W., Boivin, D., & Branton, P. E. (2001). Identification of three functions of the adenovirus e4orf6 protein that mediate p53 degradation by the E4orf6-E1B55K complex. *J Virol, 75*(2), 699-709. doi: 10.1128/JVI.75.2.699-709.2001

Reddy, V. S., Natchiar, S. K., Stewart, P. L., & Nemerow, G. R. (2010). Crystal structure of human adenovirus at 3.5 A resolution. *Science, 329*(5995), 1071-1075. doi: 10.1126/science.1187292

Reyes, E. D., Kulej, K., Pancholi, N. J., Akhtar, L. N., Avgousti, D. C., Kim, E. T., . . . Weitzman, M. D. (2017). Identifying Host Factors Associated with DNA Replicated During Virus Infection. *Mol Cell Proteomics, 16*(12), 2079-2097. doi: 10.1074/mcp.M117.067116

Rogakou, E. P., Boon, C., Redon, C., & Bonner, W. M. (1999). Megabase chromatin domains involved in DNA double-strand breaks in vivo. *J Cell Biol, 146*(5), 905-916.

Rowe, W. P., Huebner, R. J., Gilmore, L. K., Parrott, R. H., & Ward, T. G. (1953). Isolation of a cytopathogenic agent from human adenoids undergoing spontaneous degeneration in tissue culture. *Proc Soc Exp Biol Med, 84*(3), 570-573.

Roy, A. L. (2012). Biochemistry and biology of the inducible multifunctional transcription factor TFII-I: 10 years later. *Gene, 492*(1), 32-41. doi: 10.1016/j.gene.2011.10.030

Russell, W. C., Laver, W. G., & Sanderson, P. J. (1968). Internal components of adenovirus. *Nature, 219*(5159), 1127-1130.

Ryan, E. L., Hollingworth, R., & Grand, R. J. (2016). Activation of the DNA Damage Response by RNA Viruses. *Biomolecules, 6*(1), 2. doi: 10.3390/biom6010002

Salic, A., & Mitchison, T. J. (2008). A chemical method for fast and sensitive detection of DNA synthesis in vivo. *Proc Natl Acad Sci U S A, 105*(7), 2415-2420. doi: 10.1073/pnas.0712168105

Sarnow, P., Ho, Y. S., Williams, J., & Levine, A. J. (1982). Adenovirus E1b-58kd tumor antigen and SV40 large tumor antigen are physically associated with the same 54 kd cellular protein in transformed cells. *Cell, 28*(2), 387-394.

Sato, M., Tanaka, N., Hata, N., Oda, E., & Taniguchi, T. (1998). Involvement of the IRF family transcription factor IRF-3 in virus-induced activation of the IFN-beta gene. *FEBS Lett, 425*(1), 112-116.

Schwartz, R. A., Lakdawala, S. S., Eshleman, H. D., Russell, M. R., Carson, C. T., & Weitzman, M. D. (2008). Distinct requirements of adenovirus E1b55K protein for degradation of cellular substrates. *J Virol, 82*(18), 9043-9055. doi: 10.1128/JVI.00925-08

Shah, G. A., & O'Shea, C. C. (2015). Viral and Cellular Genomes Activate Distinct DNA Damage Responses. *Cell, 162*(5), 987-1002. doi: 10.1016/j.cell.2015.07.058

Sharma, S., tenOever, B. R., Grandvaux, N., Zhou, G. P., Lin, R., & Hiscott, J. (2003). Triggering the interferon antiviral response through an IKK-related pathway. *Science, 300*(5622), 1148-1151. doi: 10.1126/science.1081315

Shaw, A. R., & Ziff, E. B. (1980). Transcripts from the adenovirus-2 major late promoter yield a single early family of 3' coterminal mRNAs and five late families. *Cell, 22*(3), 905-916.

Sirbu, B. M., McDonald, W. H., Dungrawala, H., Badu-Nkansah, A., Kavanaugh, G. M., Chen, Y., . . . Cortez, D. (2013). Identification of proteins at active, stalled, and collapsed replication forks using isolation of proteins on nascent DNA (iPOND) coupled with mass spectrometry. *J Biol Chem, 288*(44), 31458-31467. doi: 10.1074/jbc.M113.511337

SivaRaman, L., & Thimmappaya, B. (1987). Two promoter-specific host factors interact with adjacent sequences in an EIA-inducible adenovirus promoter. *Proc Natl Acad Sci U S A, 84*(17), 6112-6116.

Smart, J. E., & Stillman, B. W. (1982). Adenovirus terminal protein precursor. Partial amino acid sequence and the site of covalent linkage to virus DNA. *J Biol Chem, 257*(22), 13499-13506.

Smith, M. C., Boutell, C., & Davido, D. J. (2011). HSV-1 ICP0: paving the way for viral replication. *Future Virol, 6*(4), 421-429. doi: 10.2217/fvl.11.24

Sohn, S. Y., & Hearing, P. (2012). Adenovirus regulates sumoylation of Mre11-Rad50-Nbs1 components through a paralog-specific mechanism. *J Virol, 86*(18), 9656-9665. doi: 10.1128/JVI.01273-12

Soria, C., Estermann, F. E., Espantman, K. C., & O'Shea, C. C. (2010). Heterochromatin silencing of p53 target genes by a small viral protein. *Nature, 466*(7310), 1076-1081. doi: 10.1038/nature09307

Steegenga, W. T., Riteco, N., Jochemsen, A. G., Fallaux, F. J., & Bos, J. L. (1998). The large E1B protein together with the E4orf6 protein target p53 for active degradation in adenovirus infected cells. *Oncogene, 16*(3), 349-357. doi: 10.1038/sj.onc.1201540

Steegenga, W. T., Shvarts, A., Riteco, N., Bos, J. L., & Jochemsen, A. G. (1999). Distinct regulation of p53 and p73 activity by adenovirus E1A, E1B, and E4orf6 proteins. *Mol Cell Biol, 19*(5), 3885-3894.

Stracker, T. H., Carson, C. T., & Weitzman, M. D. (2002). Adenovirus oncoproteins inactivate the Mre11-Rad50-NBS1 DNA repair complex. *Nature, 418*(6895), 348-352. doi: 10.1038/nature00863

Stracker, T. H., Lee, D. V., Carson, C. T., Araujo, F. D., Ornelles, D. A., & Weitzman, M. D. (2005). Serotype-specific reorganization of the Mre11 complex by adenoviral E4orf3 proteins. *J Virol, 79*(11), 6664-6673. doi: 10.1128/JVI.79.11.6664-6673.2005

Stros, M. (2010). HMGB proteins: interactions with DNA and chromatin. *Biochim Biophys Acta, 1799*(1-2), 101-113. doi: 10.1016/j.bbagrm.2009.09.008

Sun, W., Li, Y., Chen, L., Chen, H., You, F., Zhou, X., . . . Jiang, Z. (2009). ERIS, an endoplasmic reticulum IFN stimulator, activates innate immune signaling through dimerization. *Proc Natl Acad Sci U S A, 106*(21), 8653-8658. doi: 10.1073/pnas.0900850106

Sun, Y., Jiang, X., Chen, S., Fernandes, N., & Price, B. D. (2005). A role for the Tip60 histone acetyltransferase in the acetylation and activation of ATM. *Proc Natl Acad Sci U S A, 102*(37), 13182-13187. doi: 10.1073/pnas.0504211102

Svendsen, J. M., Smogorzewska, A., Sowa, M. E., O'Connell, B. C., Gygi, S. P., Elledge, S. J., & Harper, J. W. (2009). Mammalian BTBD12/SLX4 assembles a Holliday junction resolvase and is required for DNA repair. *Cell, 138*(1), 63-77. doi: 10.1016/j.cell.2009.06.030

Tanaka, A. J., Cho, M. T., Millan, F., Juusola, J., Retterer, K., Joshi, C., . . . Chung, W. K. (2015). Mutations in SPATA5 Are Associated with Microcephaly, Intellectual Disability, Seizures, and Hearing Loss. *Am J Hum Genet, 97*(3), 457-464. doi: 10.1016/j.ajhg.2015.07.014

Tauber, B., & Dobner, T. (2001). Molecular regulation and biological function of adenovirus early genes: the E4 ORFs. *Gene, 278*(1-2), 1-23.

Telkoparan, P., Erkek, S., Yaman, E., Alotaibi, H., Bayik, D., & Tazebay, U. H. (2013). Coiled-coil domain containing protein 124 is a novel centrosome and midbody protein that interacts with the Ras-guanine nucleotide exchange factor 1B and is involved in cytokinesis. *PLoS One, 8*(7), e69289. doi: 10.1371/journal.pone.0069289

Thimmappaya, B., Weinberger, C., Schneider, R. J., & Shenk, T. (1982). Adenovirus VAI RNA is required for efficient translation of viral mRNAs at late times after infection. *Cell, 31*(3 Pt 2), 543-551.

Thomas, G. P., & Mathews, M. B. (1980). DNA replication and the early to late transition in adenovirus infection. *Cell, 22*(2 Pt 2), 523-533.

Tollefson, A. E., Ryerse, J. S., Scaria, A., Hermiston, T. W., & Wold, W. S. (1996). The E3-11.6-kDa adenovirus death protein (ADP) is required for efficient cell death: characterization of cells infected with adp mutants. *Virology, 220*(1), 152-162. doi: 10.1006/viro.1996.0295

Tollefson, A. E., Scaria, A., Hermiston, T. W., Ryerse, J. S., Wold, L. J., & Wold, W. S. (1996). The adenovirus death protein (E3-11.6K) is required at very late stages

of infection for efficient cell lysis and release of adenovirus from infected cells. *J Virol, 70*(4), 2296-2306.

Trentin, J. J., Yabe, Y., & Taylor, G. (1962). The quest for human cancer viruses. *Science, 137*(3533), 835-841.

Turnell, A. S., & Grand, R. J. (2012). DNA viruses and the cellular DNA-damage response. *J Gen Virol, 93*(Pt 10), 2076-2097. doi: 10.1099/vir.0.044412-0

Ullman, A. J., & Hearing, P. (2008). Cellular proteins PML and Daxx mediate an innate antiviral defense antagonized by the adenovirus E4 ORF3 protein. *J Virol, 82*(15), 7325-7335. doi: 10.1128/JVI.00723-08

Ullman, A. J., Reich, N. C., & Hearing, P. (2007). Adenovirus E4 ORF3 protein inhibits the interferon-mediated antiviral response. *J Virol, 81*(9), 4744-4752. doi: 10.1128/JVI.02385-06

Van der Vliet, P. C. (1995). Adenovirus DNA replication. *Curr Top Microbiol Immunol, 199 (Pt 2)*, 1-30.

van der Vliet, P. C., & Levine, A. J. (1973). DNA-binding proteins specific for cells infected by adenovirus. *Nat New Biol, 246*(154), 170-174.

van Oostrum, J., & Burnett, R. M. (1985). Molecular composition of the adenovirus type 2 virion. *J Virol, 56*(2), 439-448.

Vasu, S., Shah, S., Orjalo, A., Park, M., Fischer, W. H., & Forbes, D. J. (2001). Novel vertebrate nucleoporins Nup133 and Nup160 play a role in mRNA export. *J Cell Biol, 155*(3), 339-354. doi: 10.1083/jcb.200108007

Velicer, L. F., & Ginsberg, H. S. (1970). Synthesis, transport, and morphogenesis of type adenovirus capsid proteins. *J Virol, 5*(3), 338-352.

Walters, R. W., Freimuth, P., Moninger, T. O., Ganske, I., Zabner, J., & Welsh, M. J. (2002). Adenovirus fiber disrupts CAR-mediated intercellular adhesion allowing virus escape. *Cell, 110*(6), 789-799.

Wathelet, M. G., Lin, C. H., Parekh, B. S., Ronco, L. V., Howley, P. M., & Maniatis, T. (1998). Virus infection induces the assembly of coordinately activated transcription factors on the IFN-beta enhancer in vivo. *Mol Cell, 1*(4), 507-518.

Weber, J. M. (2007). Synthesis and assay of recombinant adenovirus protease. *Methods Mol Med, 131*, 251-255.

Weiden, M. D., & Ginsberg, H. S. (1994). Deletion of the E4 region of the genome produces adenovirus DNA concatemers. *Proc Natl Acad Sci U S A, 91*(1), 153-157.

Weitzman, M. D. (2005). Functions of the adenovirus E4 proteins and their impact on viral vectors. *Front Biosci, 10*, 1106-1117.

Weitzman, M. D., Fisher, K. J., & Wilson, J. M. (1996). Recruitment of wild-type and recombinant adeno-associated virus into adenovirus replication centers. *J Virol, 70*(3), 1845-1854.

Winberg, G., & Shenk, T. (1984). Dissection of overlapping functions within the adenovirus type 5 E1A gene. *EMBO J, 3*(8), 1907-1912.

Wu, X., Avni, D., Chiba, T., Yan, F., Zhao, Q., Lin, Y., . . . Livingston, D. (2004). SV40 T antigen interacts with Nbs1 to disrupt DNA replication control. *Genes Dev, 18*(11), 1305-1316. doi: 10.1101/gad.1182804

Xue, Y., Johnson, J. S., Ornelles, D. A., Lieberman, J., & Engel, D. A. (2005). Adenovirus protein VII functions throughout early phase and interacts with cellular proteins SET and pp32. *J Virol, 79*(4), 2474-2483. doi: 10.1128/JVI.79.4.2474-2483.2005

Yanai, H., Ban, T., Wang, Z., Choi, M. K., Kawamura, T., Negishi, H., . . . Taniguchi, T. (2009). HMGB proteins function as universal sentinels for nucleic-acid-mediated innate immune responses. *Nature, 462*(7269), 99-103. doi: 10.1038/nature08512

Yoneyama, M., Suhara, W., Fukuhara, Y., Fukuda, M., Nishida, E., & Fujita, T. (1998). Direct triggering of the type I interferon system by virus infection: activation of a transcription factor complex containing IRF-3 and CBP/p300. *EMBO J, 17*(4), 1087-1095. doi: 10.1093/emboj/17.4.1087

Zhang, F., Romano, P. R., Nagamura-Inoue, T., Tian, B., Dever, T. E., Mathews, M. B., . . . Hinnebusch, A. G. (2001). Binding of double-stranded RNA to protein kinase PKR is required for dimerization and promotes critical autophosphorylation events in the activation loop. *J Biol Chem, 276*(27), 24946-24958. doi: 10.1074/jbc.M102108200

Zhang, J., & Chen, Q. M. (2013). Far upstream element binding protein 1: a commander of transcription, translation and beyond. *Oncogene, 32*(24), 2907-2916. doi: 10.1038/onc.2012.350

Zhong, B., Yang, Y., Li, S., Wang, Y. Y., Li, Y., Diao, F., . . . Shu, H. B. (2008). The adaptor protein MITA links virus-sensing receptors to IRF3 transcription factor activation. *Immunity, 29*(4), 538-550. doi: 10.1016/j.immuni.2008.09.003

Ziv, Y., Bar-Shira, A., Pecker, I., Russell, P., Jorgensen, T. J., Tsarfati, I., & Shiloh, Y. (1997). Recombinant ATM protein complements the cellular A-T phenotype. *Oncogene, 15*(2), 159-167. doi: 10.1038/sj.onc.1201319

Ziv, Y., Jaspers, N. G., Etkin, S., Danieli, T., Trakhtenbrot, L., Amiel, A., . . . Shiloh, Y. (1989). Cellular and molecular characteristics of an immortalized ataxia-telangiectasia (group AB) cell line. *Cancer Res, 49*(9), 2495-2501.

Zou, L., & Elledge, S. J. (2003). Sensing DNA damage through ATRIP recognition of RPA-ssDNA complexes. *Science, 300*(5625), 1542-1548. doi: 10.1126/science.1083430.